

The effect of heat shocks in skin rejuvenation

Citation for published version (APA):

Dams, S. D. (2010). *The effect of heat shocks in skin rejuvenation*. [Phd Thesis 1 (Research TU/e / Graduation TU/e), Biomedical Engineering]. Technische Universiteit Eindhoven. <https://doi.org/10.6100/IR685263>

DOI:

[10.6100/IR685263](https://doi.org/10.6100/IR685263)

Document status and date:

Published: 01/01/2010

Document Version:

Publisher's PDF, also known as Version of Record (includes final page, issue and volume numbers)

Please check the document version of this publication:

- A submitted manuscript is the version of the article upon submission and before peer-review. There can be important differences between the submitted version and the official published version of record. People interested in the research are advised to contact the author for the final version of the publication, or visit the DOI to the publisher's website.
- The final author version and the galley proof are versions of the publication after peer review.
- The final published version features the final layout of the paper including the volume, issue and page numbers.

[Link to publication](#)

General rights

Copyright and moral rights for the publications made accessible in the public portal are retained by the authors and/or other copyright owners and it is a condition of accessing publications that users recognise and abide by the legal requirements associated with these rights.

- Users may download and print one copy of any publication from the public portal for the purpose of private study or research.
- You may not further distribute the material or use it for any profit-making activity or commercial gain
- You may freely distribute the URL identifying the publication in the public portal.

If the publication is distributed under the terms of Article 25fa of the Dutch Copyright Act, indicated by the "Taverne" license above, please follow below link for the End User Agreement:

www.tue.nl/taverne

Take down policy

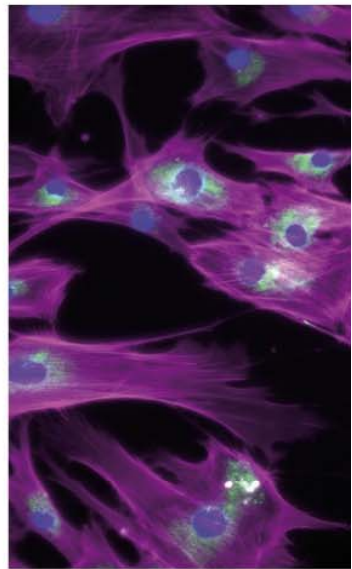
If you believe that this document breaches copyright please contact us at:

openaccess@tue.nl

providing details and we will investigate your claim.

the effect of **heat shocks** in skin rejuvenation

the effect
of **heat shocks**
in skin
rejuvenation



Susanne Dams — 2010

Susanne Dams

The effect of heat shocks in skin rejuvenation

Susanne Dams

A catalogue record is available from the Eindhoven University of Technology Library
ISBN: 978-90-386-2314-6

Cover design: B-design vormgeving

Printed by Universiteitsdrukkerij TU Eindhoven, The Netherlands

©Koninklijke Philips Electronics N.V. 2010

All rights reserved. Reproduction in whole or in part is prohibited without the written consent of the copyright owner.

The effect of heat shocks in skin rejuvenation

PROEFSCHRIFT

ter verkrijging van de graad van doctor aan de
Technische Universiteit Eindhoven, op gezag van de
rector magnificus, prof.dr.ir. C.J. van Duijn, voor een
commissie aangewezen door het College voor
Promoties in het openbaar te verdedigen
op donderdag 9 september 2010 om 16.00 uur

door

Susanne Dorien Dams

geboren te Nuenen, Gerwen en Nederwetten

Dit proefschrift is goedgekeurd door de promotor:

prof.dr.ir. F.P.T. Baaijens

Copromotor:

dr.ir. C.W.J. Oomens

Contents

List of Abbreviations	III
Summary	V
Chapter 1	1
General introduction	
Chapter 2	15
Modeling and simulation of the heat distribution in human skin caused by laser irradiation	
Chapter 3	31
The effect of pulsed heat shocks collagen type I expression in human dermal fibroblasts	
Chapter 4	47
The effect of pulse duration of the heat shock on collagen type I by human dermal fibroblasts <i>in-vitro</i>	
Chapter 5	63
The effect of thermal stimuli on dermal fibroblast in <i>ex-vivo</i> human skin	
Chapter 6	81
Procollagen gene upregulation in <i>ex-vivo</i> human skin after laser irradiation: A pilot study	
Chapter 7	93
General discussion	
Bibliography	101
Samenvatting	111
Dankwoord	113
Curriculum Vitae	115
List of Publications	117

List of Abbreviations

DAB	-	3,3'-Diaminobenzidine tetrahydrochloride
DAPI	-	4', 6-diamindino-2-phenylindole dihydrochloride
EIA	-	Enzyme Immuno Assay
HDF	-	Human dermal fibroblast
HRP	-	Horse Radish Peroxidase
HS	-	Heat shock
Hsp	-	Heat shock protein
HSR	-	Heat shock response
ICTP	-	carboxy-terminal telopeptide of collagen type I
MMP	-	Matrix metalloproteinase
MTT	-	3-[4,5-dimethylthiazol-2-yl]-2,5-diphenyl tetrazolium bromide
P1P	-	Procollagen type I carboxy-terminal Propeptide
PBS	-	Phosphate Buffered Saline
PI	-	Propidium Iodide
qPCR	-	quantative polymerase chain reaction
RMHS	-	Repeated mild heat shocks
SD	-	Standard deviation
TRITC	-	tetramethyl rhodamine B isothiocyanate

Summary

The effect of heat shocks in skin rejuvenation

The formation of wrinkles, one of the aspects of aging skin, results as a consequence of a degenerated dermis. The aged protein network, muscle contractions and gravitation result in wrinkling of the skin. Currently, in the cosmetic industry, treatments for skin rejuvenation are rapidly evolving. Only a few techniques are used to counteract the aging dermis. One of the most promising areas is non-ablative laser techniques. These techniques have clinically been tested. However, the physiological basis of their mechanisms is still to be established.

It is hypothesized that laser induced heat in the skin causes a heat shock and a subsequent heat shock response by the dermal fibroblasts. This heat shock response is said to stimulate, through heat shock proteins, the collagen synthesis by these cells. Subsequently, in addition to its thermal effect the laser also evokes a photochemical effect. The present thesis focuses on the influence of the thermal effect on the collagen production of human dermal fibroblasts in culture and in *ex-vivo* skin.

A model was developed that describes the interaction of laser light with skin resulting in the generation of heat. This model was combined with a transport model to describe the distribution of this heat through the skin. The model was used to determine the optimal laser conditions for heating and to describe the temperature distribution in the skin as a function of time.

To investigate the response of human skin to heat shocks, the initial research was performed on cell cultures. Here, human dermal fibroblasts were cultured and exposed to heat shocks of 45°C and 60°C, respectively, each with a pulse duration of 2 seconds. The results of this study showed that these heat shocks enhanced collagen type I synthesis. Subsequently, a study was performed with heat shocks of 45°C and 60°C that were applied for 2, 4, 8, 10 and 16 seconds. The conclusion from this study is that 8 to 10 second pulses at 45°C are the maximum exposure time range at which the collagen type I synthesis is optimal.

In a separate approach, viable *ex-vivo* human skin samples were immersed in PBS at both 45°C and 60°C. The 45°C heat shock did not damage the skin at all, while the 60°C heat shock appeared to reveal an initial damage response around the cells in the skin. It was demonstrated that procollagen type I as well as type III were upregulated by both 45°C and 60°C heat shocks.

Subsequently, a pilot study of a laser induced heat shock on *ex-vivo* skin study was performed. The results of this research demonstrated that the 45°C and 60°C laser induced heat shocks did not induce damage to the collagen structure of the skin samples. However, the 60°C laser induced heat shock, in conjunction with the previous *ex-vivo* skin study, appeared to reveal the presence of hsp27 in the area of the cells, suggesting early damage. The gene expression results indicated that the 45°C heat shocks upregulated procollagen type I.

In conclusion, it has been shown in this thesis that a heat shock of 45°C applied to fibroblasts or *ex-vivo* skin results in upregulation of collagen heat shock gene expression. Furthermore, the cell studies showed the relevance of the combination of time and temperature; an optimal exposure range of 8 to 10 seconds at 45°C was found to achieve the highest amount of collagen type I. Also the harmful nature of a 60°C heat shock was revealed. Showing that collagen synthesis can be enhanced by the 45°C heat shock is another step towards understanding the physiological pathways that lead to skin rejuvenation.

Chapter 1

General introduction

1.1 Skin rejuvenation

The human body grows, develops and eventually ages. The aging process affects each organ and cell, resulting in the decline of function causing health problems and eventually a decrease in the quality of life. The drive for a long and healthy life increases with prosperity. In our society today a certain vision of beauty is propagated to which one should measure up to. However, besides the obvious cosmetic reasons, health issues could in the future also play an important role in skin care. For example, skin diseases caused by excessive UV-radiation become more and more an issue (Bernerd and Asselineau, 2006; Ebling et al., 1992; Giacomoni and D'Alessio, 2007; Gilchrest and Bohr, 2006).

The skin protects us from external influences such as viruses and infections. Several functions are characteristic for the skin: it serves as a barrier, a temperature regulator, it has a prominent role in immune regulation, and it functions as a cushion for external mechanical loads (Ebling et al., 1992). It is the largest organ and is constantly exposed; therefore it should be kept in proper health. Aging of the skin results in a decreasing protective mechanism. Thus there are real advantages in retarding this aging process and many rejuvenating therapies have been proposed. However, the corresponding physiological processes are hardly understood. The present thesis is aimed at a better understanding of these processes in skin rejuvenation. Before the objective and scope can be discussed in more detail it is necessary to elaborate on the function and physiology of skin and its aging process.

1.2 Skin physiology

Like other organs the skin has the ability to grow, develop and repair. Roughly, it can be divided into three layers with on top the epidermis, followed by the dermis and the third layer is the hypodermis.

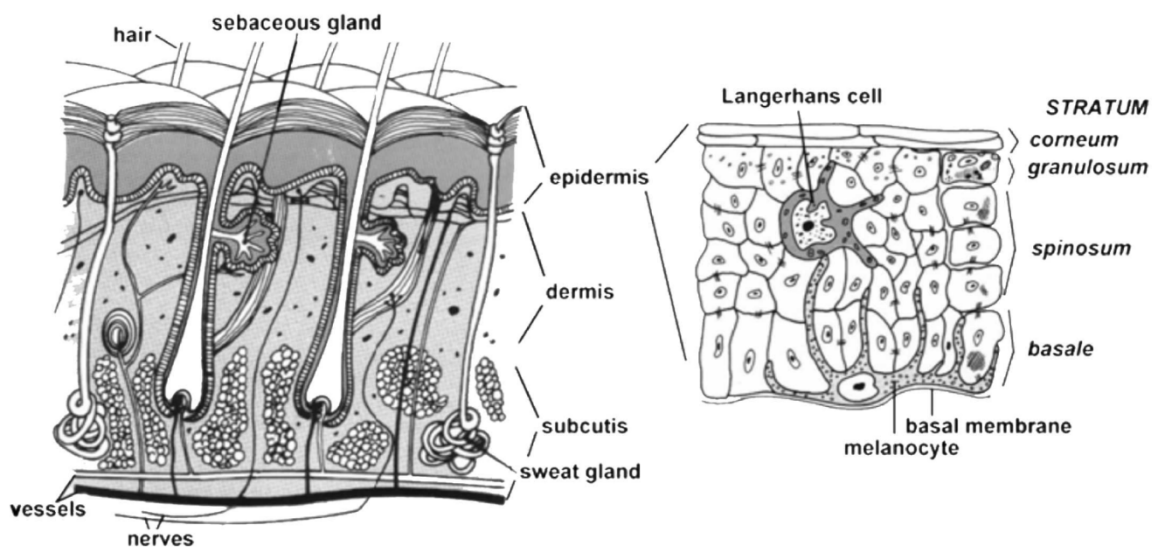


Figure 1.1: Schematic representation of a cross-section of the epidermis and dermis of the skin. The layered structure of the epidermis is depicted in more detail on the right (Farber and Rubin, 1998).

Figure 1.1 shows the two layers of the skin, most relevant for this thesis; the epidermis and the dermis.

1.2.1 Epidermis

The epidermis is 50-150 μm thick, depending on the part of the body and skin type (Lewis et al., 1994). It consists of a multilayered sheet of keratin synthesizing cells, called keratinocytes. In between those cells melanocytes, Langerhans cells and Merker cells are present. The keratinocytes are distributed in layers in order of increasing differentiation starting from the basement membrane zone, located immediately on top of the dermis. These layers, shown in figure 1.1 on the right, are called stratum basale, stratum spinosum, stratum granulosum and stratum corneum (Ebling et al., 1992; Humbert and Agache, 2004; Lewis et al., 1994; Mitchell et al., 1999).

In between the keratinocytes of the stratum basale melanocytes are situated, producing melanins, eumelanin and pheomelanin. Through melanosomes the melanins are transferred to the neighboring keratinocytes. Millions of epidermal melanin units, an association of one melanocyte with multiple keratinocytes, cause epidermal pigmentation. The color of the skin is largely based on the ratio between eumelanin and pheomelanin (Duval et al., 2002). In skin rejuvenation treatments a distinction of six different skin types, Fitzpatrick skin type I to VI, is being used. They are distinguished by the total melanin content (Fitzpatrick et al., 1961; Fitzpatrick, 1988). Type I correlates with little to no melanin content and in skin type VI melanin is in abundance (Lu et al., 1996; Roberts, 2009).

The basement membrane zone is the area where the epidermal and dermal layers are blended together. In this zone the basal membrane of the epidermis is connected to the papillary dermis through anchoring filaments (Ebling et al., 1992; Farber and Rubin, 1998).

1.2.2 Dermis

The dermis, the second layer of the skin, has a thickness that varies from 300 μm on the eyelids to 3 mm on the back (Ebling et al., 1992; Humbert and Agache, 2004). Left in figure 1.1 the dermis is depicted. The mechanical properties of the dermis are primarily determined by the supporting extracellular matrix. The main components of this matrix are proteins such as collagen, elastin, fibronectin, and proteoglycans (Ebling et al., 1992; Humbert and Agache, 2004; Mitchell et al., 1999; Prydz and Dalen, 2007).

The dermis can be divided into the papillary dermis and the reticular dermis (Farber and Rubin, 1998). The papillary dermis is a narrow zone immediately under the basement membrane zone of the epidermis. The most prominent structures are delicate collagen and elastin fibrils. Directly underneath the papillary dermis the reticular dermis is situated. This part contains most of the dermal collagen, organized into coarse bundles,

cross-linked with one another and with elastic fibers (Daamen et al., 2007; Tzaphlidou, 2007).

The majority of cells found in the dermis are the fibroblasts (Ebling et al., 1992; Farber and Rubin, 1998; Lewis et al., 1994). Fibroblasts synthesize the extracellular matrix proteins such as collagen, elastin and proteoglycans. Characteristic for these cells is that, if their activity is stimulated, for instance by heat, their endoplasmatic reticula and ribosomes become well developed and they start to synthesize heat shock proteins (Snoeckx et al., 2007).

1.3 Aging skin

Visible changes of the aging skin are roughness (dryness), wrinkling, laxity, and uneven pigmentation. Aging can biologically be defined as loss of cell function and subsequent degradation of the dermal matrix, increasing with time and illness (Krutmann, 2007; Labat-Robert and Robert, 2007; Wilhelm et al., 2007). This process is divided into intrinsic and extrinsic aging. Intrinsic aging of the skin refers to the chronological age of the skin, determined by only internal factors. Extrinsic aging is defined by external factors, such as gravity and sun light, that cause a constant exposure to mechanical stresses or irradiation, respectively (Gilchrest et al., 2007; Gilchrest, 2007c).

As a person ages several alterations occur in the skin. Internal factors result in a thinner skin, because cells, like fibroblasts, melanocytes, and keratinocytes, towards their senescent state start to divide more slowly and eventually lose their ability to replicate (Bailey, 2007; Ebling et al., 1992; Gilchrest, 2007a; Gilchrest and Bohr, 2006). Therefore, the amount of cells decreases and consequently less protein synthesis occurs. This is particularly noticeable in the dermis where less synthesis and more degradation loosens and unravels the underlying network of proteoglycans, elastin and collagen fibers, resulting in changed mechanical properties of the dermal matrix (Bailey et al., 2007; Labat-Robert and Robert, 2007). The stiffness of the skin is said to be age-related. One would expect, because of loosening and unraveling of the dermal matrix that the stiffness would decrease. However, it is reported that people under the age of 35 have a Young's Modulus of approximately $4.2 \cdot 10^5 \text{ N/m}^2$ and people above the age of 35 have an average Young's Modulus of $8.5 \cdot 10^5 \text{ N/m}^2$ (Agache et al., 2007; Branchet et al., 2007; Humbert and Agache, 2004; Smalls et al., 2006). As a result of the increasing stiffness of the dermal matrix the skin loses its ability to return to its original form, resulting in sagging and wrinkling. The formation of wrinkles also results from an interaction of permanent muscle contractions and gravity upon a thinned, inelastic dermis (Gilchrest, 2007a; Gilchrest and Bohr, 2006; Kurban and Bhawan, 2007). For example frown lines and crow's feet appear to develop due to the permanent small muscle contractions, and gravity contributes to the formation of pouches and drooping eyelids (Gilchrest, 2007b).

Additionally, the skin is exposed to light. Its optical properties play a major role in affecting the response of the skin to light. The effects are both wavelength and dose-dependent (Narurkar, 2006; Watanabe, 2008). Figure 1.2 shows the optical pathways of incident radiation into the skin (Anderson and Parrish, 2007; van Gemert et al., 1989; Welch and van Gemert, 1995).

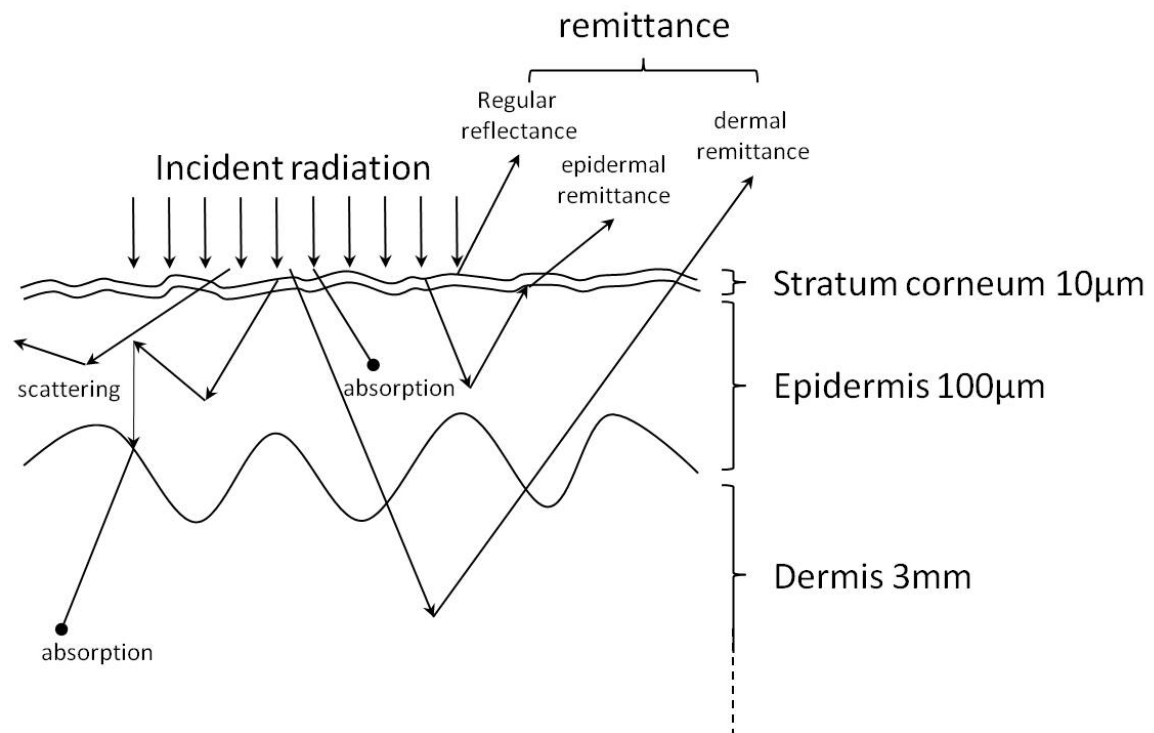


Figure 1.2: The optical pathways into the skin (van Gemert et al., 1989; Welch and van Gemert, 1995).

1.4 Skin and light

Light that penetrates into the skin is believed to have two different effects in the skin. Firstly, a thermal effect; photons are absorbed by chromophores (water, blood, and melanin) that convert the energy of the photons into heat and subsequently distribute this heat in the dermis (Capon and Mordon, 2006; Manstein et al., 2006). Secondly, a physiological effect; photons are absorbed by cytochrome-c on the membrane of the fibroblast and subsequently influence the oxidative phosphorylation. It depends on the wavelength and the energy of the photon if it will have a stimulating or an inhibiting effect on the oxidative phosphorylation (Dinh, 2006).

Incident photons must pass through the stratum corneum before they reach the viable epidermis and dermis. For normally incident photons a small part is reflected (regular reflectance, figure 1.2) due to the change in refractive index between air and stratum corneum. This reflectance for healthy skin is between 4% and 7% for a perpendicular beam of any wavelength (van Gemert et al., 1989). The remaining portion of the light is

transmitted further into the tissue. Besides propagating, the epidermis absorbs light too. The absorption property results from melanin and water. The melanin absorption level depends on the volume fraction of the melanin present in the epidermis, varying from 1.3% (skin type I) to 43% (skin type VI) (Bashkatov et al., 2005; Troy and Thennadil, 2001; van Gemert et al., 1989). Since melanin and water content decrease with age (Gilchrest, 2007a; Yaar et al., 2007), the absorption will decrease as well. The main chromophores in the dermis are water and hemoglobin (Troy and Thennadil, 2001). However, due to the change in dermal composition, decrease in amount and thickness of fibers, the optical properties, such as absorption and scattering, will decrease with age (Humbert and Agache, 2004; van Gemert et al., 1989).

1.5 Rejuvenation methods

To rejuvenate the skin the effects of aging must be stopped or reversed. As a result of continuous research it is perceived that most aging symptoms can be treated (Bjerring, 2006; Giacomoni and Rein, 2007; Sadick, 2006). Treatments that counteract the dryness and uneven pigmentation focus on the epidermis. Treatments to decrease the wrinkle depth and to improve the skin laxity are focused on the dermis. However, fundamental knowledge about the presumed physiological changes as a result of the rejuvenation treatments is missing. Some of the assumed mechanisms are associated with inflicting different degrees of skin damage (table 1.1), causing different degrees of wound healing that is assumed to result in a rejuvenated skin (Bjerring, 2006; Giacomoni and Rein, 2007; Sadick, 2006). Other theories suggest enhancement of synthesizing dermal components by stimulating fibroblasts will also result in skin rejuvenation (Dinh, 2006; Hamblin and Demidova, 2007; Kameyama, 2008).

Table 1.1: An overview of the different rejuvenation treatments including their corresponding processes. Based on literature literature (Biesman, 2007; Bjerring, 2006; Bowler, 2007; Dierickx and Anderson, 2007; Dierickx, 2007; Dinh, 2006; Giacomoni and Rein, 2007; Goldberg, 2006; Hamblin and Demidova, 2007; Manstein et al., Narurkar, 2006; Sadick, 2006; Sadick et al., 2006; Sadick, 2007; Swelstad and Gutowski, 2006; Weiss et al., 2006; White et al., 2007).

Technique	Treatment	Result after treatment			
		Damaging the skin	Spectrum of traumatizing → damaging the dermis	Removing stratum corneum	No damage
Optical	LED				×
	Non-ablative lasers		×		
	IPL		×		
	Fractional photothermolysis		×		
	Ablative lasers	×			
Electrical	Monopolar RF		×		
	Bipolar RF		×		
Mechanical	Micro-dermabrasion			×	
	Focused ultrasound		×		
	Dermabrasion	×			
Chemical	Superficial peel			×	
	Deep peel	×			

As depicted in table 1.1 and 1.2 the rejuvenation methods can be divided into four groups based on the used technique; optical, electrical, mechanical, and chemical. In the following paragraphs the treatments will be explained briefly, using the order as given in the first column of the tables.

Table 1.2: An overview of the efficacy of the rejuvenation treatments based on literature (Biesman, 2007; Bjerring, 2006; Bowler, 2007; Dierickx and Anderson, 2007; Dierickx, 2007; Dinh, 2006; Giacomoni and Rein, 2007; Goldberg, 2006; Hamblin and Demidova, 2007; Manstein et al., Narurkar, 2006; Sadick, 2006; Sadick et al., 2006; Sadick, 2007; Swelstad and Gutowski, 2006; Weiss et al., 2006; White et al., 2007). The efficacy of the treatment is indicated with ++ and + (positive), - and - - (negative). No difference before and after treatment is indicated with ‘o’ (neutral), and not reported with ‘?’.

Technique	Treatment	Aging characteristics						Efficacy	Down time	Risk potential
		Deep wrinkles	Fine lines	Skin tone	Skin texture	Spider veins	Pore size			
Optical	LED	-	o	o	o	o	o	o	++	++
	Non-ablative lasers	-	+	+	+	+	+	+	+	+
	IPL	-	+	+	+	+	+	+	-	-
	Fractional photothermolysis	-	+	+	+	+	+	+	-	-
	Ablative lasers	+	+	+	+	+	+	+	--	--
Electrical	Monopolar RF	o	+	-	-	-	o	o	o	?
	Bipolar RF	o	+	o	o	o	o	o	+	?
Mechanical	Micro-dermabrasion	-	o	+	+	o	o	o	--	--
	Focused ultrasound	?	?	?	?	?	?	?	?	?
	Dermabrasion	+	+	+	+	+	+	+	+	+
Chemical	Superficial peel	-	o	+	+	o	o	o	+	+
	Deep peel	+	+	+	+	+	+	+	--	--

1.5.1 Optical techniques

All optical treatments cause two effects, a thermal and a photochemical effect, as mentioned in paragraph 1.4. However, differences between treatments occur, due to the used spectrum and the amount of power that is applied. In the text below the dominating effect of the optical techniques will be explained.

Low-level light therapy, as mentioned, is performed with light emitting diodes, LEDs. The emitted photons are absorbed and produce a biological response. As a result this treatment does not inflict any damage to the skin, table 1.1. All biological systems have a unique absorption spectrum; this uniqueness determines which wavelengths of light will be absorbed (Dinh, 2006; Hamblin and Demidova, 2007; Weiss et al., 2006). The mechanism of low-power laser therapy at the cellular level is based upon the absorption of monochromatic visible and near infrared (NIR) radiation by components that play a role in the cellular respiratory chain, the oxidative phosphorylation. Absorption of these photons causes changes in redox properties of these molecules and acceleration of electron transfer, the so called primary reactions. Primary reactions in mitochondria are

followed by a cascade of secondary reactions, photo-signal transduction and amplification of cellular signalling. These reactions occur in cell cytoplasm, membrane, and nucleus. This process is known as photomodulation. Furthermore, it is suggested that the primary photo acceptor for the red-NIR range in mammalian cells is a cytochrome-c oxidase, an electron carrier in the oxidative phosphorylation (Dinh, 2006; Hamblin and Demidova, 2007).

Low-level light therapy aims to enhance collagen and elastin synthesis without causing injury, table 1.1 (Dinh, 2006; Hamblin and Demidova, 2007; Weiss et al., 2006). The method uses light emitting diodes, LEDs, for stimulation of the cells, but it does not traumatize or damage the skin. As a result no visible difference between before and after treatment can be noticed (table 1.2).

Laser treatments make use of chromophores. Chromophores are molecules, like water, haemoglobin, and melanin, that are capable of converting the energy of the photon into heat (Bjerring et al., 2006; Capon and Mordon, 2006; Dinh, 2006; Hamblin and Demidova, 2007; Sadick, 2006; Weiss et al., 2006). It is hypothesized that this heat shock triggers a heat shock response (HSR), resulting in the production of heat shock proteins. These proteins induce an inflammation reaction in the dermis (Capon and Mordon, 2006; Sadick, 2006). The damaging effect in the dermis is believed to induce a wound healing response (Bjerring et al., 2006; Capon and Mordon, 2006; Goldberg, 2006). The intact epidermis serves as a natural bandage, ensuring a low risk of infection and a relatively short recovery period (Bjerring, 2006; Geronemus, 2006; Manstein et al., 2006). The spectrum of lasers for non-ablative laser treatment is chosen in such a way that these lasers are able to selectively create thermal damage, using different chromophores, without losing the integrity of the epidermis.

Among the non-ablative technologies, intense-pulsed-light (IPL) technology involves application of a broadband, filtered flash lamp source directed to the skin. Modification of various parameters allows flexibility in treatment. These parameters include wavelength, energy fluency, pulse footprint, pulse duration, pulse delay, pulse sequence and temperature control of the skin (Bjerring et al., 2006; Capon and Mordon, 2006; Dierickx and Anderson, 2007; Goldberg, 2006; Sadick, 2006; Weiss et al., 2006).

Fractional photothermolysis uses a laser with a wavelength that is absorbed by aqueous tissue and is therefore not restricted to specific target tissue. It creates a dense pattern of epidermal and dermal microscopic wounds, but leaves the stratum corneum intact. The tissue around these microscopic wounds remains undamaged (Geronemus, 2006; Manstein et al., 2006).

The spectrum of treatments between stimulating and damaging the skin is wide. This area, from non-ablative lasers to fractional photothermolysis, is rapidly evolving and multiple treatments are developed. The positive effect of these treatments is that they

affect the dermis, but leave the epidermis more or less intact. However, the results of these treatments vary from traumatizing cells up to damaging the dermis, table 1.1. As an adverse effect of inflicting more damage to the skin, the risk of infections and scar formation increases as well (Manstein et al., 2006; Sadick et al., 2006; Sadick, 2007; White et al., 2007). Due to these different degrees of imposing injury to the skin, the results of these treatments vary from no difference to reducing wrinkles (table 1.2).

The spectrum of ablative lasers, treatments that cause the most skin damage, is chosen such that the targeted chromophore is water. The high amount of electromagnetic energy is absorbed by water molecules in the epidermis and part of the dermis. This conversion into heat results in vaporizing of the tissue water, leading to the ablation of the epidermis and part of the dermis (Dierickx and Anderson, 2007; Goldberg, 2006).

Ablative lasers remove the entire epidermis and part of the dermis, creating a deep wound and new skin is formed by the subsequent wound healing. Clinical studies have shown that the healing process requires a long time (long 'down time') and that it is hard to control, table 1.1. Therefore, the risk potential (table 1.2), the risk of developing scars and infections, is high (Dierickx and Anderson, 2007; Goldberg, 2006). However, the efficacy of these treatments is very good when the mentioned complications do not occur (table 1.2).

1.5.2 Electrical techniques

Monopolar conductive radio frequency generates a current that flows through the body from a single electrode with a grounding to close the electrical circuit. Sub-dermal heating occurs in the area around the electrode. Bipolar conductive radio frequency makes use of two electrodes that generate the current. However, it penetrates less deep than the current generated with monopolar RF (Biesman, 2007; Bowler, 2007; Narurkar, 2006).

Like the non-ablative laser, IPL and fractional photothermolysis treatments, treatments using RF affect the dermis, without harming the epidermis. Similarly, these treatments vary in the amount of damage they inflict to the dermis, table 1.1 (Manstein et al., 2006; Sadick et al., 2006; Sadick, 2007; White et al., 2007). These techniques are still in development. Therefore, the information about the efficacy of these treatments is scarce. Supposedly, the result will vary with the amount of inflicted damage (table 1.2).

1.5.3 Mechanical techniques

Microdermabrasion and dermabrasion damage the top layer of the skin, using small crystals to respectively scrape off a part or the entire epidermis (Dierickx and Anderson, 2007; Swelstad and Gutowski, 2006). Focused ultrasound generates a focal heating point in the dermis by mechanical forces induced by the longitudinal waves. The energy of ultrasound can be focused in the skin at 4.5 mm to create microscopic lesions (White et al., 2007).

Micro-dermabrasion only focuses on counteracting the aging signs in the epidermis. It removes the stratum corneum, dead cells, and therefore leaves the dermis and the viable epidermis intact, table 1.1 (Dierickx, 2007; Swelstad and Gutowski, 2006). The efficacy of these treatments in terms of wrinkle reduction is neutral, as shown in table 1.2.

Dermabrasion, on the other hand, scrapes of the entire epidermis, creating an open wound, table 1.1. Like the ablative laser treatments, the efficacy of dermabrasion can be very high (table 1.2), when complications, such as infection and scar formation, do not occur.

1.5.4 Chemical techniques

Superficial and deep chemical peeling use topical formulas to remove, respectively, a part or the entire epidermis (Swelstad and Gutowski, 2006). The depth of the peeling depends on the chemicals that are used.

The results of the chemical techniques can be compared to those of the mechanical techniques. Superficial chemical peelings, like micro-dermabrasion, only counteract the aging signs in the epidermis. As a result the efficacy is neutral, as shown in table 1.2. The deep chemical peelings remove the entire epidermis, like dermabrasion. It also has the same risk potential, down time and efficacy (Dierickx, 2007; Swelstad and Gutowski, 2006).

1.6 Relevant dermal proteins

Collagen, elastin, and proteoglycans are, as discussed earlier, the main extracellular matrix components of the dermal matrix. A very important aspect of skin rejuvenation is strongly related to the synthesis of these dermal components. It is therefore necessary to elaborate a little more on these proteins. Furthermore, heat shock proteins, as an essential facet of the response to thermal stimuli, will be discussed.

1.6.1 Collagen

Collagen represents the main fibrillar component of connective tissue and skin. Furthermore, it provides the skin its mechanical stiffness and strength (Knott and Bailey, 2007; Smalls et al., 2006). Collagen molecules are composed of three polypeptides. The intermolecular cross-links provide the continuous polymeric network and give collagen its unique properties of high tensile strength and stiffness. Collagen can be divided into different types based the aminoacid sequence in the α -chains (Ebling et al., 1992; Goldberg, 2006; Lewis et al., 1994). Collagen type I and type III are the most dominant collagen types in the skin. The adult human dermis consists for 80% of collagen type I. This collagen type represents the bulk of newly formed fully evolved collagen seen after ablative and most non-ablative dermal remodeling. Approximately 10% of the adult human dermis is type III collagen (Ebling et al., 1992; Goldberg, 2006).

1.6.2 Collagen synthesis and remodeling

Collagen consists of a hierarchical structure (figure 1.3) ranging from fibers down to a triple helical organization. The collagen fibers are composed of fibril bundles, consisting of hundreds of microfibrils. The microfibrils are assemblies of 5 collagen triple helices. Rope-like helices are formed out of three α -chains, each containing approximately 1000 amino acids.

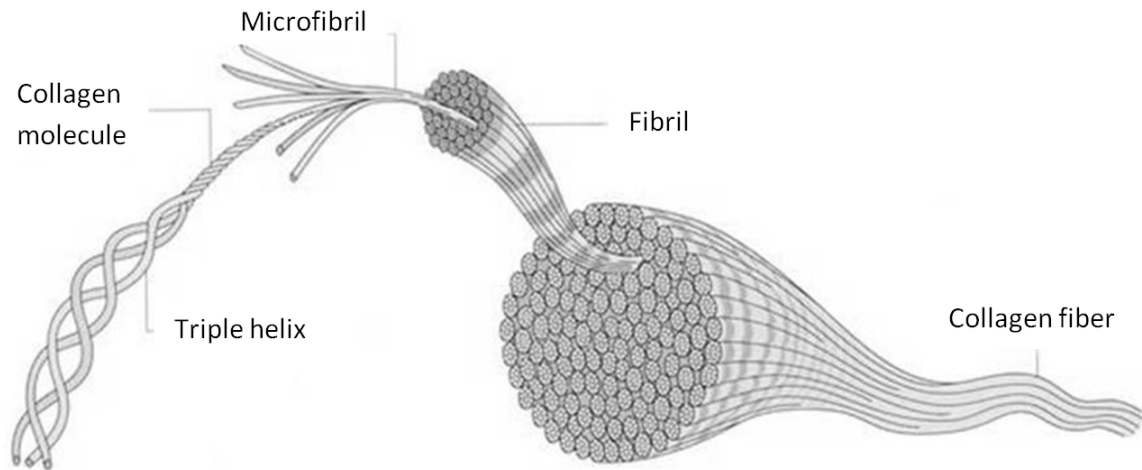


Figure 1.3: Formation of a collagen fiber (Lewis et al., 1994).

Variations in the amino acid content of the α -chains result in slightly different structural components. These distinctions evolve in the nuclei of the cells where mRNA is transcribed from the different genes that encode for the different types of procollagen. This specific mRNA is subsequently translated into the various amino acids. This enables early detection of a specific type of procollagen by means of measuring gene expression. Collagen synthesis takes place both inside the cell and subsequently in the extracellular space (Ebling et al., 1992; Farber and Rubin, 1998; Lewis et al., 1994). Inside the cell in the ribosomes along the Rough Endoplasmic Reticulum, RER, three peptide chains are formed. These peptide chains, known as procollagen, have registration peptides on each end. These peptide chains are sent into the lumen of the RER. Subsequently, signal peptides are cleaved inside the RER to form procollagen chains. Hydroxylation of lysine and proline amino acids occurs inside the lumen. This process depends on Ascorbic Acid (Vitamin C) as a cofactor. Glycosylation of specific hydroxylated amino acid occurs. The triple helical structure is formed inside the RER. The triple helical formation can be seen in figure 1.4. Procollagen is transported to the Golgi apparatus, where it is packaged and secreted through the membrane.

Outside the cell, registration peptides are cleaved and tropocollagen is formed by procollagen peptidase. Multiple tropocollagen molecules form collagen fibrils, and multiple collagen fibrils form into collagen fibers. This formation is shown in figure 1.4.

1.6.5 Heat shock proteins

Heat shock proteins, Hsps, are diverse and essential components of cell physiology. Most of the Hsps are molecular chaperones and have a protective role. They are named according to their molecular weight in kilo-Daltons, ranging from 10 to 110. Their expression can be elevated in the cells exposed to several stress factors, for example a heat shock. They provide a working environment for correct polypeptide folding, and perform a pivotal role not only in protein assembly but also in repair and transportation of proteins. A thermal stimulus that is applied by non-ablative treatments induces a temperature increase. This activates heat shock factors, which are inactively present under unstressed conditions, by changing the membrane composition and by unfolding proteins. The elevated level of activated heat shock factors results in an increase in Hsp-gene transcription and subsequent protein synthesis (Snoeckx et al., 2007). In the present thesis we are interested in the transcription of certain heat shock proteins. Three heat shock proteins are of interest to use as biomarkers, namely Hsp27, Hsp47, and Hsp70.

1.6.5.1 Heat shock protein 27

Heat shock protein 27, Hsp27, is a constitutive protein and an anti-apoptotic molecule that protects cells from apoptosis. Hsp27 can act both upstream of mitochondria, by inhibiting the release of cytochrome-c as a pro-apoptotic factor, and downstream of mitochondria, by preventing caspase-3 and -9 activation; enzymes that play a central role in the execution phase of a cell (Frank et al., 2004). It is phosphorylated upon stress and associates with structural proteins, among other things in the cytoskeleton and nucleus. There it governs re-folding of other proteins. Heat shock mediated denaturation of proteins was prevented by adding Hsp27 (Snoeckx et al., 2007).

1.6.5.2 Heat shock protein 47

Heat shock protein 47, Hsp47, is a constitutive protein and serves as a collagen type I-specific molecular chaperone. It is localized in the endoplasmic reticulum and plays an essential role in collagen biosynthesis in skin fibroblasts by transporting procollagen from the RER to the Golgi system. Hsp47 enables the correct three-dimensional conformation of procollagen chains and prevents their aggregation and precipitation (Hirano et al., 2004; Kuroda et al., 1998; Verrico et al., 2001; Verrico and Moore, 1997).

1.6.5.3 Heat shock protein 70

Heat shock protein 70, Hsp70, is a highly inducible protein and prevents aggregation and induces dissolution of aggregates. In response to stress, Hsp70 binds to denatured proteins, preventing their intracellular aggregation and precipitation, whilst targeting them for the appropriate environment for refolding or proteolysis. Hsp70 also plays a role in suppressing apoptosis of cells (Bonelli et al., 1999; Marshall and Kind, 2007; Ohtsuka and Laszlo, 2007; Snoeckx et al., 2007).

1.7 Aim and outline

Many skin rejuvenation techniques have been developed. A thorough understanding in the physiological changes in the skin as a result of the treatment is still lacking. In the present thesis we focus on the non-ablative treatments that generate heat in the dermis. Particularly, non-ablative laser techniques, because they have the ability to selectively heat the dermis.

The goal of the present thesis is to study the effect of heat pulses on fibroblasts, in particular collagen type I synthesis. The work is focused on the question whether or not collagen production in cultured cells and in *ex-vivo* skin can be stimulated by the generation of heat and which conditions are optimal for this purpose.

First we investigated the heat distribution caused by laser irradiation in skin, using a skin model. This includes a simulation model to determine the photon distribution combined with a heat transfer model to calculate the generated heat (chapter 2). This is important as it provides laser parameters and an estimation of the exposure time to heat shock cultured cells. Subsequently, the pulse duration from the model is used to study the effect of 45°C and 60°C heat shock on human dermal fibroblasts (chapter 3). Differences in collagen and heat shock proteins are quantified with time at gene expression level. In addition, the secretion of collagen synthesis and degradation markers is investigated as a function of time. The cell study continues with investigating the effect of different exposure times of the heat shocks of 45°C and 60°C on the collagen amount together with the heat shock protein gene expression levels of cultured human dermal fibroblasts (chapter 4). The outcome reveals different responses of the cultured cells between 45°C and 60°C heat shocks. Therefore, the effect of similar thermal stimuli on the gene expressions of collagen and heat shock proteins of dermal fibroblasts in human *ex-vivo* skin was studied by immersing the skin samples in heated phosphate buffered saline (chapter 5). Furthermore, to complete this thesis the effect of laser irradiation, with parameter setting acquired in chapter 2, on the gene expressions of collagen and heat shock proteins of dermal fibroblasts in human *ex-vivo* skin samples is investigated (chapter 6). To conclude this thesis, chapter 7 presents a general discussion based on the findings of the presented studies.

Chapter 2

Modeling and simulation of the heat distribution in human skin caused by laser irradiation

Abstract

With increasing age the characteristics of the human skin change and its appearance becomes different resulting in wrinkling and sagging of the skin. Treatment of aging skin with light based devices is a rapidly evolving area. Characteristic temperatures that are reached within the skin by non-ablative therapy are in the range of 45°C and 60°C. To study the interaction of a laser with *ex-vivo* skin a model system is developed. This paper presents a model combining Monte Carlo simulation to determine the distribution of heat generated by the photons from the laser with a finite element analysis to solve the transport of heat equation through skin. The end result is a temperature distribution as function of time and position in the skin. The model is used to determine which spectrum, power, and beam diameter are needed to heat the dermis of a human *ex-vivo* skin sample to 45°C and 60°C, with as little heat generation in the epidermis as possible. Additionally, a preliminary *ex-vivo* skin study with the calculated laser parameters is performed for validation. We show with this model that a 976 laser with 1 W and a beam diameter of 4 mm are the best settings for this study. Additionally, we demonstrate that it requires approximately 8 and 23 seconds to achieve 45°C and 60°C, respectively, with this kind of laser.

This chapter is based on S.D. Dams, Y. Luan, A.M. Nuijs, C.W.J. Oomens, F.P.T. Baaijens. *Modeling and simulation of heat distribution in human skin caused by laser irradiation.* (submitted)

2.1 Introduction

The skin is a complex heterogeneous medium, where the proteins, blood and cells are spatially distributed in different layers. The skin comprises three layers: epidermis, dermis and hypodermis. The epidermis can be subdivided into two sub-layers: the non-living epidermis, stratum corneum, and the living epidermis. The stratum corneum, with a thickness of 10 - 20 μm , only consists of dead squamous cells, with relatively low water content. The living epidermis, approximately 50 - 150 μm in thickness, contains most of the skin pigmentation, melanin, which is produced in melanocytes. It is composed of four layers: stratum basale, stratum spinosum, stratum granulosum and stratum lucidum (Ebling et al., 1992; Humbert and Agache, 2004). The dermis is a vascular layer with a thickness of 0.3 - 3 mm. Based on the distribution of blood vessels, the dermis can be subdivided into four layers (Bashkatov et al., 2005; Humbert and Agache, 2004): the papillary dermis with a thickness of about 150 μm , the upper blood net plexus which is 100 μm thick, the reticular dermis of approximately 1- 4 mm in thickness and the deep blood net plexus with a thickness of 100 μm . The hypodermis is a subcutaneous adipose tissue of up to 3 cm in thickness in the abdomen (Bashkatov et al., 2005; Ebling et al., 1992; Humbert and Agache, 2004). It is formed by an aggregation of fat cells containing stored lipids in the form of a number of small droplets. There are capillaries and nerves among the fat cells that provide for the metabolic activity of the fat tissue (Ebling et al., 1992; Lewis et al., 1994).

With increasing age the characteristics of the skin change and its appearance becomes different (Dimri et al., 2007). Visible changes are wrinkling and laxity (Bjerring, 2006; Diridollou et al., 2007; Gilchrest, 2007a; Gilchrest, 2007b; Gilchrest and Bohr, 2006; Leveque et al., 2007a; Swelstad and Gutowski, 2006). The causes of these changes can be attributed to two important alterations occurring in the dermal layer of the skin. Firstly, the ability decreases for fibroblasts to proliferate, resulting in less synthesis of dermal components. This causes thinning of the dermis. This leads to an increased susceptibility to damage. Secondly, the elastin and collagen fibers become more susceptible to damage, which leads to loosening and unraveling of the underlying network, resulting in wrinkling and sagging of the skin (Gilchrest, 2007b; Kurban and Bhawan, 2007; Leveque et al., 2007b).

Treatment of aging skin with different rejuvenation methods is a fast developing area. Among these methods, laser-based cosmetic surgery is evolving most rapidly. The underlying mechanism is the thermal effect of photon skin interaction in response to visible and near-infrared laser light. This effect can lead to thermal damage. The extent of this thermal injury of the tissue is governed by the heat deposition caused by the photon absorption in the skin and its subsequent heat radiation with its temperature dependent reactions (Welch et al., 1989b; Welch et al., 1991).

Ablative laser cosmetic surgery vaporizes the top layer of the skin and the skin upon healing reveals a fresh new surface layer. Since the targeted chromophore is water, the CO₂ laser or Er:YAG laser is commonly used, because of its relatively strong absorption by water in the far-infrared wavelength range (Eze and Kumar, 2010). The process of recovery is slow, because the keratinocytes and fibroblasts from the healthy part of the skin have to migrate to append for healing. Moreover, side effects of this method include edema, infection, pigmentary changes, and scarring (Pearlman, 2006). In contrast, the absence of epidermal damage in non-ablative dermal remodeling results in a decreased recovery time. The results of non-ablative laser treatments vary, as a consequence of the different settings in temperature and exposure time, from damaging to mildly traumatizing the skin. Hereby, the dermal tissue is selectively damaged or traumatized, leaving the skin surface intact (Eze and Kumar, 2010). This is achieved by using appropriate laser irradiation parameters: spectrum, energy density, pulse duration, spot size and spatial profile, as well as cooling of the epidermis during irradiation (Capon and Mordon, 2006; Laubach et al., 2006; Weiss et al., 2006).

It is believed that the thermal trauma that is induced denatures dermal collagen and stimulates collagen synthesis to promote the healing response (Capon and Mordon, 2006; Laubach et al., 2006; Narurkar, 2006; Weiss et al., 2006). The result is skin thickening and tightening. Typical lasers that are used for non-ablative rejuvenation are the 532 nm pulsed-dye lasers and lasers that emit in the 676 – 1540 nm region where absorption by water is not so strong. These types of lasers include Q-switched 1064nm Nd:YAG lasers, 976nm diode lasers, 1320nm long-pulsed Nd:YAG lasers, 1540nm Er:Glass lasers and 1440nm diode lasers (Narurkar, 2006; Pearlman, 2006).

In the present study, we focus on the heating process in the dermis by non-ablative laser treatments that do not cause damage to the skin. Characteristic temperatures that are reached within the skin are 45°C, which is a typical temperature used in photodynamic therapy (Capon and Mordon, 2006; Verrico et al., 2001; Verrico and Moore, 1997), and 60°C, which is known to induce denaturation of collagen. However, the amount of collagen contraction is determined by a combination of time and temperature (Ruiz-Esparza, 2006).

The characteristics of photon propagation include absorption and scattering events within skin tissue, reflection and transmission at boundaries. Photons can be absorbed by chromophores (e.g. melanin in the epidermis, hemoglobin and water in the dermis) that convert the energy into heat, which diffuses into the skin (Atiyeh and Dibo, 2009; Capon and Mordon, 2006; Sadick, 2006). These chromophores have different absorption spectra, resulting in absorption of photons of different wavelengths.

The epidermis propagates and absorbs light. The absorption of photons depends on the wavelength of the laser. Photons are absorbed in the epidermis by natural chromophores, such as water and melanin, mainly produced in the stratum basale. The

melanin absorption level depends on the volume fraction of the melanin content, varying from 1.3% (skin type I) to 43% (skin type VI) (Bashkatov et al., 2005; Troy and Thennadil, 2001; van Gemert et al., 1989). For the dermis, in the visible spectral range, the main chromophore is hemoglobin (Troy and Thennadil, 2001). Absorption by hemoglobin is defined by the haemoglobin oxygen saturation, because oxy- and de-oxy hemoglobin have slightly different absorption spectra. In the IR spectral range absorption properties of the dermis are determined by the water absorption. The hypodermis is characterized by a negligible absorption of light and most light reaching this layer is scattered back to the upper layer (Humbert and Agache, 2004; van Gemert et al., 1989). In general, the absorption properties of the entire skin are defined by the hemoglobin and water content in the dermis and the melanin density in the epidermis.

Another important phenomenon is scattering, where the direction of photon propagation is changed, especially in the visible and near-IR wavelength range (400nm-1200nm) (Bashkatov et al., 2005). The scattering property of human skin can be divided into two parts: surface scattering and subsurface scattering (Welch et al., 1989a; Welch et al., 1989b). Surface scattering is caused by the folds in the stratum corneum and is described by Fresnel equations (van Gemert et al., 1989; Welch et al., 1989b). About 5-7% of the light incident on the stratum corneum is reflected at the surface (Bashkatov et al., 2005; Humbert and Agache, 2004; Troy and Thennadil, 2001; van Gemert et al., 1989). The remaining portion of the light is transmitted further into the tissue. The skin is characterized as a forward scattering media (Humbert and Agache, 2004; Troy and Thennadil, 2001). Two types of subsurface scattering occur within the skin layers, which can be described for particles larger than the wavelength of light, Mie scattering, and for particles much smaller than the wavelength of light, Rayleigh scattering (Welch and van Gemert, 1995). In the dermis, the scattering properties of the skin are defined by the scattering properties of the reticular dermis (Groff et al., 2008; Humbert and Agache, 2004; Sturesson and Andersson-Engels, 1995; Troy and Thennadil, 2001). Collagen fibers (cylindrical with about 2.8 μm in diameter) lead to Mie scattering, while micro-structures are responsible for Rayleigh scattering (Groff et al., 2008; Humbert and Agache, 2004). Light is scattered multiple times inside the dermis before it is either transmitted to another layer or absorbed.

An exact evaluation of light propagation and the subsequent heat distribution in tissue requires a model that characterizes the tissue structure and optical properties. The skin can be considered to be a multi-layered structure, with each layer assumed to be isotropic and homogeneous. Several methods for constructing a well-designed model have been reported in literature (Eze and Kumar, 2010; Sturesson and Andersson-Engels, 1995; van Gemert et al., 1989). Gamborg *et al.* used a CCD camera to measure energy storage, and analyzed the heat transfer using FEMLAB (Gamborg Andersen et al., 2010). Crochet *et al.* applied the Monte Carlo method to simulate heat generation in skin, while using a finite difference method for the heat diffusion process (Crochet et al., 2006).

This paper presents a model combining Monte Carlo simulation with finite element analysis to describe the heat and temperature distribution in *ex-vivo* skin, caused by laser irradiation, as a function of the position and time. The model is used to predict the desired spectrum, power, and beam diameter needed to heat the dermis of the skin to 45°C and 60°C, without compromising the epidermis. Preliminary *ex-vivo* skin studies with calculated laser settings are used as an initial validation of the model.

2.2 Methods

2.2.1 Parameter study

We consider the skin to be a two-layered structure distinguishing between the epidermis and the dermis. The epidermis is considered to be 0.05 mm thick and the dermis 0.95 mm in thickness. The size and shape of the model is defined according to our *ex-vivo* validation experiments, where the size of the skin sample is 1.0 mm in height, 1.0 cm in width and 4.0 cm in length.

2.2.2 Monte Carlo simulation

The Monte Carlo method for laser-tissue interaction is used in this simulation. A package of photons is launched and reaches the skin surface. This photon package is given a weight, W , which is equal to 1. It propagates to an interaction site with a certain step size with a rotation angle and a deflection angle, assuming all particles behave similarly. At each interaction site the package deposits a portion of its energy to the site, determined by the tissue optical properties. The energy that is transferred to the interaction site is determined by the weight that the photon package deposits. The change of weight is defined as (Crochet et al., 2006; van Gemert et al., 1989; Welch and van Gemert, 1995):

$$\Delta W = W \frac{\mu_a}{\mu_a + \mu_s} \quad (2.1)$$

Where μ_a is the absorption coefficient and μ_s is the scattering coefficient. The action of the photon package will be terminated when the value of ΔW is below a defined threshold. In this simulation the photon package was terminated when one hundredth of its original weight was left after its interactions with the surrounding media. The value is chosen arbitrarily in such a way that efficiency and accuracy are optimal. A new photon package is launched after this termination process and the procedure is repeated. When the simulation is completed for a sufficient number of photon packages (typically 10^6 packages), an absorption power density matrix is generated for the given tissue configuration. This matrix corresponds to the amount of laser power that is absorbed by the area in the form of power density (Crochet et al., 2006; Welch and Gardner, 1997; Welch and van Gemert, 1995). The multiplication of the photon absorption probability density with the laser power results in the total power that is absorbed in the area (Crochet et al., 2006; van Gemert et al., 1989; Welch et al., 1989a).

The absorbed power at each location can be used as the heat source for the thermal diffusion process.

2.2.3 Finite element analysis

For the calculation of the thermal diffusion process in the skin sample a finite element analysis was performed, using Matlab[®] (R2008b, The MathWorks BV, Eindhoven, The Netherlands) together with Comsol (Multiphysics 3.5, Zoetermeer, The Netherlands). The diffusion equation with constant thermal properties and steady heat generation can be used for laser tissue interactions (van Gemert et al., 1989; Welch et al., 1989a):

$$\nabla \cdot (k\nabla T) = q - \rho C_p \frac{\partial T}{\partial t} \quad (2.2)$$

Where q is the heat generation rate inside the region (the energy density per unit time), T is the temperature, k is the thermal conductivity of the tissue, ρ is the density, and C_p represents the specific heat. Since the temperature increase is not sufficiently large, constant thermal properties may be assumed. The heat generation rate is calculated as (Crochet et al., 2006; Welch et al., 1989a):

$$q = P_{abs} \times P_{laser} \quad (2.3)$$

Where the photon absorption probability, P_{abs} , represents the portion of the photon energy deposited in a unit volume. These data are obtained through the Monte Carlo simulation. P_{laser} is the laser power. From these equations the temperature increase as a function of position and time can be calculated.

Table 2.1: Skin optical properties determined at 37°C used for Monte Carlo simulation input (Bashkatov et al., 2005; Groff et al., 2008; Troy and Thennadil, 2001; van Gemert et al., 1989; Welch and van Gemert, 1995).

Wavelength [nm]	Absorption coefficient, μ_a [cm ⁻¹]	Scattering coefficient, μ_s [cm ⁻¹]	Refractive index, n
532	1.28	322.57	1.38
635	0.6	247.31	1.38
976	0.38	174	1.38
1064	0.25	167.63	1.38

Based on the literature we have tested four different wavelengths, as depicted in table 2.1. These wavelengths were chosen, because they are absorbed by different and the most important chromophores in the skin (table 2.2). The requirements on the wavelengths were such that laser irradiation allows:

1. Homogeneous heating of the skin in the longitudinal direction; $T_{epidermis} \approx T_{dermis}$.
2. The homogeneously heated area should be as large as possible.

3. Appropriate heating efficiency to achieve 45°C as well as 60°C. Time to reach T_{desired} should be short.

Table 2.2: The different wavelengths and matching chromophores (P.Bjerring et al., 2006; R.R.Anderson and J.A.Parrish, 2007).

Wavelength [nm]	Chromophores			
	Melanin	Hemoglobin	Oxy-Hemoglobin	Water
532	×	×		
635	×			
976			×	×
1064			×	×

2.2.4 Simulation procedure

A finite element analysis was performed using the heat generation rate obtained through Monte Carlo simulations followed by data processing in Matlab. The outcome was visualized in terms of heat and temperature distribution in time and space. Figure 2.1 shows the flow of the entire simulation process.

Since the source of the energy is the laser, the beam properties must be taken into consideration. Different parameter sets were tested. The laser beam was considered to have a top-hat distribution in all simulations. This flat incident beam is constructed of multiple concentric rings, where each ring has an equally weighted number of photons. The result is an isotropic incident beam. The desired radius can be achieved by adjusting the number of rings. A total of 10^6 photon packages were used in each of the simulations in this study. Tables 2.1 and 2.3 contain the optical and thermal properties of human skin, respectively. The laser beam parameters, resulting from the parameter study and the configuration as used in the final simulation are depicted in table 2.4. The size of the geometry is based on the stretched *ex-vivo* skin sample.

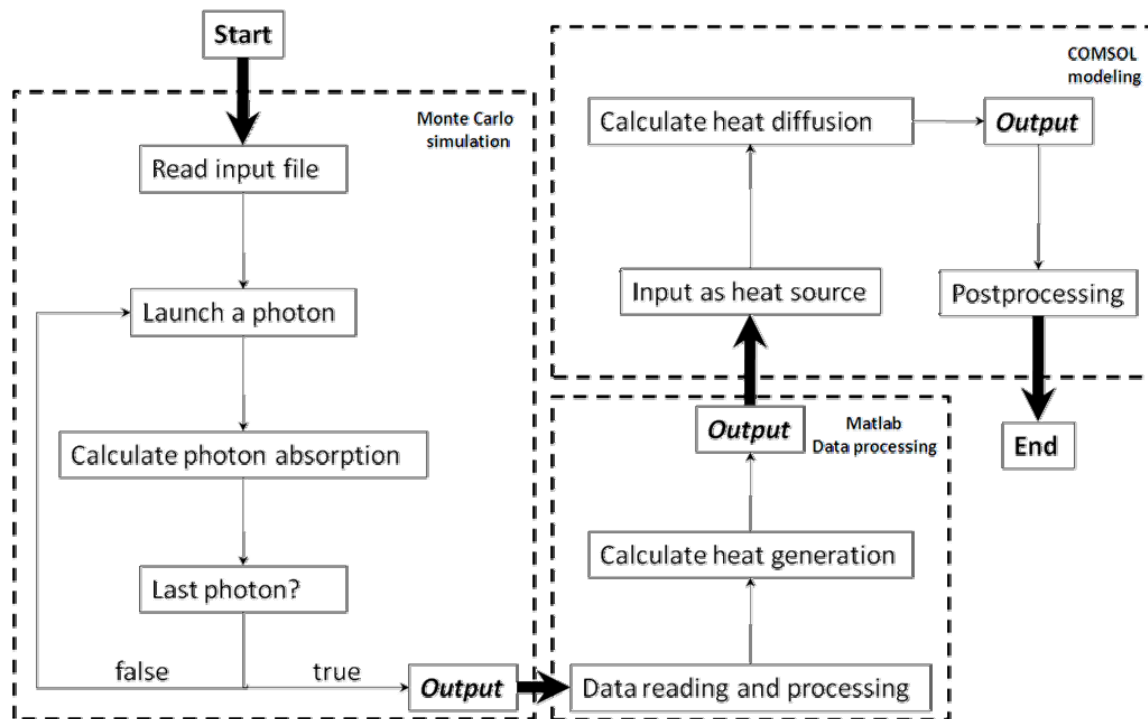
Table 2.3: Skin thermal properties used for finite element analyses (Bashkatov et al., 2005; Groff et al., 2008; Troy and Thennadil, 2001; van Gemert et al., 1989; Welch and van Gemert, 1995).

Tissue	Density, ρ [kg/m ³]	Thermal conductivity, k [W/(m*K)]	Specific heat, C_p [J/(kg*K)]	Initial temperature [°C]
Epidermis	1200	0.24	3590	37
Dermis	1200	0.45	3300	37

Table 2.4: Input parameters of experimental conditions.

Wavelength [nm]	x- range [μm]	y- range [μm]	Sample thickness [μm]	Beam		Laser power [W]	Number of photons
				type	radius [mm]		
976	10000	20000	1000	Top- hat	2	1	10^6

Using the finite element analysis, the temperature increase as a function of space and time is obtained. This heat generation is taken to be constant throughout the irradiation process. The energy transport is governed by the thermal properties of the area as given in table 2.3 (Welch and van Gemert, 1995).

**Figure 2.1:** Architecture of the model (Crochet et al., 2006).

2.2.5 Validation of the model

2.2.5.1 Experimental setup

All validation experiments were performed using a laser irradiation system that has been built with settings according to the outcome of the simulations. Figure 2.2 shows the experimental setup. The laser, a 976 nm laser diode (Sheaumann, Marlborough, USA) is connected to the computer through a laser driver (VueMetrix, Sunnyvale, USA) with compatible software installed. The laser is attached to the cooling system (Laser2000, Vinkeveen, The Netherlands) with a thermal insulation layer in between to cool the laser

diode during the experiments. A power meter (Melles Griot, Didam, The Netherlands) is used to calibrate the power on the surface of skin sample before experiments. The skin sample is exposed to the laser diode, and the dynamic temperature is measured using a thermocouple (VoltCraft, Oldenzaal, The Netherlands) and an infrared camera (FLIR, Berchem, Belgium).

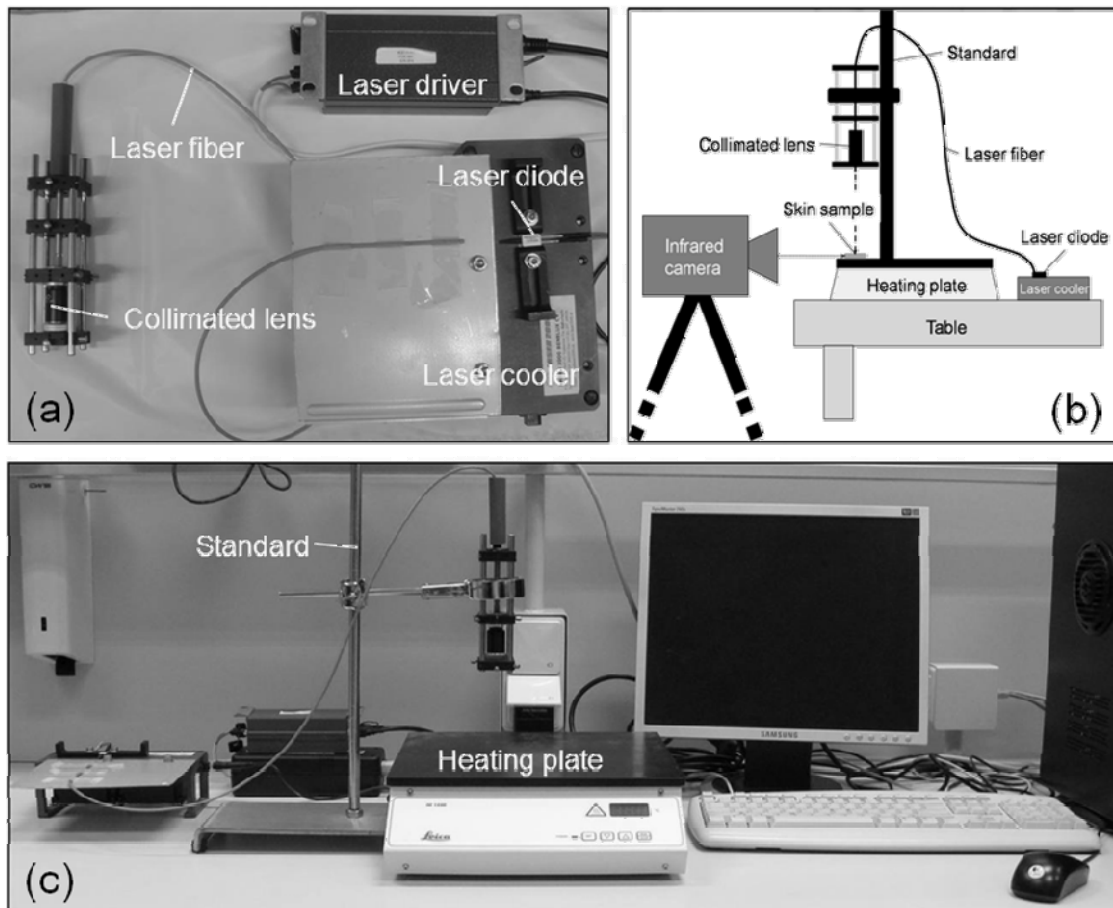


Figure 2.2: The experimental setup as used in the validation experiments. (a) A close-up of the laser driver, cooler and a 976 nm laser diode placed in a holder fixed and lined out with a collimated objective attached. (b) Schematic representation laser set up with infrared camera. (c) The setup in total with heating plate and control device.

2.2.5.2 Beam profile measurement

The intensity distribution of laser beam is measured by moving the spot with a translational stage over the fixed power meter. The sensor of the power meter is covered by a 200 μm pinhole. The measurements are performed every 0.5 mm in x and y direction. Figure 2.3 shows the uniform spot intensity of a top-hat distributed laser beam.

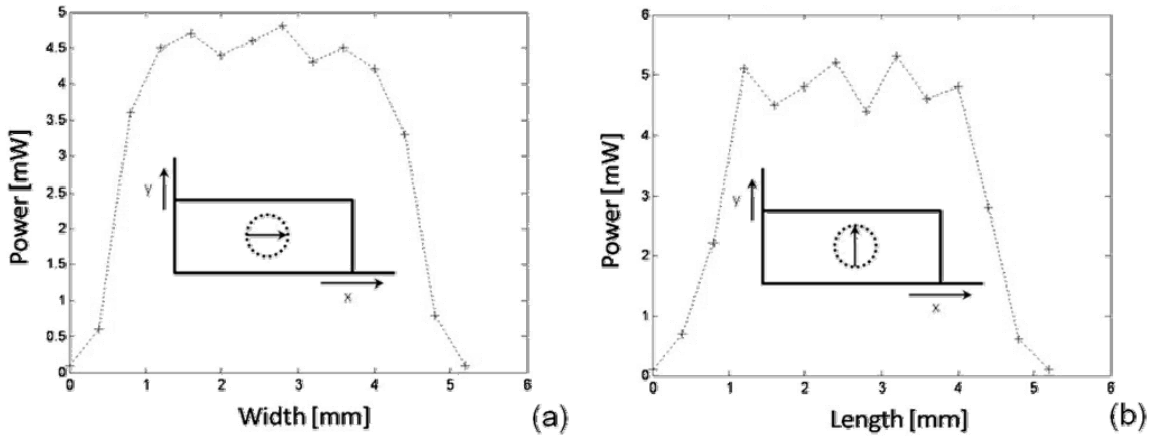


Figure 2.3: Results of the beam profile measurement of the 976 nm laser diode. The x-axis depicts the width of the collimated laser beam; the y-axis shows the measured power. (a) Shows the beam profile in x-direction and (b) shows the beam profile in y-direction.

Calibration of the laser was carried out to determine the relation between the applied current through the laser and the emitted power. The power meter is used for this calibration.

2.2.6 Preparation of skin samples

Ex-vivo human skin was obtained from the Catharina Hospital in Eindhoven. This material was anonymized after the procedure, making tracing back to the patient impossible. The procedure was in conformity with the code of conduct for use of human material as stated by the Dutch Federation of Biomedical Scientific Societies. Sample preparation was carried out within 3 hours after harvesting of the tissue. The skin was stretched in order to cut slices of 1 mm thickness with a dermatome (Humeca, Enschede, The Netherlands). To ensure the accuracy of measurement, we chose 4cm×1cm×1mm skin samples. Samples were placed in a small amount of culture medium at 37 °C during the experiments.

2.2.7 Experimental procedure

The thermocouple probe was fixed on a 37°C heating plate (Leica, Meppel, The Netherlands) in the middle of the beam. An infrared camera was adjusted to the same height as the skin sample to obtain a lateral view (figure 2.2(b)). The infrared camera automatically took images at a frequency of 0.2 Hz. The camera resolution is 320×240 pixels. The images from the infrared camera were used for further analyses.

2.3 Results

2.3.1 Heat distribution modeling

2.3.1.1 Parametric study

As shown in table 2.5, lasers with wavelengths of 635 nm and 1064 nm need substantially more time to heat the skin samples compared to the lasers with wavelengths of 532 nm and 976 nm. The wavelength of 976 nm minimally heats the epidermis and heats the dermis to the required temperatures in the shortest amount of time. At this wavelength, it takes 7.9 seconds and 26 seconds for the dermis to reach the desired temperature of 45°C and 60°C, respectively. As can be noticed at the wavelength of 532 nm these temperatures are achieved in a shorter time, 7.5 and 20 seconds, respectively. However, it only takes 5.5 and 16 seconds to achieve those temperatures in the epidermis, meaning that this layer will continue to heat up for 2 and 4 seconds, respectively. The difference in heating time between the epidermis and dermis should be in a similar time period; otherwise the epidermis will become too hot. At 976 nm wavelength this additional heating time is only 1.0 seconds for both 45°C and 60°C. Therefore, it can be said that the 976 nm wavelength fits our requirements best.

Table 2.5: Results parameter study to determine wavelength, $P = 1 \text{ W}$ and $\varnothing = 4 \text{ mm}$.

Wavelength [nm]	Desired temperature [°C]	Laser irradiation time epidermis [s]	Laser irradiation time dermis [s]	Δt [s]
532	45	5.5	7.5	2
	60	16	20	4
635	45	70	80	10
	60	180	200	20
976	45	6.9	7.9	1.0
	60	25.0	26.0	1.0
1064	45	11.7	13.8	2.1
	60	40	45	5

To determine the laser power and beam diameter we tested different power settings, 0.1 and 1 W, and a variety of beam diameters, 1, 2 and 4 mm. For practical applications, the heated area should be large enough to be able to visualize it. The results are shown in table 2.6. It can be seen that, to achieve an as large as possible area that is homogeneously heated in the longitudinal direction, the power should be 1 W and the beam diameter 4 mm.

Table 2.6: Results parameter study to determine beam diameter and power. Time to heat epidermis and dermis, respectively, at 1mm and 0 mm correspond to the positions in the inset in figure 2.4.

Power [W]	Diameter [mm]	T _{desired} [°C]	Time to heat epidermis (1 mm) [s]	Time to heat dermis (0 mm) [s]	Δt [s]
0.1	1	45	18.3	21.9	3.6
		60	70.8	74.6	3.8
	2	45	31.7	34.6	2.9
		60	149.7	152.7	3
	4	45	45.5	47.6	2.1
		60	228.7	230.7	2
1	1	45	0.4	1.8	1.4
		60	2.3	3.7	1.4
	2	45	1.3	1.9	0.6
		60	4.9	5.6	0.7
	4	45	6.9	7.9	1
		60	25	26	1

2.3.1.2 Temperature distribution in skin

The test conditions relate to the *in-vitro* situation of the *ex-vivo* skin experiments, where prior to laser irradiation the sample was placed at 37°C. The simulations were run using the selected laser with the determined laser parameters; a wavelength of 976 nm, 4 mm in diameter and a power of 1 W. The temperature to cool down to was set at 37°C. The boundary conditions, temperature, T, and heat flux, ϕ , were set to 37°C and 5 W/(m²K) (Kim and Guo, 2007; Sturesson and Andersson-Engels, 1995; Welch and van Gemert, 1995).

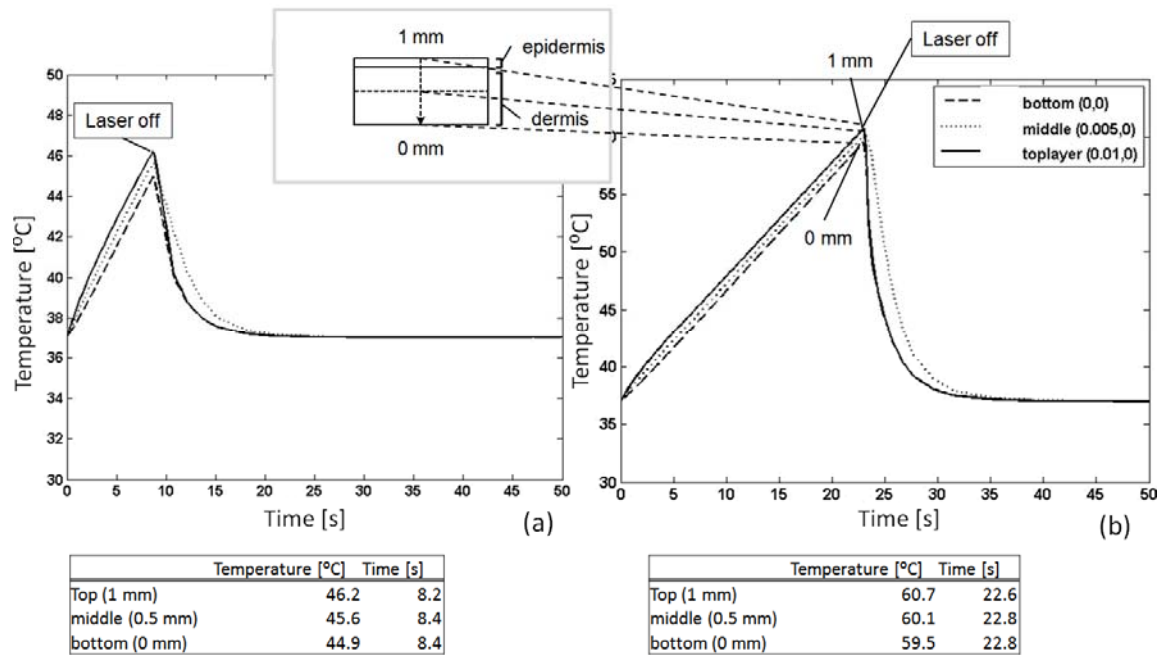


Figure 2.4: Visualization of the temperature change, along the symmetry axis of the sample from 0 mm to 1 mm (indicated in the inset), of the heating and cooling process by the 976 nm laser diode with a beam diameter of 4 mm and a power of 1 W. The x-axis depicts the time in seconds and the y-axis the temperature in degrees Celsius. The corresponding values are depicted in the tables below. (a) Heating to 45°C and cooling process. (b) Heating to 60°C and cooling process.

Figure 2.4 depicts the results of the simulations. The heat distribution in the center of the skin sample along the longitudinal axis is shown. In figure 2.4 (a) the heating process of the skin to 45°C and its subsequent cooling is shown. The irradiation of the skin sample heated to 60°C and its recovery of the dermis to 37°C is demonstrated in figure 2.4 (b). It takes roughly 8 seconds to heat the the dermis to 45°C. To achieve 60°C at in the dermis, it needs to be exposed to the laser for approximately 23 seconds.

2.3.2 Validation skin model

Prior to the validation experiments on *ex-vivo* human skin the experimental setup was calibrated to the acquired settings from the simulation.

2.3.2.1 Heat distribution validation

The temperature changes caused by the laser irradiation are visualized with the infrared camera as shown in figure 2.5 (b) next to the visualization of the simulation results in figure 2.5 (a). The lateral view in figure 2.5 (b) shows the 37°C heating plate on the bottom and the skin sample on top. The relatively cooler area between the heating plate and the *ex-vivo* skin sample can subscribed to the lateral view. The skin sample was placed close to the border of the heating plate. However, the uncovered part of the cooling plate is in contact with room temperature (approximately 20°C).

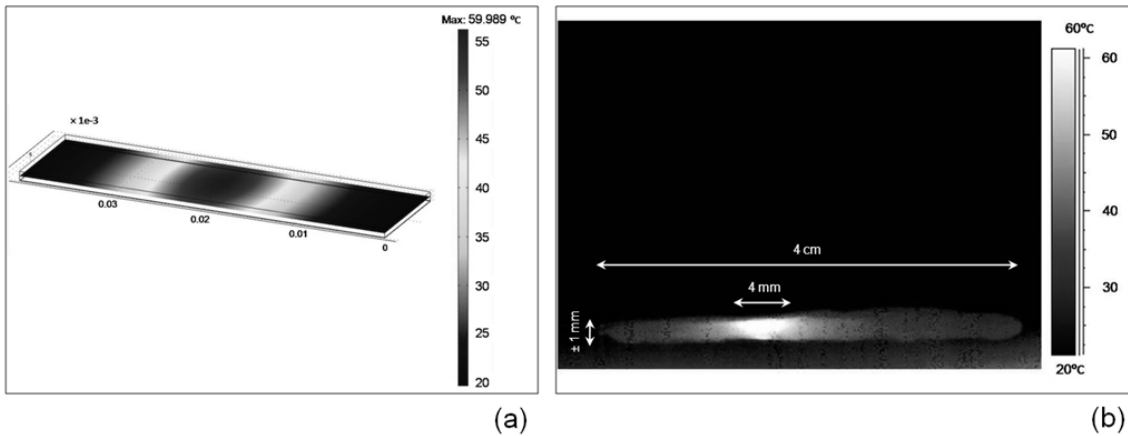


Figure 2.5: The simulation and experimental visualization of the heating process to 60°C. (a) The heat distribution as calculated by the simulation at $t = 25$ [s]. (b) The heat distribution after 29 ± 3 [s] laser irradiation by the 976 nm laser diode, diameter 4 mm and with a power 1 W.

A linear regression analysis was performed to determine the temperatures of 45°C and 60°C at the bottom of the skin samples. Mean values of 9 ± 2 seconds and 29 ± 4 seconds, respectively, were calculated (table 2.7).

Table 2.7: Results 976 nm diode laser, 4mm diameter, 1 W.

	Time to reach 45°C in the dermis [s]	Time to reach 60°C in the dermis [s]
Simulation	8.4	22.8
Infrared camera	9 ± 2	29 ± 4

2.4 Discussion

In this study a mathematical model was developed to predict the temperature field in human skin under laser irradiation. It combines a Monte Carlo simulation with finite element analysis to model transport of heat through the skin. The model was validated by means of experiments with ex-vivo human skin samples. A parametric study revealed the optimal laser wavelength of 976 nm for heating the skin to 45°C and 60°C.

The model was developed for a parametric study to obtain the best wavelength, beam diameter and power to achieve temperatures of 45°C and 60°C in human skin. These temperatures are chosen, because of their relevance in rejuvenating skin treatments. The temperature of 45°C was preferred because it is often applied in photodynamic therapy (Capon and Mordon, 2006), and 60°C was selected because this temperature is characteristic for protein denaturation (Ebling et al., 1992; Farber and Rubin, 1998; Mitchell et al., 1999). The different wavelengths for initial testing (table 2.1) are based on lasers that are currently used for skin treatment. The simulations showed that the 976 nm laser matched our requirements of longitudinal homogeneous heating and a relatively short time span to reach the desired temperatures of 45°C and 60°C.

Additionally, we further optimized the parameters power and beam diameter at this wavelength. It suggested that the optimal power is 1 W and the most adequate beam diameter is 4 mm.

In our simulations of the *in-vivo* situation it is shown that the temperatures of 45°C and 60°C are reached in 8.4 and 22.6 seconds, respectively (figure 2.4). Since the temperature at the epidermis is approximately 1°C higher than 1 mm into the dermis in the center of the laser beam, we also consider the skin sample to be nearly homogeneously heated in the longitudinal direction.

In our simulation the parameters are wavelength-dependent. However, they should also be temperature-dependent, because the optical parameters change with temperature of skin samples under laser irradiation (Anderson and Parrish, 2007; Tuchin et al., 2010; van Gemert et al., 1989; Welch and van Gemert, 1995). The scattering coefficient becomes higher when the temperature in the skin increases. This increase occurs because of denaturation of proteins in the dermis that change the structure of the dermal matrix into a denser configuration (Anderson and Parrish, 2007; Welch and van Gemert, 1995). However, our parametric studies showed that a temperature-dependent scattering coefficient in the heating process to 45°C or 60°C did not cause different heat distributions.

Also the anisotropy and refractive index depend on the structure of the dermis. The absorption coefficient, on the other hand, depends on the amount of water available in the skin. When the skin temperature rises, water starts to evaporate, resulting in a decreased absorption coefficient.

The results of the validation experiments of the heating process to 60°C showed a reasonable correlation with the simulated results (figure 2.5). The temperature of the skin sample was visualized with an infrared camera. An average of 6 images showed that 60°C was reached within 29 ± 4 seconds. This time span is in reasonable agreement with 25 seconds in the simulation. However, it should be taken into account that more extensive validation is necessary.

The main goal in non-ablative skin rejuvenation is to selectively heat the dermis without damage in the epidermal layer. The results obtained in this study demonstrate the feasibility of such a treatment regimen and the method developed in this study can be used effectively to guide these or similar treatment procedures. Furthermore, this skin model could in time provide a tool to predict the temperature distribution in the skin of each patient with its unique skin properties.

Chapter 3

The effect of pulsed heat shocks on collagen type I expression in human dermal fibroblasts

Abstract

The formation of wrinkles is associated with degeneration of the collagen matrix. For regeneration of the matrix, fibroblasts need to be stimulated in producing new collagen. In this study, the effect of short pulsed heat shocks on gene expression of procollagen type I, procollagen type III, hsp27, hsp47, and hsp70 and on expression of remodeling markers, P1P and ICTP, of human dermal fibroblasts in vitro, is investigated. Temperatures of 45°C and 60°C were used for the heat shocks. Proliferation rates, viability and metabolic activity were measured directly after the pulsed heat shocks and quantitative PCR was performed at five different time points after the heat shocks. Enzyme Immuno Assays were performed to determine the concentrations of P1P and ICTP. Results showed a decreased proliferation rate of the 60°C heat shocked cells, whereas the viability and metabolic activity did not differ. Furthermore, gene expressions were upregulated in both 45°C and 60°C heat shocked cells. However, remodeling marker analyses showed a larger amount of collagen produced by 60°C heat shocked cells. It can be concluded that these findings together with upregulation in gene expression show that it is possible to stimulate the cells to produce more collagen with short pulsed heat shocks.

The content of this chapter is based on: S.D. Dams, M.de Liefde-van Beest, A.M. Nuijs, C.W.J. Oomens, F.P.T. Baaijens. *Pulsed heat shocks enhance procollagen type I and procollagen type III expression in human dermal fibroblasts*. *Skin Res. and Techn.*, 16(3): 354-364, 2010.

3.1 Introduction

The skin is the largest organ of the human body. Like other organs it has the ability to grow, develop and repair itself. Roughly, the skin can be divided into three layers; the epidermis, dermis and hypodermis. The epidermis is 50-150 μm thick, depending on the part of the body and skin type (Lewis et al., 1994). It consists of a multilayered sheet of keratin synthesizing cells, keratinocytes, located immediately on top of the dermis (Farber and Rubin, 1998; Humbert and Agache, 2004; Lewis et al., 1994; Mitchell et al., 1999). Beneath the epidermis, the dermis is located with a varying thickness of 300 μm on the eyelids to 3 mm on the back (Ebling et al., 1992). The main component of the dermis is the supporting extracellular matrix, consisting of complexes of supportive proteins, such as collagen, elastin and proteoglycans, synthesized by dermal fibroblasts (Ebling et al., 1992; Geronemus, 2006). The dermis can be divided into the papillary dermis, situated directly under the epidermis, and the reticular dermis, located between the papillary dermis and the hypodermis (Farber and Rubin, 1998). The hypodermis insulates the body and plays an important role in wound healing and immune response (Ebling et al., 1992). This subcutaneous layer is the deepest layer of the skin and is composed primarily of fat cells.

As well as any other organ of the human body the skin ages. With increasing age the characteristics of the skin change and its appearance becomes different (Dimri et al., 2007). Visible changes are roughness (dryness), wrinkling, laxity, and uneven pigmentation (Bjerring, 2006; Diridollou et al., 2007; Gilchrest et al., 2007; Gilchrest, 2007b; Gilchrest and Bohr, 2006; Leveque et al., 2007a). These features are due to two important alterations that occur in the different layers of the skin. In this study we focus on changes in the dermal layer; wrinkling and laxity. Firstly, the fibroblasts divide more slowly and the dermis becomes thinner, thereby having an increased susceptibility to damage. Secondly, the underlying network of elastin and collagen fibers loosens and unravels, resulting in wrinkling and sagging of the skin (Gilchrest, 2007a; Kurban and Bhawan, 2007). The aging process can be divided into intrinsic aging, changes in e.g. dermal components like collagen, elastic fibers, proteoglycans and fibroblasts, and extrinsic aging, which is caused by external factors e.g. damage by UV-radiation (Ebling et al., 1992; Geronemus, 2006; Gilchrest, 2007c; Gilchrest, 2007d).

Rejuvenation of the skin aims at reversing the intrinsic and extrinsic causes of skin aging at both levels of the epidermis and the dermis. Among the rejuvenation methods used, non-ablative techniques are gaining popularity: in contrast to ablative techniques, that ablate the entire epidermis, these non-ablative methods claim to induce dermal remodeling without obvious epidermal injury, using a thermal approach. Light sources, like lasers and broad band lamps, radio frequency and ultrasound are techniques that can be used as non-ablative rejuvenation methods. The energy is applied as short nanosecond to millisecond pulses, or in a continuous wave resulting in a local

temperature increase (Bjerring, 2006; Capon and Mordon, 2006; Geronemus, 2006; Sadick, 2006).

It has been hypothesized that the generation of heat would cause collagen injury and contraction (Ebling et al., 1992; Geronemus, 2006; Gilchrest, 2007c; Sadick, 2006). Subsequently, this thermal injury could lead to a wound healing response (Goldberg, 2006; Sadick, 2006), where first collagen type III is synthesized and subsequently is substituted by collagen type I to approach the ratio of normal young skin (Capon and Mordon, 2006; Stadelmann et al., 2006). Another study suggests that dermal fibroblasts react to thermal injury with a heat shock response. This reaction of fibroblasts to the heat shocks results in the synthesis of heat shock proteins to protect themselves and their protein network (Bjerring et al., 2007). Relevant heat shock proteins for skin regeneration are

- hsp70; a highly inducible protein that is overproduced when a cell encounters a rapid increase of temperature (Bowers et al., 2007; Kovalchin et al., 2006; Marshall and Kind, 2007; Ohtsuka and Laszlo, 2007; Snoeckx et al., 2007; Souil et al., 2001),
- hsp47; a constitutive protein that binds and transports procollagen from endoplasmic reticulum to the Golgi system and plays an active role in collagen type I synthesis (Naitoh et al., 2001; Tasab et al., 2000; Verrico et al., 2001; Verrico and Moore, 1997), and
- hsp27; a constitutive protein that in case of overexpression protects the cell from apoptosis, resulting from a heat shock (Frank et al., 2004; Hirano et al., 2004; Snoeckx et al., 2007).

However, little physiological evidence of the heat shock response theory can be found in literature. Nevertheless, several studies have investigated the response of dermal fibroblasts to repeated mild heat shocks (RMHS). Their results showed that repeated mild (39°C - 42°C) heat shocks have beneficial effects on aged cells, resulting in an increase in procollagen type I and hsp47 and a decrease in the expression of hsp27 (Geronemus, 2006; Mayes and Holyoak, 2008; Rattan, 1998). Nonetheless, the duration of the heat shocks applied was between 30 minutes and 1 hour, which is relatively long and could induce thermotolerance (Ohtsuka and Laszlo, 2007). Moreover, the effect of the heat shocks on procollagen type III expression, as an indication of regeneration of the extracellular matrix has not been studied.

We aim to reverse the inherent aging processes in the dermis; in particular to counteract the behavior of the embedded fibroblasts. The focus of the work will be the degenerated collagen matrix. For regeneration of the collagen matrix dermal fibroblasts need to be stimulated to synthesize new collagen in line with the wound healing process where first collagen type III is produced followed by synthesis of collagen type I. To obtain an early indication if the collagen types indeed are produced we examined the

gene expression of these proteins. In this study we aim to increase the expression of procollagen type I and procollagen type III of human dermal fibroblasts by applying short pulsed heat shocks. Furthermore, we make use of heat shock proteins 70, 47 and 27 as biomarkers for respectively recognition of the heat shock, as a precursor for collagen synthesis, and for protection from apoptosis. In addition, to gain an insight into the regeneration process, the secretion of specific collagen remodeling markers was investigated with time: collagen synthesis marker P1P (procollagen type I carboxy-terminal propeptide) and collagen degradation marker ICTP (carboxy-terminal telopeptide of type I).

3.2 Materials and Methods

3.2.1 Cell culture

Cryopreserved human dermal fibroblasts were obtained from the European Collection of Cell Cultures (Salsbury, United Kingdom). Cells were grown at 37°C, 5% CO₂ and 95% humidity, in Dulbecco's advanced Modified Eagle's Medium (DMEM) (GIBCO, Invitrogen™, Breda, The Netherlands) supplemented with 10% fetal bovine serum (Greiner bio-one, Germany), 1% Glutamax (BioWhittaker™, Verviers, Belgium) and 0.1% Gentamycin (BioWhittaker™, Verviers, Belgium). Cells were grown until near confluency before passaging in a 1:2 ratio. After four serial passagings the cells were transferred to 6-wells plates for heat shock.

3.2.2 Heat shocks

Three distinct heat shock temperatures were used; 45°C, which can be induced by non-ablative techniques (Capon and Mordon, 2006; Verrico et al., 2001; Verrico and Moore, 1997), 60°C as a characteristic temperature for protein denaturation (Verrico and Moore, 1997) and 90°C to determine the limit of survival of the cells. The pulse duration of the heat shocks was chosen at approximately 2 seconds to approach the thermal heating time induced by non-ablative methods. The time points were chosen to enable early detection of changes by means of gene expression.

The pulsed heat shocks with temperatures of 45°C and 60°C were applied and as a control group cells were rinsed with 37°C Phosphate-Buffered Saline (PBS). The heat shocks were applied by rinsing the cell cultures twice with 1 ml heated PBS, which results in a heat shock duration of 2 seconds per rinsing. During the experiment cell cultures were placed on a heating plate of 37°C. After the pulsed heat shocks part of the cells were used for growth and viability curves, another part of the cells was used to measure the metabolic activity and the remainder was used for quantitative Polymerase Chain Reaction (qPCR).

3.2.3 Determination of the growth rate and viability of the cells

An equivalent of six 6-wells plates per temperature were used for the determination of the growth rate and viability of the fibroblasts. Cells were harvested for counting by trypsinization at six different time points; before and directly after the heat shocks to determine detachment of cells, and at $t = 2, 4, 7,$ and 9 days after the heat shocks. Until harvesting, the cells were kept under standard culture conditions with refreshments of culture medium every other day. After harvesting at each time point, the total number of cells, C_t , and number of non-viable cells, C_{nv} , were counted. Counting of the cells was performed using the Nucleocounter™ (Chemometec, Allerød, Denmark) following the protocol of the manufacturer. The growth rate was assessed using the average C_t per time point. An estimation of the viability was made out of the percentage of living cells.

3.2.4 Determination of the metabolic activity of the cells

The metabolic activity was measured using the 3-[4,5-dimethylthiazol-2-yl]-2,5-diphenyl tetrazolium bromide (MTT) based in vitro toxicology assay kit (Sigma, Breda, Nederland). Six 6-wells plates per temperature per measurement were used. Cells were used directly after the heat shocks to determine the metabolic activity. Per well 250 μ l MTT solution (M 5655, Sigma, Breda, The Netherlands) was added immediately and the 6-wells plates were placed at 37°C for 45 minutes. Subsequently, 250 μ l solubilization solution (M 8910, Sigma, Breda, The Netherlands) was added to each well and the 6-wells plates were placed on a shaker (Titramax 1000, Heidl Instruments, Germany) at 300 rpm for another 30 minutes. Metabolically active cells cleaved the molecules of the MTT solution resulting in an insoluble substrate of formazan crystals. After the 45 minutes of incubation the crystals were dissolved in acidified isopropanol resulting in a purple solution. Absorbance was spectrophotometrically measured at a wavelength of 570 nm (Biotek Synergy, Beun de Ronde, The Netherlands).

3.2.5 Determination of gene expression levels of heat shock proteins 27, 47, 70 and procollagen type I and III

Six 6-wells plates per temperature were used for qPCR. Cells were harvested by trypsinization at five different time points ($t = 5, 15, 35, 65, 95$ min) after the heat shocks and stored as dry pellets at -80°C. Total RNA was isolated using RNeasy kit (Qiagen, Venlo, The Netherlands) using the manufacturer's protocol. The concentration and purity of the total RNA was determined at OD 260/280 nm measurements (Nanodrop, Isogen, The Netherlands). RNA integrity was assessed using gel-electrophoresis. 500 ng RNA and random primers were used for cDNA synthesis using M-MLV reverse transcriptase (Invitrogen™, Breda, The Netherlands). Gene expression analysis was performed on an iCycler Real-Time PCR detection system (Biorad, Veenendaal, The Netherlands) using iQ™ SYBR®-Green supermix (Biorad, Veenendaal, The Netherlands). Primers for hsp27, hsp47, hsp70 and procollagen type I and III were designed with Beacon software using the DNA sequences obtained from the gene bank. For all primers used (Table 1), temperature gradients were performed to set the optimal annealing

temperature and dilution curves were assessed to check the efficiency of the primers. Results were normalized using reference genes β -Actin and GAPDH, obtained from Primerdesign (SouthHampton, U.K.), determined by Genorm (Vandesompele et al., 2002) to be best suited. Relative changes in quantity levels, $2^{-\Delta Ct}$, were calculated using Bio-Rad iQ5 software.

Table 3.1: Sequences of oligo's, genbank accession numbers, amplification fragments and annealing temperatures used for quantitative PCR.

Oligo	Sequence 5'-3'	Accession No.	Amplification fragment	Annealing temperature (°C)
Hsp70 FW	CGGAGGCGTGATGACTGC	BC002453	96 bp	59
Hsp70 REV	GTTGTCCGAGTAGGTGGTGAAG			
Hsp47 FW	TTGAGTTGGACACAGATG	AB010273	108 bp	59
Hsp47 REV	GCACTAGGAAGATGAAGG			
Hsp27 FW	ATCACCATCCCAGTCACCTTC	NM_001540	80 bp	59
Hsp27 REV	TTGGCGGCAGTCTCATCG			
ProColl1 FW	AATCACCTGCGTACAGAACGG	NM_000088	120 bp	59
ProColl1 REV	TCGTCACAGATCACGTCATCG			
ProColl3 FW	CCCAGAACATCACATATCAC	NM_000090	140 bp	59
ProColl3 REV	CAA GAGGAACACATATGGAG			

3.2.6 Determination of collagen type I remodeling markers

Concentrations of the markers for collagen synthesis, P1P, and collagen degradation, ICTP, were determined in the culture medium by means of enzyme immuno assays (EIA). P1P was measured using a procollagen type I C-peptide EIA kit (Takara Bio, Otsu, Shiga, Japan). ICTP was determined using a quantitative enzyme immunoassay designed for in vitro measurement of carboxy-terminal cross-linked telopeptide of human type I collagen (Orion Diagnostica, Espoo, Finland). Each assay was performed according to the recommendations of the suppliers. The assays were performed on medium samples of the HDFs obtained after 90 minutes, 24 and 48 hours after the pulsed heat shocks of 45°C and 60°C. For the control group medium samples of HDFs were measured at similar time points after culturing. The data were normalized to their corresponding amount of cells, resulting in concentration P1P and ICTP per cell.

3.2.7 Immunocytochemistry

To study the synthesis of collagen type I by the HDFs after the applied pulsed heat shocks immunofluorescent staining with an antibody for collagen type I (Sigma Aldrich, Breda, The Netherlands) was used. Cells were fixated 90 minutes, 24 and 48 hours after the pulsed heat shocks with 10% of formalin for 10 minutes before the staining

procedure was performed. The actin filaments of the cells were stained with Phalloidin-TRITC (Sigma, Breda, The Netherlands) and the cell nuclei with DAPI (Sigma, Breda, The Netherlands). The results were visualized with fluorescence microscopy at room temperature (Axiovert 200M, Zeiss B.V., Göttingen, Germany) with a 20× objective (Zeiss LD ACHROPLAN) and a NA of 0.4. A Zeiss AxioCam HRM Camera was used together with Zeiss AxioVision Rel. 4.8 acquisition software to record representative images.

3.2.8 Statistical analysis

Data are presented as mean \pm SD (standard deviation) for a sample measurement of $n = 6$. Comparisons between the control and experimented groups were performed by a two-tailed t-test. Differences were considered significant at $p < 0.05$.

3.3 Results

3.3.1 Influence of repeated heat shocks on growth rate and viability of cultured human dermal fibroblasts

Figure 3.1(a) shows the growth curves of the different groups of heat shocked cells. The proliferation rate of cells heat shocked at 45°C is similar to that of the control group of 37°C, while the cells heat shocked at 60°C proliferated much slower. The negative slope in the growth curve of the 90°C heat shocked cells indicates that the cells had reduced in number due to their death.

The viability of the fibroblasts, as depicted in figure 3.1(b), shows that the cells heat shocked at either 45°C or 60°C retained a similar viability as the control group, in the range of 90 to 98%. In case of the 60°C heat shocked cells this is noteworthy namely, that despite the retardation of the proliferation, the viability remains high. The viability of the cells heat shocked at 90°C, as represented in figure 3.1(b), decreased dramatically to 0% within four days. The presence of cell death after 4 days is necessarily associated with the growth rate data (figure 3.1(a)).

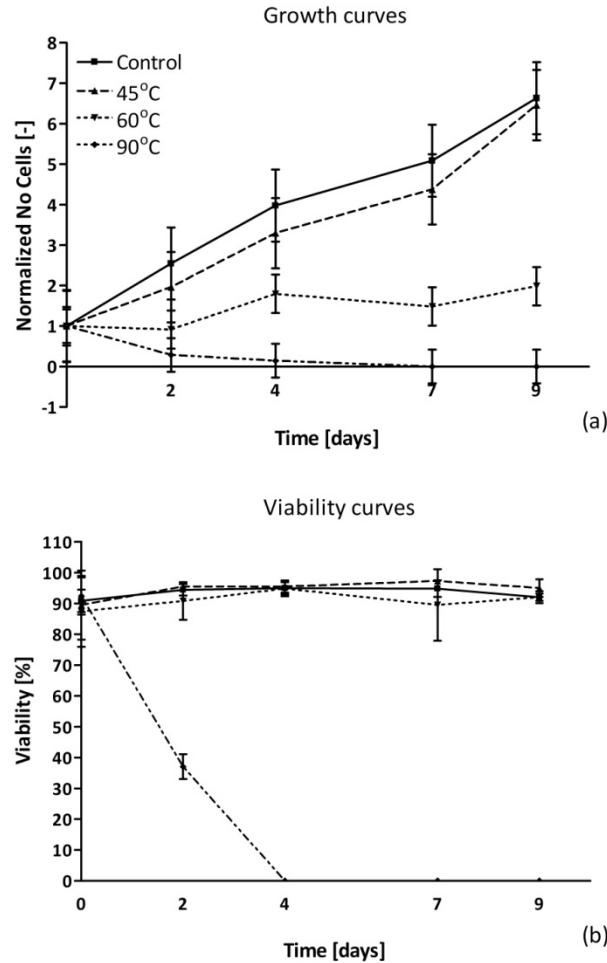


Figure 3.1: (a) Growth rate of human dermal fibroblasts after exposure to different pulsed heat shocks; the control was kept at 37°C. The x-axis depicts the time in days and the y-axis shows the number of cells normalized to their begin situation. The error bars at each point are calculated standard deviations ($n = 6$). Note: the decreased growth rate of 60°C heat shocked cells. (b) Viability curves of human dermal fibroblasts after being exposed to pulsed heat shocks; the control was kept at 37°C. The x-axis depicts the time in days and the y-axis shows the viability, percentage of living cells, calculated from C_t and C_{nv} . The error bars at each point are calculated standard deviations ($n = 6$). Note: the viability of the 60°C heat shocked cells.

3.3.2 Influence of heat shocks on metabolic activity of cultured human dermal fibroblasts

The effect of the heat shocks on the metabolic activity is illustrated in figure 3.2. The absorption levels are proportional to the metabolic activity. Furthermore, all results are normalized to the absorption level of the control group. It can be seen that the absorption levels of the 45°C and the 60°C heat shocked cells are 0.76 ± 0.10 ($p < 0.01$) and 0.79 ± 0.06 ($p < 0.01$), respectively. However, there is no significant difference in the metabolic rates of cells heat shocked at 45°C and 60°C. The absorption level of the 90°C heat shocked cells is 0.04 ± 0.02 , which is significantly lower than that of the control value ($p < 0.001$). This low metabolic activity confirms that these cells are dead.

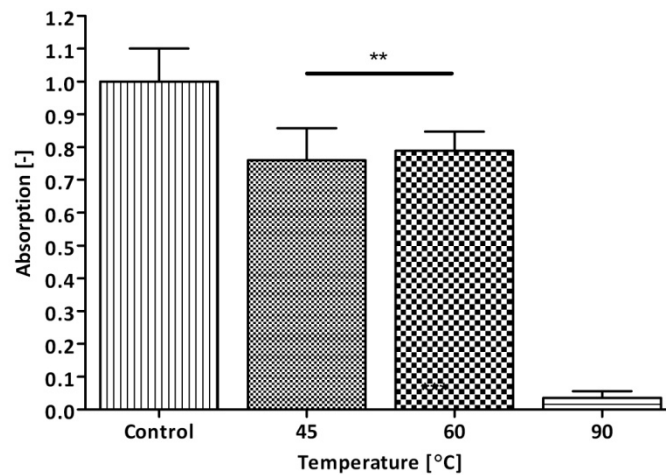


Figure 3.2: The metabolic activity of human dermal fibroblasts after exposure to a pulsed heat shock; the control was kept at 37°C. The x-axis depicts the control and the different heat shock temperatures. The y-axis shows the absorption levels normalized to the control. The data are shown as the mean \pm SD for $n = 6$ run in triplicates. Significant differences are shown at ** $p < 0.01$ and *** $p < 0.001$. Note: the absorption is proportional to the metabolic activity.

It is noted that the metabolic activity of 45°C and the 90°C heat shocked cells is in accordance with the growth rate and viability measurements. However, it should be noted that the 60°C heat shocked cells, although their proliferation rate has decreased, are still metabolically as active as the faster growing 45°C heat shocked cells.

3.3.3 Effect of heat shocks on the expression of heat shock proteins 27, 47 and 70

The relative quantities of hsp70 and their control are depicted in figures 3.3(a) and (b). After the pulsed heat shocks of 45°C the expression significantly increased after 35 minutes ($p < 0.05$) as shown in figure 3.3(a). The corresponding values of gene expression of hsp70 are significantly higher at the elevated 60°C temperature ($p < 0.001$ in all cases). Indeed, there is a monotonic increase in the expression of hsp70 in the 95 minutes following the 60°C pulsed heat shocks (figure 3.3(b)).

Figures 3.3(c) and (d) represent the relative quantities of hsp47 at the various time points after the pulsed heat shocks. These data show that the heat shock of 45°C resulted in a significant increase after 35 minutes ($p < 0.01$) while, after the 60°C pulsed heat shock, a significant increase in hsp47 mRNA level was seen after 95 minutes ($p < 0.01$).

Regarding the expression of hsp27, figure 3.3(e) shows an overall significant decrease in gene expression ($p < 0.001$) after the pulsed heat shocks of 45°C. The 60°C heat shocks also resulted in a significant decrease ($p < 0.001$) as illustrated in figure 3.3(f), although, with time, the expression was restored to near the control value.

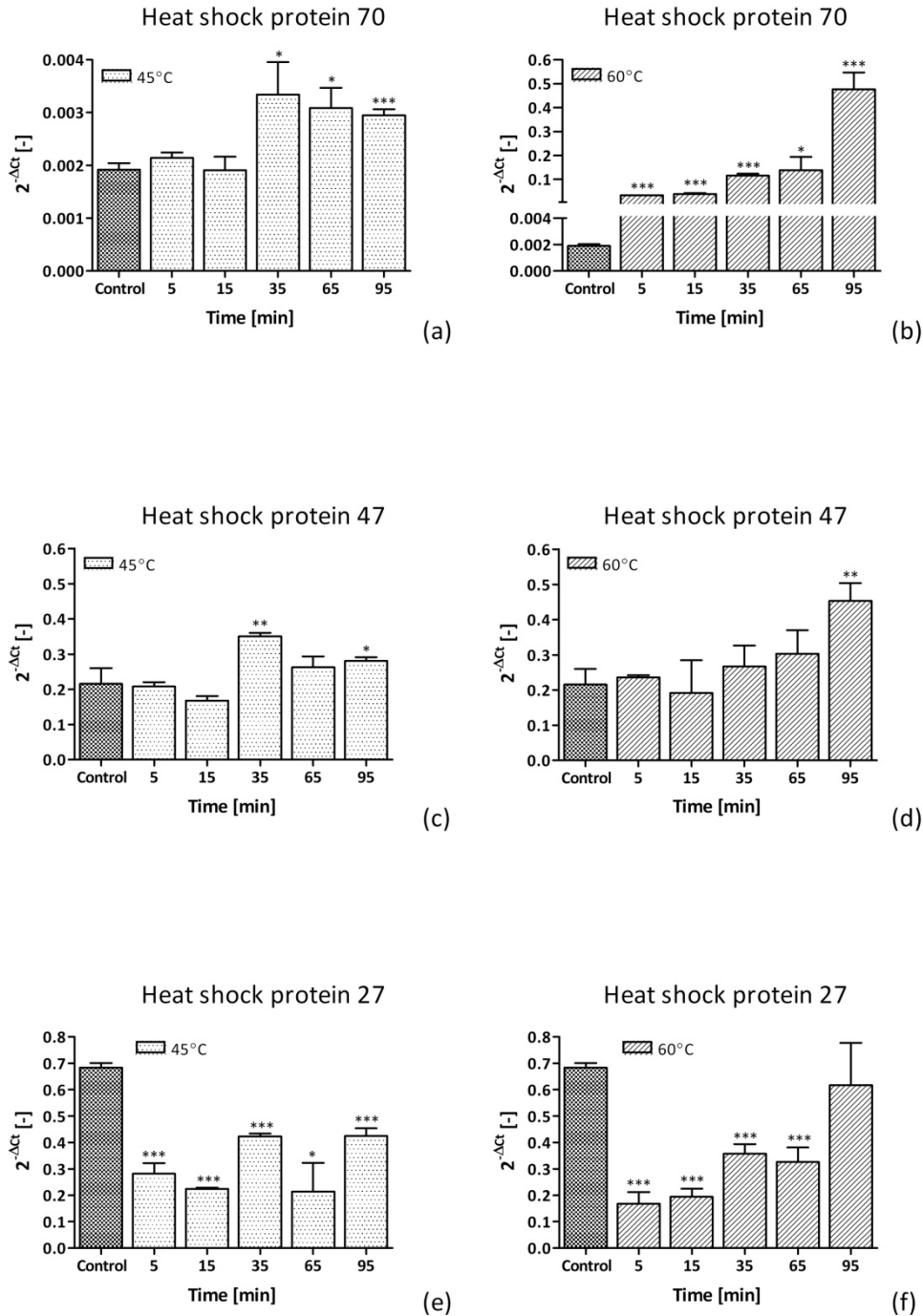


Figure 3.3: Relative quantity of heat shock protein 70, heat shock protein 47 and heat shock protein 27 at the different time points after exposure to pulsed heat shocks. The control was kept at 37°C and the data are relative to the reference genes β -Actin and GAPDH. The x-axis depicts the control and the different points in time given in minutes. The y-axis shows the relative quantity of mRNA, respectively hsp70, hsp47 and hsp27, calculated with $2^{-\Delta Ct}$. Data are shown as the mean \pm SD for three independent experiments each run in duplo with significant differences compared to control at * $p < 0.05$, ** $p < 0.01$ and *** $p < 0.001$. (a) Hsp70 after 45°C pulsed heat shocks. (b) Hsp70 after 60°C pulsed heat shocks. (c) Hsp47 after 45°C pulsed heat shocks. (d) Hsp 47 after 60°C pulsed heat shocks. (e) Hsp 27 after 45°C pulsed heat shocks. (f) Hsp 27 after 60°C pulsed heat shocks

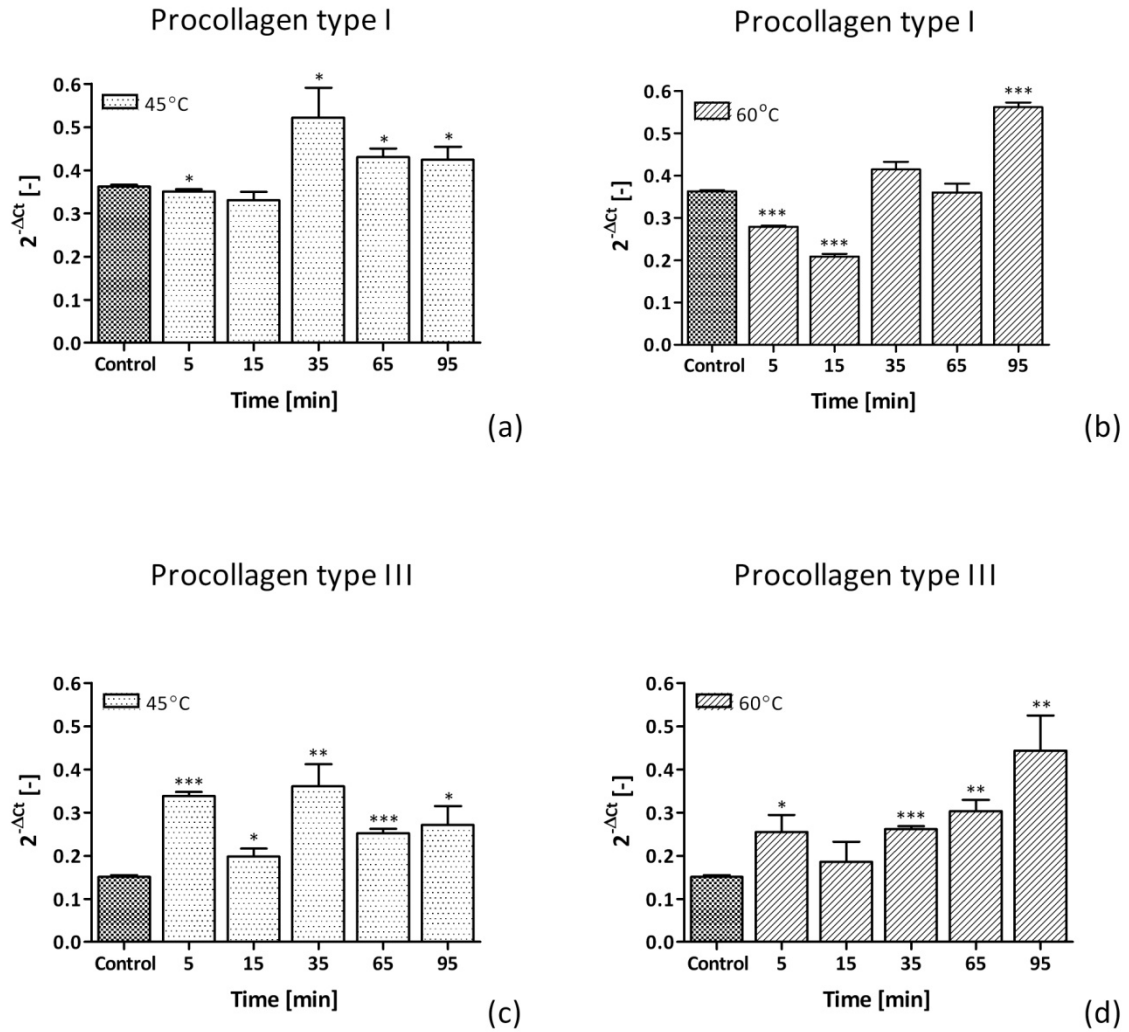


Figure 3.4: Relative quantity of procollagen type I and procollagen type III at the different time points after exposure to pulsed heat shocks. The control was kept at 37°C and the data are relative to the reference genes β -Actin and GAPDH. The x-axis depicts the control and the different points in time given in minutes. The y-axis shows the relative quantity of mRNA of procollagen type III and procollagen type I calculated with $2^{-\Delta Ct}$. Data are shown as the mean \pm SD for three independent experiments each run in duplo with significant differences compared to control at * $p < 0.05$, ** $p < 0.01$ and *** $p < 0.001$. (a) Procollagen type I after 45°C pulsed heat shocks. (b) Procollagen type I after 60°C pulsed heat shocks. (c) Procollagen type III after 45°C pulsed heat shocks. (d) Procollagen type III after 60°C pulsed heat shocks.

3.3.4 Effect of heat shocks on the expression of procollagen type I and III

The results of the 45°C and 60°C pulsed heat shocks on the expression of procollagen type I are shown in figures 3.4(a) and (b), respectively. A significant decrease in expression ($p < 0.001$) can be seen in the first 15 minutes after the 60°C pulsed heat shocks. After 35 minutes an increasing trend up to a significant increase in expression ($p < 0.05$) is noticed as presented in figure 3.4(b). The 45°C and 60°C pulsed heat shocks resulted in a significant increase after 35 minutes and 95 minutes, respectively. It is

noticed that these significant time points of upregulation are similar to the time points of upregulation of hsp47 for both heat shock temperatures (figures 3.3(c) and (d)).

Figures 3.4(c) and (d) depict the relative quantities of procollagen type III mRNA of the control and after heat shocks of 45°C and 60°C, respectively. Even after 5 minutes, there is a significant increase in expression at both heat shock temperatures. However, there is a clear distinction between the two groups: at later time points with a continuing increase in gene expression for 60°C heat shocked cells, but little trend with time for the 45°C heat shocked cells.

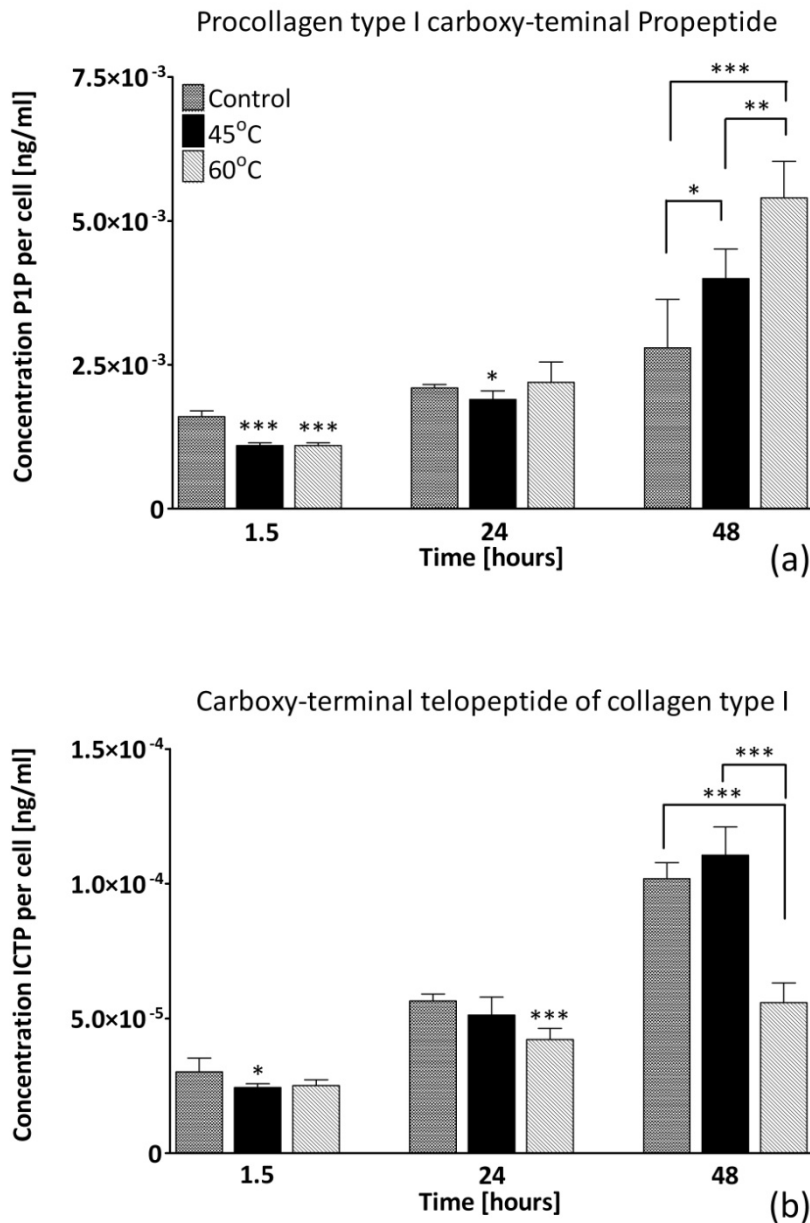


Figure 3.5: Absolute concentrations per cell of P1P (a) and ICTP (b) in culture medium. The x-axis depicts the time in hours and the y-axis the concentration per cell in ng/ml * $p < 0.05$, ** $p < 0.001$, and *** $p < 0.0001$ represent the significant differences between the heat shocked groups and the control group. Medium samples of the control group were obtained at similar time points, 90 minutes, 24 and 48 hours after culturing.

3.3.5 Effect heat shocks on collagen remodeling markers

The effects of the pulsed heat shocks on specific collagen remodeling markers for collagen synthesis (P1P) and degradation (ICTP) are shown in figure 3.5. The concentrations of P1P produced by the cells after the 45°C and the 60°C pulsed heat shocks increase with time and at 48 hours statistically significant higher values of P1P can be seen compared to the control values (figure 3.5a). It is worthy of note that the amount of P1P produced by the cells heat shocked at 60°C is also significantly higher compared to the amount of P1P produced after 45°C pulsed heat shocks ($p < 0.01$). This appears to be in agreement with the gene expression results that precede this protein synthesis.

Whereas the concentration of ICTP after the 45°C pulsed heat shocks at 24 hours are similar to control values, the corresponding values for 60°C heat shocks are statistically significantly lower (figure 3.5(b)). This trend is maintained at 48 hours. This significant increase and reduction of P1P and ICTP, respectively, results in higher net collagen content produced by cells being treated with the 60°C pulsed heat shocks compared to the net collagen content that is produced by the 45°C heat shocked cells and the control.

3.3.6 Immunofluorescence

Examination of the synthesis of collagen type I by immunofluorescent staining demonstrated more collagen type I formation after 48 hours by cells that underwent 60°C pulsed heat shocks (figure 3.6(c)) compared to the cells that were heat shocked at 45°C (figure 3.6(b)). It is noteworthy to point out that these findings are in agreement with the gene expression results and the results of the enzyme immune assays for P1P and ICTP.

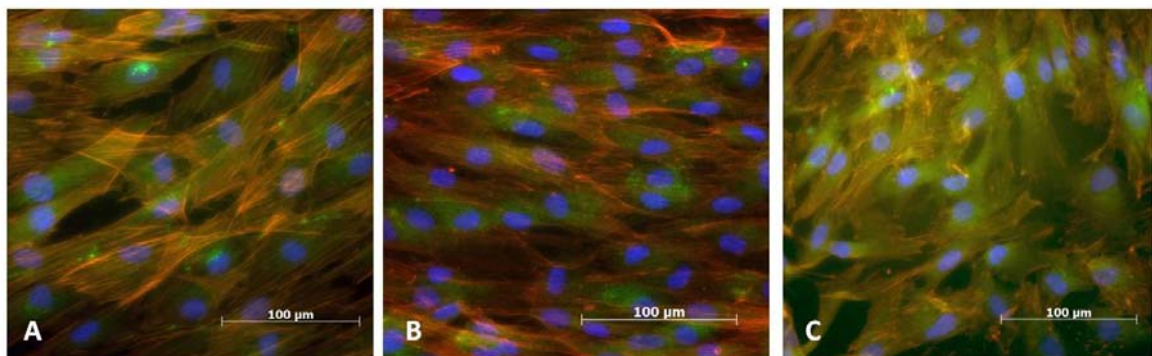


Figure 3.6: Immunofluorescent staining for collagen type I after 48 hours of the control group (a), 45°C heat shocked cells (b), and 60°C heat shocked cells (c). Green indicates collagen type I, red indicates the actin filaments (Phalloidin) of the cells and blue depicts the cell nuclei (DAPI).

3.4 Discussion

This study demonstrates that pulsed heat shocks stimulate the human dermal fibroblasts in-vitro to upregulate gene expression of procollagen type I and procollagen type III as an initial response. Our results show that the stimulation by the pulsed heat shocks at both heat shock temperatures, 45°C and 60°C, caused an upregulation in gene expression of procollagen type I and procollagen type III after 35 and 5 minutes respectively.

Procollagen type I expression has previously been shown to be upregulated after 3 hours by human dermal fibroblasts treated with repeated mild heat shocks of 30 minute duration at 41°C (Mayes and Holyoak, 2008). However, our results demonstrate, after application of short pulsed heat shocks of 45°C and 60°C, that an upregulation of procollagen type I can be noticed within 35 minutes. We have also found that the early response in upregulation of hsp47 of the cells to both heat shock temperatures, 45°C and 60°C, is similar to the early response in upregulation of procollagen type I. These findings are consistent with results shown in literature, which report that hsp47 has the ability to bind procollagen I for transportation to the Golgi system. Furthermore, it is stated that hsp47 takes an active role in the collagen type I synthesis (Naitoh et al., 2001; Tasab et al., 2000; Verrico et al., 2001). Therefore, our results substantiate that these physiological processes are initiated at a very early stage following thermal stimulation.

It is hypothesized that the effect of heat generation in the dermis would cause collagen denaturation and injury, which subsequently would lead to a wound healing response (Capon and Mordon, 2006). From this perspective, it is known that collagen type III is the first protein that will be deposited to heal the extracellular matrix. Subsequently, this protein will be replaced by collagen type I (Farber and Rubin, 1998). Therefore, to detect early extracellular matrix regeneration procollagen type I and III are effective biomarkers. Additionally, we hypothesize a differential expression with increasing time steps between the 45°C and the 60°C heat shocks. We suggest that the 60°C pulsed heat shocks would result in a more pronounced stimulation of the cells compared to the 45°C pulsed heat shocks. With regard to these findings, we suggest that the 60°C pulsed heat shocks have a beneficial effect in the process of regeneration of the collagen matrix. Rejuvenation is a complex physiological process that can be related to the complex physiology of wound healing. The complexity of these physiological pathways goes beyond our research; nevertheless, our results demonstrate that the heat shocks stimulate the cells into producing more collagen. Therefore, it is tempting to speculate that our findings are in accordance with a wound healing response, where first collagen type III is deposited and subsequently substituted by collagen type I, as our results have shown a direct upregulation of procollagen type III followed by an upregulation of procollagen type I after 35-95 minutes (figures 3.4(a-d)).

Besides quantification of collagen on gene expression level, specific collagen markers were investigated. Markers for collagen synthesis (P1P) and degradation (ICTP) were measured to provide insight in the effect of pulsed heat shocks on human dermal fibroblasts on the overall collagen turnover. Synthesis of collagen from their precursor molecules, procollagen, occurs by releasing procollagen propeptides (P1P). The balance between synthesis and degradation, the net collagen content, appeared to be dependent on the temperature of the pulsed heat shocks. Our results show that collagen synthesis is enhanced by pulsed heat shocks at both 45°C and 60°C (figure 3.5(a)). At the same time, the concentration of collagen degradation marker, ICTP, which is released upon cleavage of collagen by MMPs, was significantly lower than the control after pulsed heat shocks of 60°C, but did not differ from the control after pulsed heat shocks of 45°C (figure 3.5b). This shows that the stimulus of the 60°C pulsed heat shocks results in more collagen synthesis and less collagen degradation and therefore an enhanced amount of net collagen content than the 45°C heat shocked stimulus. The results of the immunofluorescent staining support these findings (figure 3.6).

As mentioned in the introduction heat shock protein 70 is routinely used as biomarker. Hsp70 indicates that the cells recognize the heat shock (Mayes and Holyoak, 2008; Rattan, 1998; Verbeke et al., 2007). Our results show by the increased levels of hsp70 mRNA that we have proven that both heat shock temperatures have evidently stimulated the cells, which is in accordance with other studies (Snoeckx et al., 2007; Verbeke et al., 2007). We observed strongly elevated mRNA levels even 5 minutes after the pulsed heat shock of 60°C and we cannot exclude the possibility that the mRNA levels would continue rising beyond the time of the experiment, namely 95 minutes. This rising trend remains to be established.

It has been reported that repeated mild heat shocks of 41°C for 60 minutes result in a decreased expression of hsp27 (Verbeke et al., 2007). We also observed a downregulation of hsp27 in 45°C heat shocked cells as well as in 60°C heat shocked cells, but in contrast to the mentioned study, our results of the expression at 60°C heat shocked cells after 95 minutes are not significantly different compared to the control values (figure 3.3(f)). Another study reports that hsp27 plays a role in protecting cells against apoptosis (Frank et al., 2004). We have observed that after a pulsed heat shock of 90°C, besides the obvious death of the cells after four days, hsp27 was strongly upregulated within 60 minutes (data not shown). Therefore, our findings imply that the heat shock temperatures, 45°C and 60°C, do not endanger the viability of the fibroblasts.

Repeated mild heat shocks of 41°C for 60 minutes do not influence the proliferation rate of the cells (Rattan, 1998). In our study, we did not observe any change in proliferation rate after the 45°C pulsed heat shocks. However, we have found that the influence of the heat shocks of 60°C for 2 seconds resulted in lower proliferation rate than that of

the control group and that of the cells heat shocked at 45°C (figure 3.1(a)). Taking the results of the viability curves and the metabolic activity into account, both in line with the results of the 45°C heat shocked cells and controls, a possible explanation for this difference is that the 60°C heat shocked cells use preferentially their energy to synthesize proteins as opposed to cell proliferation.

Only a few studies have investigated the response of human dermal fibroblasts to heat shocks. The temperature and duration that were chosen in those studies was 41°C and 60 minutes (Mayes and Holyoak, 2008; Rattan, 1998; Verbeke et al., 2007). To approach the heat shock duration of the rejuvenation methods used by dermatologists, such as the non-ablative laser techniques, we have chosen to apply heat shocks with a shorter duration. However, we are aware that the heat shock duration could play an important role in the response of the human dermal fibroblasts. The temperatures we have chosen also differ from these studies, because it is reported in literature that a characteristic temperature reached in the dermis after laser treatment is between 42 and 45°C (Verrico et al., 2001). In addition, a 60°C heat shock temperature was chosen, because it is known that this is a threshold temperature for protein denaturation (Ebling et al., 1992; Farber and Rubin, 1998). However, it should be recognised that changes in the parameters pulse duration and temperature could result in a different response of human dermal fibroblasts (Altshuler et al., 2007; Watanabe, 2008).

Heat shock response of human dermal fibroblasts induced by either laser treatments or pulsed heat shocks is poorly understood. In this study we have shown that an early detection of the cell response to pulsed heat shocks is possible. It is evident that the pulsed heat shocks of 60°C enable the dermal fibroblasts to reduce their proliferation rate without compromising their viability and metabolic activity. Furthermore, we have demonstrated that these short pulsed heat shocks of 45°C and 60°C cause an upregulation of procollagen type I as well as of procollagen type III. Moreover, we hypothesized a tendency difference in expression with increasing time steps between the 45°C and the 60°C heat shocks. Therefore, the 60°C pulsed heat shocks would result in a more pronounced stimulation of the cells compared to the 45°C pulsed heat shocks. In addition we have strengthened this hypothesis with the measurement of remodeling markers, where we have shown that the 60°C stimulus resulted in higher net collagen content (figure 3.5 and 3.6). With regard to these findings, it can be suggested that the 60°C pulsed heat shocks have, in the early stage of regeneration, a more substantial effect than the 45°C pulsed heat shocks in the process of regeneration of the collagen matrix.

Chapter 4

The effect of pulse duration of the heat shock on collagen type I by human dermal fibroblasts *in-vitro*

Abstract

The formation of wrinkles is associated with degeneration of the collagen matrix of the skin. For regeneration of the matrix fibroblasts need to be stimulated in producing new collagen. In this study, the effect of pulse duration of heat shocks on gene expression of procollagen type I, procollagen type III, hsp27, hsp47, and hsp70 and on expression of remodeling markers, P1P and ICTP, of human dermal fibroblasts *in vitro*, is investigated. Temperatures of 45°C and 60°C were used as heat shock temperatures which were exposed at times of 2, 4, 8, 10, 16, and 21 seconds. Proliferation rates, viability and metabolic activity were measured directly after the pulsed heat shocks and quantitative PCR was performed at three different time points after the heat shocks. Enzyme Immuno Assays were performed to determine the concentrations of P1P and ICTP. Results showed a decreased proliferation rate and severe cell loss after the 60°C heat shock. Gene expressions were upregulated in 45°C heat shocked cells. Remodeling marker analysis showed the largest net production of collagen by cells exposed to 45°C heat shocks for 8 to 10 seconds. It can be concluded that with short pulsed heat shocks it is possible to stimulate cells without traumatizing them to enhance new collagen formation.

The contents of this chapter are based on S.D. Dams, M.de Liefde-van Beest, A.M. Nuijs, C.W.J. Oomens, F.P.T. Baaijens. *Influence of pulse duration of heat shocks on collagen type I expression in human dermal fibroblasts. (submitted)*

4.1 Introduction

In skin rejuvenation dermal fibroblasts play an essential role in the active growth, development and repair of the skin. Fibroblasts are situated in the dermis. The dermis can be divided into the papillary dermis, situated directly under the epidermis, the top-layer that serves as the primary barrier against influences from the external environment (Lewis et al., 1994), and the reticular dermis, located between the papillary dermis and the hypodermis, which is the deeper layer and is involved in the wound healing and immune response (Farber and Rubin, 1998). The main component that defines the dermis is the extracellular matrix consisting of complexes of supportive proteins, such as collagen, elastin and proteoglycans, synthesized by dermal fibroblasts (Ebling et al., 1992; Geronemus, 2006).

Fibroblasts change with age with an increase in size, but a decrease in their mitotic and synthetic potential (Gilchrest, 2007a; Kurban and Bhawan, 2007; Ramos-e-Silva and da Silva Carneiro, 2007). Senescent fibroblasts lose their capability to replicate, due to a shortening of the telomere sequence, until it is no longer present. Then the capacity of the cell to replicate is lost (Gilchrest, 2007a; Gilchrest and Bohr, 2006).

The dermal components change as well with age. Collagen fibers become thicker and more susceptible to damage. Furthermore, after the age of 25 the collagen content of the dermis decreases 1% per year (Kurban and Bhawan, 2007; Ramos-e-Silva and da Silva Carneiro, 2007). Furthermore, elastic fibers decrease in number and fragment with age. The amount of ground substance, which is the amorphous material composed of proteoglycans, plasma constituents, metabolites, water, and ions present within the intracellular space, decreases with age (Gilchrest, 2007b; Kurban and Bhawan, 2007; Ramos-e-Silva and da Silva Carneiro, 2007). These changes contribute to the degradation of the underlying network of elastin and collagen fibers, resulting in wrinkling and sagging of the skin (Gilchrest, 2007b; Kurban and Bhawan, 2007).

UV radiation damages collagen fibers and causes accumulation of abnormal elastin. In response to this accumulation large amounts of metalloproteinases (MMPs) are produced (Gilchrest, 2007b; Gilchrest, 2007c; Ramos-e-Silva and da Silva Carneiro, 2007). The fibroblasts from the dermis are one of the major sources of matrix metalloproteinases after exposure to UV radiation. The normal function in this case is generally positive, namely to remodel the sun-injured tissue by manufacturing and reforming collagen. However, when following prolonged exposure to the sun, it is an imperfect damaging process, because some of the metalloproteinases produced by sunlight actually degrade collagen (Ebling et al., 1992; Gilchrest, 2007c). The result is an uneven formation of collagen fibers. Repetition of this imperfect skin remodeling causes wrinkles to form (Ebling et al., 1992; Gilchrest et al., 2007; Gilchrest, 2007c; Ramos-e-Silva and da Silva Carneiro, 2007; West, 2007; Yaar et al., 2007).

Rejuvenation of the skin aims at stopping or reversing of the features of aging. Although, this can also be achieved in the epidermis, the focus of the present work is on the dermis where the aim is to stimulate the fibroblasts to regenerate the aged collagen matrix. To renew the dermal matrix most rejuvenation techniques aim to induce thermal stress in the dermis. Among these methods, non-ablative techniques claim to induce dermal remodeling without global epidermal injury, using a thermal approach. The energy is applied as short nanosecond to millisecond pulses, or in a continuous wave resulting in a local temperature increase (Bjerring, 2006; Capon and Mordon, 2006; Geronemus, 2006; Sadick, 2006). The locally generated heat diffuses throughout the skin resulting in a temperature gradient (Altshuler et al., 2007). Through this inhomogeneous heating process of the skin, fibroblasts encounter heat shocks of different temperatures with different durations.

Heat shocks, which can be applied by various techniques, directly cause a heat shock response, HSR (Bjerring et al., 2006; Capon and Mordon, 2006). The HSR might induce temporary changes in cellular metabolism and might be responsible for the release and production of growth factors and increase the rate of cell proliferation. One of the changes is associated with a stimulated expression of heat shock proteins, which can play a major role in the inflammatory reaction process and wound healing (Capon and Mordon, 2006; Geronemus, 2006). Another physiological process that has been suggested is that the generation of heat causes collagen injury and contraction and subsequent repair of collagen injury by activating and recruiting fibroblasts (Geronemus, 2006).

The previous chapter has indicated that a pulsed heat shock of two seconds of both 45°C and 60°C can result in an increase of procollagen type I synthesis, preceded by an increase of procollagen type I gene expression, by human dermal fibroblasts *in-vitro* (Dams et al., 2010). Moreover, repeated mild heat shocks, with temperatures of 39°C up to 42°C and a duration of 30 minutes up to 1 hour, have beneficial effects on aged fibroblasts, resulting in an increase in procollagen type I and hsp47 and a decrease in the expression of hsp27 (Geronemus, 2006; Mayes and Holyoak, 2008; Rattan, 1998). Relevant heat shock proteins for skin regeneration are: (1) hsp70; a highly inducible protein that is overproduced when a cell encounters a swift change to a higher temperature (Bowers et al., 2007; Marshall and Kind, 2007; Ohtsuka and Laszlo, 2007; Snoeckx et al., 2007; Souil et al., 2001; Tandara et al., 2007), (2) hsp47; a constitutive protein that binds and transports procollagen from the endoplasmic reticulum to the Golgi system and plays an active role in collagen type I synthesis (Brown et al., 2007; Naitoh et al., 2001; Verrico and Moore, 1997), and (3) hsp27; a constitutive protein that when overexpressed can protect the cell from apoptosis when it encounters a heat shock (Frank et al., 2004; Hirano et al., 2004; Snoeckx et al., 2007). However, it must be taken into account that fibroblasts exposed to non-lethal heat shocks acquire a transient

resistance to such a heat challenge, a phenomenon termed thermotolerance (Ohtsuka and Laszlo, 2007).

Non-ablative rejuvenation techniques, based on inducing thermal stimuli, are already used extensively in clinical practice. However, the processes that are taking place as a result of skin treatment or the influences of the pulse duration in combination with the chosen temperature are still not fully understood. Thermal exposure times used in non-ablative devices vary from nanoseconds to minutes (Watanabe, 2008). Different settings in pulse duration and temperature are said to enable different treatments of skin rejuvenation (Capon and Mordon, 2006; Watanabe, 2008). The present research aims at exploring the effect of different pulse durations of heat shocks of 45°C or 60°C applied to human dermal fibroblasts.

The gene expression associated with procollagen type I and type III for human dermal fibroblasts exposed to pulsed heat shocks with different pulse durations is studied. Furthermore, heat shock proteins 70, 47 and 27 are used as biomarkers for respectively recognition of the heat shock, as a precursor for collagen synthesis, and for protection from apoptosis. In addition, to further examine the regeneration process, the temporal secretion of specific collagen remodeling markers is investigated, namely, collagen synthesis marker P1P (procollagen type I carboxy-terminal propeptide) and collagen degradation marker ICTP (carboxy-terminal telopeptide of type I), assuming such an increase in collagen synthesis is one of the required phenomena in skin rejuvenation (Bjerring et al., 2007; Capon and Mordon, 2006; Narurkar, 2007; White et al., 2007).

4.2 Materials and Methods

4.2.1 Cell culture

Human dermal fibroblasts from a 51 year old male (European Collection of Cell Cultures, Salsbury, United Kingdom) were grown in culture flasks (Nunc™, Roskilde, Denmark) at 37°C, 5% CO₂ and 95% humidity, in Dulbecco's advanced Modified Eagle's Medium (DMEM) (GIBCO, Invitrogen™, Breda, The Netherlands) supplemented with 10% fetal bovine serum (Greiner bio-one, Germany), 1% Glutamax (BioWhittaker™, Verviers, Belgium) and 0.1% Gentamycin (BioWhittaker™, Verviers, Belgium). When cell density reached near-confluency they were passaged in a 1:2 ratio. After four serial passagings the cells were seeded onto chamber slides (4 and 8 wells, Nunc™) and underwent heat shock treatments within 24 hours.

4.2.2 Heat shocks

For the heat shocks two temperatures were used; 45°C, which can be induced by non-ablative techniques (Capon and Mordon, 2006; Verrico et al., 2001; Verrico and Moore, 1997) and 60°C as a characteristic temperature for protein denaturation (Verrico and Moore, 1997). For each temperature six different pulse durations were chosen: 2, 4, 8,

10, 16 and 21 seconds. These durations were chosen based on our previous work on human *ex-vivo* skin (chapter 5 and 6). Heat shocks were applied by immersing the slides in 45°C or 60°C phosphated buffered saline (PBS) for the desired exposure time. After the heat shocks the wells were filled with 500 µl culture medium of 37°C.

The main experiment incorporated thirteen different test conditions: six different exposure times for each temperature and a control maintained at 37°C. Each test condition was measured at three points in time: 1.5, 24 and 48 hours. Growth and viability measurements were also performed after the 48 hours up to 7 days. Before and after the experimental procedure cell cultures were placed in the incubator. This experiment was carried out four independent times.

For each time point 500 µl of culture medium on the cells was removed and frozen at -80°C for subsequent measurement of remodeling markers procollagen type I C-peptide (P1P) and C-terminal telopeptide of collagen type I (ICTP). Cells were then collected by trypsinization at the different time points, resuspended in culture medium and centrifuged (1000 *g*, 5 minutes). Each time point the cell pellets were resuspended, for determining growth and viability curves, and stored at -80°C, for quantitative polymerase chain reaction (qPCR) analysis. Additionally, one chamber slide per time point was fixed with 10% formalin for 10 minutes and subsequently washed and stored in PBS at 4°C for subsequent immunofluorescence analysis.

4.2.3 Determination of the growth rate and viability of the cells

Growth rate and viability of the fibroblasts were determined by harvesting the cells for counting at several time points; before and directly after the heat shocks to determine detachment of cells, and at $t = 1.5$ h, 1 day, 2, 5 and 7 days after the heat shocks. Until harvesting, the cells were kept under standard culture conditions with refreshments of culture medium every other day. After harvesting at each time point, the total number of cells, C_t , and number of non-viable cells, C_{nv} , were counted. Counting of the cells was performed using the Nucleocounter™ (Chemometec, Allerød, Denmark) following the protocol of the manufacturer. The growth rate was assessed using the average C_t per time point. The viability, percentage of living cells, was calculated from C_t and C_{nv} .

4.2.4 Determination of the metabolic activity of the cells

Cells were used directly after the heat shocks to determine the metabolic activity, using the 3-[4,5-dimethylthiazol-2-yl]-2,5-diphenyl tetrazolium bromide (MTT) based *in vitro* toxicology assay kit (Sigma, Breda, Nederland). Per well 150 µl MTT solution (M 5655, Sigma, Breda, The Netherlands) was added immediately and the chamber slides were placed at 37°C for 45 minutes. Metabolically active cells cleaved the molecules of the MTT solution resulting in precipitation of formazan crystals. Subsequently, 150 µl solubilization solution (M 8910, Sigma, Breda, The Netherlands) was added to each well and the slides were placed on a shaker (Titramax 1000, Heidl Instruments, Germany) at 300 rpm for a further 30 minutes, dissolving the crystals in acidified isopropanol

resulting in a purple solution. Absorbance was spectrophotometrically measured at a wavelength of 570 nm (Biotek Synergy, Beun de Ronde, The Netherlands).

4.2.5 Determination of gene expression levels of heat shock proteins 27, 47, 70 and procollagen type I and III

For qPCR analysis total RNA was isolated using RNeasy kit (Qiagen, Venlo, The Netherlands) using the manufacturer's protocol. The concentration and purity of the total RNA was determined at OD 260/280 nm measurements (Nanodrop, Isogen, The Netherlands). RNA integrity was assessed using gel-electrophoresis. Random primers and 225 ng RNA were used for cDNA synthesis using M-MLV reverse transcriptase (Invitrogen™, Breda, The Netherlands). Gene expression analysis was performed on an iCycler Real-Time PCR detection system (Biorad, Veenendaal, The Netherlands) using iQ™ SYBR®-Green supermix (Biorad, Veenendaal, The Netherlands). Primers for hsp27, hsp47, hsp70 and procollagen type I and III were used as by Dams *et al.* (Dams et al., 2010). Results were normalized using reference genes β -Actin and GAPDH, obtained from Primerdesign (South Hampton, U.K.). Fold changes, $2^{-\Delta\Delta Ct}$, were calculated manually.

4.2.6 Determination of collagen type I remodeling markers

Concentrations of the markers for collagen synthesis, P1P, and collagen degradation, ICTP, were determined in the culture medium by means of enzyme immuno assays (EIA). P1P was measured using a procollagen type I C-peptide EIA kit (Takara Bio, Otsu, Shiga, Japan). ICTP was determined using a quantitative enzyme immunoassay designed for in vitro measurement of carboxy-terminal cross-linked telopeptide of human type I collagen (Orion Diagnostica, Espoo, Finland). Each assay was performed according to the recommendations of the suppliers. The assays were performed on the acquired medium samples. The EIA data were normalized to their corresponding amount of cells, resulting in concentration P1P and ICTP per cell.

4.2.7 Immunofluorescence

To study the synthesis of collagen type I by the HDFs after the applied pulsed heat shocks immunofluorescent staining with an antibody for collagen type I (Sigma Aldrich, Breda, The Netherlands) was used. The actin filaments of the cells were stained with Phalloidin-TRITC (Sigma, Breda, The Netherlands) and the cell nuclei with DAPI (Sigma, Breda, The Netherlands). The results were visualized with fluorescence microscopy at room temperature (Axiovert 200M, Zeiss B.V., Göttingen, Germany) with a 20× objective (Zeiss LD ACHROPLAN) and a NA of 0.4. A Zeiss AxioCam HRM Camera was used together with Zeiss AxioVision Rel. 4.8 acquisition software to take representative images.

4.2.8 Statistical analysis

Data are presented as mean \pm standard deviation (SD) for a sample measurement of $n = 4$. Comparisons between the control and the experimental groups were performed using

a two-tailed *t*-test. Differences were considered to be significant at $p < 0.05$. Furthermore, differences between groups were tested by using analysis of variances followed by a Dunnett's multiple comparison tests. Groups were considered to be different at $p < 0.05$.

4.3 Results

4.3.1 Human dermal fibroblast proliferation and viability

The proliferation rate of cells exposed to the different heat shocks is depicted in figure 4.1(a).

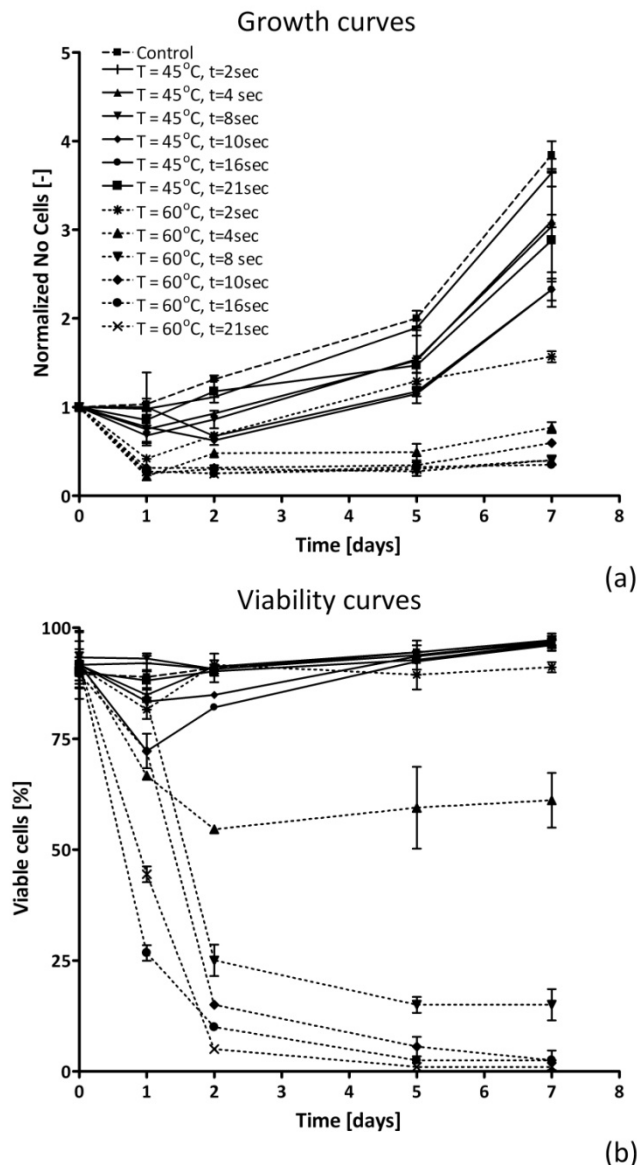


Figure 4.1: Growth rate and viability curves of human dermal fibroblasts after exposure to different pulsed heat shocks; the control was kept at 37°C. (a) Growth curves. The x-axis depicts the time in days and the y-axis shows the number of cells normalized to their begin situation. The error bars at each point are calculated standard deviations ($n = 4$). Note: the severe cell loss at the 60°C heat shocked cells cultures. (b) Viability curves. The x-axis depicts the time in days and the y-axis shows the viability, percentage of living cells, calculated from C_t and C_{nv} . The error bars at each point are calculated standard deviations ($n = 4$). Note: the decreased viability of the 60°C heat shocked cells.

The number of cells per measurement point is normalized to the number of cells prior to the heat shock. The growth rate of the control is shown as the black dashed line. The 45°C heat shocks, as depicted by the black solid lines (figure 4.1(a)), cause a slightly lower proliferation rate of the cells than the control cells. By contrast the growth curves of the cells heat shocked at 60°C for more than 2 seconds reveal severe cell loss, as indicated by the black dotted lines in figure 4.1(a).

Figure 4.1(b) indicated the calculated viability of the control and the heat shocked cells. The viability of the 45°C heat shocked cells was similar to the control group for all exposure times. The 60°C heat shocked cells indicate that pulse durations beyond 4 seconds, result in a decrease in viability to less than 25%. After an exposure time of 4 seconds approximately 50% of cells survive. The percentage of viable cells after a 2 second heat shock of 60°C is shown to be slightly lower, approximately 90%, compared to control values (96-98%).

4.3.2 Influence of heat shock exposure time on metabolic activity

The complete results of the metabolic activity of the cells per test condition per measurement point of both heat shock temperatures are depicted in table 4.1. Absorption values are normalized to the corresponding amount of cells. An overview of this data can be visualized with the color scale indicated in figure 4.2. White depicts no difference compared to the corresponding control situation. A color scale of 5 steps is used to distinguish the differences between the groups. The shades of colors that are assigned to the different measurement points are based on the values from table 4.1. It can be seen that beyond an exposure time of 16 seconds for the 45°C heat shocked cells the metabolic activity of all cells is extremely low compared to the control values.

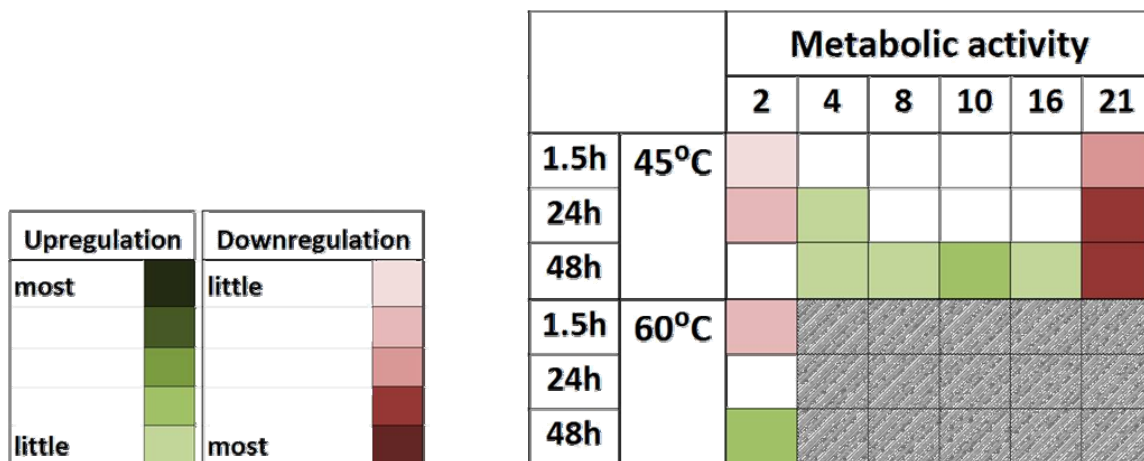


Figure 4.2: The color scale visualization of the metabolic activity of human dermal fibroblasts after exposure to the different heat shock conditions based on the data from table 4.1. The data were normalized to the control situation; the control was kept at 37°C. White depicts no difference compared to the corresponding control situation. Light up to dark green indicates more to extensively more metabolically active cells than the control. Light up to dark red depicts a lower to extremely lower metabolic activity compared to the corresponding control. Grey depicts the removed time points. Note: the absorption is proportional to the metabolic activity.

Up to an exposure time of 16 seconds, on the other hand, the metabolic activity increases with time and after 48 hours heat shock of 45°C result in an upregulation of metabolic activity compared to controls.

Given the extreme cell loss in the cases where the cells were exposed to 60°C for more than 2 seconds (figure 4.1(b)) we conclude that results on metabolic activity and gene expression of the few remaining cells were not relevant. Therefore, we decided to remove these data from further analyses and assigned them the color grey.

4.3.3 Gene expression of heat shock proteins 27, 47 and 70

In figure 4.3 the gene expressions of heat shock proteins, hsp70, hsp47 and hsp27 are depicted on the color scale, with white indicating no difference compared to the control group. The shades of colors that are assigned to the different time points are based on the values from table 4.1. Per gene, a color scale of 5 steps is used to distinguish the differences between the groups.

		Heat shock protein 70					Heat shock protein 47					Heat shock protein 27								
		2	4	8	10	16	21	2	4	8	10	16	21	2	4	8	10	16	21	
1.5h	45°C	Light Green	Light Green	Light Green	Light Green	Light Green	Light Green	Light Green	Light Green	Light Green	Light Green	Light Green	Light Green	Light Green	Light Green	Light Green	Light Green	Light Green	Light Green	Light Green
24h		Light Green	Light Green	Light Green	Light Green	Light Green	Light Green	Light Green	Light Green	Light Green	Light Green	Light Green	Light Green	Light Green	Light Green	Light Green	Light Green	Light Green	Light Green	Light Green
48h		Light Green	Light Green	Light Green	Light Green	Light Green	Light Green	Light Green	Light Green	Light Green	Light Green	Light Green	Light Green	Light Green	Light Green	Light Green	Light Green	Light Green	Light Green	Light Green
1.5h	60°C	Grey	Grey	Grey	Grey	Grey	Grey	Grey	Grey	Grey	Grey	Grey	Grey	Grey	Grey	Grey	Grey	Grey	Grey	Grey
24h		Grey	Grey	Grey	Grey	Grey	Grey	Grey	Grey	Grey	Grey	Grey	Grey	Grey	Grey	Grey	Grey	Grey	Grey	Grey
48h		Grey	Grey	Grey	Grey	Grey	Grey	Grey	Grey	Grey	Grey	Grey	Grey	Grey	Grey	Grey	Grey	Grey	Grey	Grey

Figure 4.3: Visualization of the differences in fold changes compared to the control of heat shock protein 70, heat shock protein 47 and heat shock protein 27 at the different time points after exposure to the heat shocks with pulse durations of 2, 4, 8, 10, 16 and 21 seconds based on the data of table 4.1. The data are relative to the reference genes β -Actin and GAPDH. White indicates no difference compared to the control situation. Light green up to dark green corresponds to a little to an extensive upregulation. Light red up to dark red indicates slight to severe downregulation. Grey depicts the removed time points.

The upregulated gene expression of the 45°C heat shock cells generally returned to control levels within 48 hours for all exposure times, indicating that these gene expressions have reached the highest upregulation between 1.5 and 48 hours. Two exceptions to this trend are the gene expressions of hsp70 and hsp47 for the cells exposed to 45°C for more than 10 seconds, which are still upregulated after 48 hours. Furthermore, extensive upregulation for hsp47 is noticed in cells heat shocked with 45°C with exposure time ranging from 4-10 seconds. Additionally, an increase in upregulation of hsp 27 coinciding with an increase in exposure time is seen at 24 hours in cells after exposure to 45°C. In case of the 2 second 60°C heat shocked cells, all genes remain upregulated at 48 hours. Extensive upregulation of hsp70 is noticed already after 24 hours and is continued at 48 hours.

Table 4.1: I: Metabolic activity; The absorption values per cell of the metabolic activity test of all test conditions. Values are normalized to the corresponding control values and depicted as the mean \pm standard deviation (n = 4). II: Gene expression heat shock proteins; The fold change of heat shock proteins 70, 47 and 27 of all the test conditions. Data are relative to the reference genes β -Actin and GAPDH. Values shown as mean \pm standard deviation (n = 4). III: Gene expression procollagen; The fold change of procollagen type I and type III of all the test conditions. Data are relative to the reference genes β -Actin and GAPDH. Values shown as mean \pm standard deviation (n = 4). IV: Remodeling markers; Concentrations P1P and ICTP per cell of all test conditions. Values are normalized to the corresponding control values and depicted as the mean \pm standard deviation (n = 4).

Absorption per cell [-]	Metabolic activity																		
	2		4		8		10		16		21								
	1.5h	2.4h	1.5h	2.4h	1.5h	2.4h	1.5h	2.4h	1.5h	2.4h	1.5h	2.4h							
I 45°C	0.89 ± 0.07	0.74 ± 0.66	0.61 ± 0.5	0.73 ± 0.38	0.63 ± 0.33	0.39 ± 0.06	0.76 ± 0.03	1.18 ± 0.09	0.97 ± 0.12	1.10 ± 0.15	0.72 ± 0.09	0.26 ± 0.03	0.99 ± 0.10	1.13 ± 0.08	1.24 ± 0.06	1.9 ± 0.09	1.21 ± 0.05	0.57 ± 0.10	
60°C	0.63 ± 0.07																		
1.5h	1.14 ± 0.19																		
2.4h	1.77 ± 0.05																		
Fold change \pm SD																			
Heat shock protein 70																			
II 45°C	6.11 ± 0.45	2.85 ± 0.06	3.70 ± 0.28	2.12 ± 0.31	3.04 ± 0.20	3.29 ± 0.22	2.88 ± 0.19	2.99 ± 0.15	2.93 ± 0.09	1.02 ± 0.34	1.44 ± 0.47	1.12 ± 0.37	1.28 ± 0.31	0.93 ± 0.29	0.83 ± 0.25	0.78 ± 0.31	1.11 ± 0.17	1.22 ± 0.26	
2.4h	6.44 ± 0.26	5.22 ± 0.28	6.75 ± 0.31	5.68 ± 0.28	13.14 ± 0.68	7.00 ± 0.59	22.89 ± 0.42	30.66 ± 3.61	39.4 ± 5.13	27.2 ± 3.22	4.83 ± 1.94	3.48 ± 1.94	3.27 ± 0.23	4.00 ± 0.15	4.83 ± 0.75	4.20 ± 0.06	27.27 ± 0.98	26.04 ± 0.79	
4.8h	0.83 ± 0.26	0.89 ± 0.24	0.85 ± 0.25	0.99 ± 0.13	6.28 ± 0.22	2.39 ± 0.26	1.15 ± 0.17	1.13 ± 0.17	0.94 ± 0.08	0.98 ± 0.06	9.44 ± 3.27	4.1 ± 0.35	0.95 ± 0.08	0.95 ± 0.29	1.03 ± 0.06	1.02 ± 0.3	0.99 ± 0.34	0.79 ± 0.22	
1.5h	7.35 ± 1.00						2.53 ± 0.30						2.38 ± 0.15						
2.4h	67.07 ± 3.30						1.95 ± 0.05						4.66 ± 0.10						
4.8h	104.88 ± 12.0						1.73 ± 0.24						4.29 ± 0.20						
Fold change \pm SD																			
Collagen type I																			
III 45°C	4.52 ± 0.26	2.87 ± 0.17	1.94 ± 0.28	2.11 ± 0.43	1.12 ± 0.26	1.11 ± 0.28	40.83 ± 3.01	17.16 ± 2.40	5.89 ± 1.36	1.63 ± 0.35	1.59 ± 0.19	1.06 ± 0.11	7.29 ± 0.29	8.97 ± 0.26	12.9 ± 0.22	11.06 ± 1.32	11.64 ± 0.30	10.07 ± 0.39	23.42 ± 3.20
2.4h	1.12 ± 0.19	0.98 ± 0.06	0.99 ± 0.05	1.16 ± 0.18	0.96 ± 0.42	0.81 ± 0.26	1.04 ± 0.50	0.91 ± 0.10	1.03 ± 0.17	1.04 ± 0.12	0.96 ± 0.25	0.99 ± 0.10	1.12 ± 0.19	0.98 ± 0.06	0.99 ± 0.05	1.16 ± 0.18	0.96 ± 0.42	0.81 ± 0.26	1.04 ± 0.50
4.8h	2.02 ± 0.33						2.6 ± 0.58						2.09 ± 0.18						2.6 ± 0.58
1.5h	2.09 ± 0.18						1.01 ± 0.01						2.09 ± 0.18						1.01 ± 0.01
2.4h	2.03 ± 0.18						0.48 ± 0.17						2.03 ± 0.18						0.48 ± 0.17
Fold change \pm SD																			
Collagen type III																			
IV 45°C	0.67 ± 0.03	0.77 ± 0.08	1.22 ± 0.01	1.32 ± 0.01	0.44 ± 0.02	0.54 ± 0.02	0.81 ± 0.05	0.51 ± 0.05	0.40 ± 0.05	0.37 ± 0.03	0.44 ± 0.01	1.27 ± 0.28	0.91 ± 0.04	1.00 ± 0.04	1.21 ± 0.04	1.67 ± 0.08	1.16 ± 0.08	0.64 ± 0.06	0.91 ± 0.12
2.4h	1.21 ± 0.10	2.10 ± 0.09	1.23 ± 0.11	1.26 ± 0.04	0.78 ± 0.02	0.39 ± 0.05	1.09 ± 0.10	0.42 ± 0.05	0.47 ± 0.05	0.54 ± 0.06	0.41 ± 0.08	0.30 ± 0.3	1.21 ± 0.10	2.10 ± 0.09	1.23 ± 0.11	1.26 ± 0.04	0.78 ± 0.02	0.39 ± 0.05	1.09 ± 0.10
4.8h	0.68 ± 0.03						0.83 ± 0.07						0.68 ± 0.03						0.83 ± 0.07
1.5h	1.03 ± 0.17						0.75 ± 0.07						1.03 ± 0.17						0.75 ± 0.07
2.4h	1.66 ± 0.06						0.55 ± 0.07						1.66 ± 0.06						0.55 ± 0.07
4.8h																			
Fold change \pm SD																			
ICTP																			
Concentration per cell [ng/ml]																			
II 45°C	0.67 ± 0.03	0.77 ± 0.08	1.22 ± 0.01	1.32 ± 0.01	0.44 ± 0.02	0.54 ± 0.02	0.81 ± 0.05	0.51 ± 0.05	0.40 ± 0.05	0.37 ± 0.03	0.44 ± 0.01	1.27 ± 0.28	0.91 ± 0.04	1.00 ± 0.04	1.21 ± 0.04	1.67 ± 0.08	1.16 ± 0.08	0.64 ± 0.06	0.91 ± 0.12
2.4h	1.21 ± 0.10	2.10 ± 0.09	1.23 ± 0.11	1.26 ± 0.04	0.78 ± 0.02	0.39 ± 0.05	1.09 ± 0.10	0.42 ± 0.05	0.47 ± 0.05	0.54 ± 0.06	0.41 ± 0.08	0.30 ± 0.3	1.21 ± 0.10	2.10 ± 0.09	1.23 ± 0.11	1.26 ± 0.04	0.78 ± 0.02	0.39 ± 0.05	1.09 ± 0.10
4.8h	0.68 ± 0.03						0.83 ± 0.07						0.68 ± 0.03						0.83 ± 0.07
1.5h	1.03 ± 0.17						0.75 ± 0.07						1.03 ± 0.17						0.75 ± 0.07
2.4h	1.66 ± 0.06						0.55 ± 0.07						1.66 ± 0.06						0.55 ± 0.07
4.8h																			

4.3.4 Gene expression of procollagen type I and III

A similar color scale is used to show the gene expression of procollagen type I and III for all time points as illustrated in figure 4.4. The different shades of colors that are assigned to the different values of each time point are based on the values from table 4.1. After exposure to heat shock of 45°C for each of the pulse durations, there is a maximum upregulation for both procollagen types I and III gene expression at 24 hours. Subsequent gene expression decreases to values similar to control by 48 hours. In contrast to the shorter exposure times, procollagen type III gene expression of cells exposed to 45°C beyond 10 seconds is extensively upregulated. The results of the 2 seconds at 60°C heat shocked cells show a different pattern, with procollagen type I being upregulated within 1.5 hours and remaining upregulated after 48 hours. Procollagen type III gene expression, on the other hand, starts with upregulation at 1.5 hours and within 48 hours this gene is downregulated.

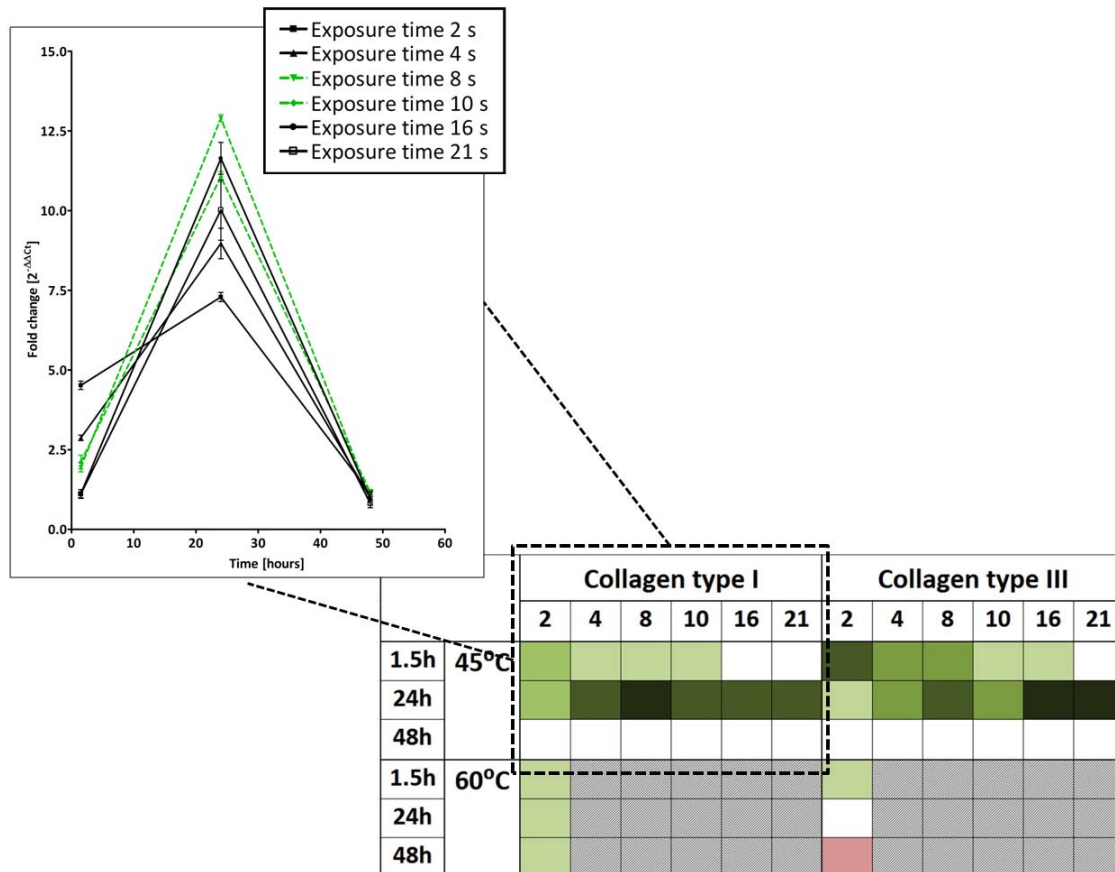


Figure 4.4: Visualization of the differences in fold changes of procollagen type I and procollagen type III compared to the control at the different time points after exposure to pulsed heat shocks with pulse durations of 2, 4, 8, 10, 16 and 21 seconds based on the values from table 4.1. The data are relative to the reference genes β -Actin and GAPDH. White indicates no difference compared to the control situation. Light green up to dark green corresponds to a little to an extensive upregulation. Light red up to dark red indicates slight to severe downregulation. Grey depicts the removed time points.

4.3.5 Effect of pulse duration on collagen remodeling markers

The effect of the different pulse durations of the 45°C and 60°C heat shocks on the remodeling markers P1P, synthesis, and ICTP, degradation, are depicted in figure 4.5. The same color scale is used for visualization of the data as for the gene expression results. All concentrations at all time points are normalized to their corresponding amount of cells, resulting in concentrations P1P and ICTP per cell. The five different shades of green and red that are assigned to the different time points are based on the values from table 4.1.

From the ICTP concentrations, it can be seen that the degradation of collagen type I is overall less compared to the control group. The concentration of P1P, and thus collagen synthesis, after the heat shocks of 45°C with exposure time up to 10 seconds, on the other hand, is shown to be significantly higher than the control situation after 48 hours ($p < 0.001$). The 2 second heat shock of 60°C also shows a higher concentration P1P after 48 hours. Exposure times beyond 10 seconds lead to a much lower concentration of P1P, compared to the control.

		P1P						ICTP					
		2	4	8	10	16	21	2	4	8	10	16	21
1.5h 24h 48h	45°C	Light red	Dark red	Light green	Light green	Dark red	Light red	Light red	Dark red	Dark red	Dark red	Dark red	White
		Light red	White	Light green	Light green	Light green	Light red	Light red	Light red	Dark red	Dark red	Light red	Light red
		Light green	Dark green	Light green	Light green	Light red	Dark red	Light green	Dark red	Dark red	Dark red	Dark red	Dark red
1.5h 24h 48h	60°C	Light red	Grey	Grey	Grey	Grey	Grey	Light red	Grey	Grey	Grey	Grey	Grey
		Light green	Grey	Grey	Grey	Grey	Grey	Light red	Grey	Grey	Grey	Grey	Grey
		Light green	Grey	Grey	Grey	Grey	Grey	Dark red	Grey	Grey	Grey	Grey	Grey

Figure 4.5: Color scale visualization of the concentrations per cell of P1P and ICTP in culture medium based on the data from table 4.1. The data were normalized to the control situation; the control was kept at 37°C. White depicts no difference compared to the corresponding control situation. Light up to dark green indicates more to extensively more P1P or ICTP compared to the control. Light up to dark red depicts a lower to extremely lower concentration of P1P or ICTP compared to the corresponding control. Grey depicts the removed time points.

4.3.6 Immunofluorescence

Immunofluorescent staining of the cells heat shocked with 45°C and 60°C for 10 and 4 seconds, respectively, and control cells are shown in figure 4.6. Red depicts the actin filaments of the cells, blue the nuclei and green indicates collagen type I. Examination of the synthesis of collagen type I, using this staining, demonstrated more collagen type I formation after 48 hours by cells that underwent 45°C heat shocks (figure 4.6(b)), compared to the control cells that were maintained at 37°C (figure 6(a)). In agreement

with the remodeling marker data (figure 4.5), the immunostaining of the cells exposed for 10 seconds to 45°C show more expression. Figure 4.6c shows that the heat shock of 60°C severely disrupted the cytoskeleton of the cells as indicated by the arrows.

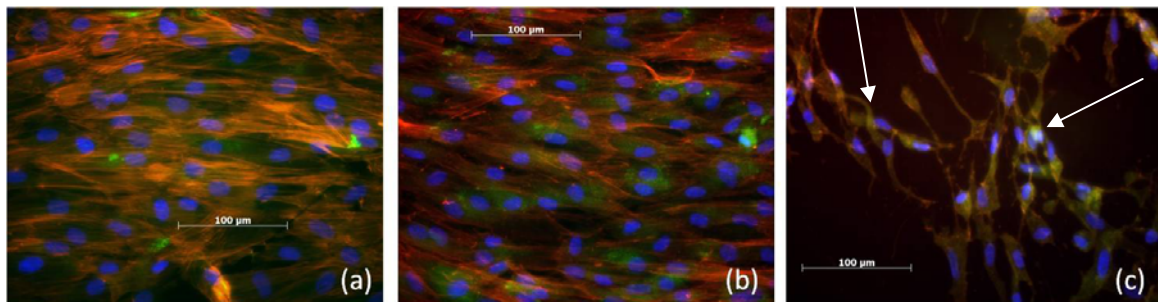


Figure 4.6: Immunofluorescent staining for collagen type I after 48 hours of the control (a) cells exposed to a 45°C heat shock for 10 seconds (b), and cells exposed to a 60°C heat shock for 4 seconds (c). Green indicates collagen type I, red indicates the actin filaments (Phalloidin) of the cells and blue depicts the cell nuclei (DAPI). Note: the lower cell density and the degradation of the actin filaments after a 60°C heat shock.

4.4 Discussion

This study demonstrates that heat shocks of 45°C for 8 to 10 seconds applied to human dermal fibroblasts *in-vitro* result in the highest amount of net collagen content (figure 4.5). These high levels of collagen type I are shown to be preceded by upregulation of procollagen type I gene expression (figure 4.4).

Procollagen type I expression has previously been shown to be upregulated very shortly after short pulsed heat shocks (Dams et al., 2010). The present study also demonstrates an early upregulation of procollagen type I. Moreover, it is noticed that gene expression of procollagen type I by cells, exposed to 45°C for all exposure times, has returned to the level of the control situation at 48 hours, indicating that the highest upregulation must have occurred between 1.5 and 48 hours. A similar trend was also observed for the gene expression of hsp47. Since hsp47 has the ability to bind procollagen I for transportation to the Golgi system and takes an active role in the collagen type I synthesis (Dams et al., 2010; Naitoh et al., 2001; Tasab et al., 2000; Verrico and Moore, 1997), it can be suggested that our findings are consistent with this physiological process.

Apart from quantification of collagen on gene expression level, markers for collagen synthesis (P1P) and degradation (ICTP) were measured to provide more understanding in the effect of heat shocks on the collagen metabolic balance. Procollagen propeptides (P1P) are cleaved from procollagen, which is a precursor molecule, during synthesis of collagen type I. The balance between synthesis and degradation, resulting in the net collagen content, clearly depends on the temperature and pulse duration of the heat shocks. Our results suggest that collagen type I synthesis is highest after heat shocks of 45°C of 8 to 10 seconds. For the same exposure times at 45°C the concentration of collagen degradation marker, ICTP, which is released upon cleavage of collagen by

MMPs, was significantly lower than the control (figure 4.5). This results in the highest amount of net collagen after treatment 45°C for 8 and 10 seconds. In addition, our findings demonstrated that the 45°C heat shock induces a 24 hour upregulation of procollagen type III.

Heat shock protein 70 is used as biomarker to indicate that the cells recognize the heat shock (Mayes and Holyoak, 2008; Rattan, 1998; Verbeke et al., 2007). It is clear from the expression of hsp70 that we have demonstrated that both heat shock temperatures can stimulate the fibroblasts, which is in accordance with other studies (Snoeckx et al., 2007; Verbeke et al., 2007). However, it is noticed that the expression of hsp70 by the cells after being exposed to 45°C beyond 10 seconds remains upregulated. A similar trend is noticed for the gene expression of hsp47. We suggest that a 45°C heat shock with an exposure time beyond 10 seconds has a traumatizing effect on the cells, which results in a negative response in collagen production of these cells.

The gene expression of hsp27 after the 45°C heat shocks is upregulated at 24 hours and an increasing upregulation is seen with increasing exposure times. However, after 48 hours the gene expressions have returned to the control level, meaning that those cells are no longer compromised.

A previous study reported that repeated mild heat shocks of 41°C for 60 minutes did not influence the proliferation rate of the cells (Rattan, 1998). In the present study, no significant changes in proliferation rate were observed after the 45°C heat shocks either (figure 4.1(a)).

The procollagen type III gene expression by cells exposed to the 60°C heat shock returned to control levels at 24 hours and was subsequently downregulated at 48 hours. However, these cells continue upregulating procollagen type I at 48 hours. We have found that the influence of the heat shocks of 60°C for exposure times beyond 2 seconds resulted in lower proliferation rate than that of the control group (figure 4.1(a)). A similar trend was evident with the viability, which decreases to 10%-50% within 2 days. Accordingly, any further analysis was considered only to reflect severe cell loss as opposed to temperature changes due to heat shocks.

The effect of heat generation in the dermis is thought to cause collagen denaturation and injury, leading to a wound healing response (Capon and Mordon, 2006). From this perspective it is known that collagen type III is the first protein that will be deposited to heal the extracellular matrix. Subsequently, this protein will be replaced by collagen type I (Farber and Rubin, 1998). Therefore, to detect early extracellular matrix regeneration procollagen type I and III are effective biomarkers. Rejuvenation is a complex physiological process that, assuming that an increase in collagen synthesis is one of the desired phenomena, can be related to the intricate physiology of wound healing. The complexity of these physiological pathways is beyond the scope of our research;

nevertheless, our results demonstrate that the heat shocks stimulate the cells into producing more collagen.

There are clear differences in the physiological processes activated during stimulation at the two temperatures. Hypothetically, it can be suggested that with the 45°C heat shock the cells are mildly stimulated, while at 60°C the cells are damaged, as demonstrated by our immunofluorescent staining results, where a severely compromised cytoskeleton can be seen (figure 4.6c). Additionally, our gene expression results of hsp27, a damage marker, reveal a continuous upregulation after the heat shock of 60°C, which supports our suggestion. This does not mean, however, that 60°C pulses cannot be useful in practice. It is clear that at a local level cells are damaged, but in *in-vivo* skin this will trigger a wound healing response that may also be beneficial for rejuvenation.

These findings are based on *in-vitro* cell cultures. However, the response of cells in a three dimensional environment in skin may be different. Therefore, for future research this study should be extended towards ex-vivo or in-vivo skin studies. Moreover, in this study only temperatures of 45°C and 60°C were used. However, after our findings of severe cell loss at 60°C, investigating temperatures in between 45°C and 60°C might prove an interesting avenue of future research.

Chapter 5

The effect of thermal stimuli on dermal fibroblast in *ex-vivo* human skin

Abstract

Background: Well-known characteristics of aging skin are the development of fine lines and wrinkles, but also changes in skin tone, skin texture, thickness and moisture content are features of aging. Rejuvenation of the skin aims at reversing the signs of aging and can be established in the epidermis as well as in the dermis. In addition, aged dermis has a degenerated collagen matrix. To regenerate this matrix, fibroblasts need to be stimulated into synthesizing new collagen. **Aims:** In this study, the effects of heat shocks of different temperatures on human dermal fibroblasts in *ex vivo* skin on the expression of procollagen 1, procollagen 3, hsp27, hsp47, and hsp70 are investigated. **Materials & Methods:** The heat shocks were applied on *ex-vivo* skin samples by immersing the samples in heated PBS at 45°C or 60°C. Metabolic activity was measured and, at similar time points, propidium-iodide-calcein staining was performed to establish cell viability. Quantitative PCR was performed after the heat shock to determine gene expression levels relative to the reference temperature. Furthermore, PicroSirius Red and Haematoxylin stainings were performed to visualize the collagen network and the cells. **Results:** The skin samples appeared to be viable and metabolically active. Histology demonstrated that the heat shocks did not influence the structure of the collagen network or cell appearance. Quantitative PCR results showed that, in contrast to the 45°C heat shock, the 60°C heat shock resulted in significant upregulations of procollagen type I and III, Hsp 70 and Hsp47. **Conclusion:** A 60°C heat shock stimulates the human dermal fibroblasts in *ex-vivo* skin to upregulate their procollagen type I and type III expression.

The contents of this chapter are based on S.D. Dams, M. de Liefde-van Beest, A.M. Nuijs, C.W.J.Oomens, F.P.T. Baaijens. *Heat shocks enhance procollagen type I and III expression in fibroblasts in ex vivo human skin*. Skin Res. Tech. (submitted)

5.1 Introduction

The skin is the largest organ of the human body. Like other organs it has the ability to grow, develop and repair itself. Roughly, the skin can be divided into three layers; the epidermis, dermis and hypodermis. The epidermis is 50-150 μm thick, depending on the part of the body and skin type (Lewis et al., 1994). The dermis thickness varies from 300 μm on the eyelids to 3 mm on the back (Ebling et al., 1992). The main component of the dermis is the supporting extracellular matrix. This matrix consists of complexes of supportive proteins, such as collagen, elastin and proteoglycans, which are synthesized by dermal fibroblasts (Ebling et al., 1992; Geronemus, 2006). The dermis can be divided into the papillary dermis, situated directly under the epidermis, and the reticular dermis, located between the papillary dermis and the hypodermis (Farber and Rubin, 1998). The hypodermis, also called the subcutaneous layer, is the deepest layer and is composed primarily of fat cells (Ebling et al., 1992).

As well as any other organ of the human body the skin ages. With increasing age the characteristics of the skin change and its appearance becomes different (Dimri et al., 2007). Visible changes are roughness (dryness), wrinkling, laxity, and uneven pigmentation (Bjerring, 2006; Diridollou et al., 2007; Gilchrest, 2007a; Gilchrest, 2007c; Gilchrest and Bohr, 2006; Leveque et al., 2007b; Swelstad and Gutowski, 2006). These features are due to two important alterations that occur in the different layers of the skin. In the present study we are interested in changes, wrinkling and laxity, in the dermis. Firstly, the fibroblasts divide more slowly and the dermis becomes thinner, thereby having an increased susceptibility for damage. Secondly, the underlying network of elastin and collagen fibers loosens and unravels, resulting in wrinkling and sagging of the skin (Gilchrest, 2007b; Kurban and Bhawan, 2007). The aging process can be described by changes in e.g. dermal components like collagen, elastic fibers, proteoglycans and fibroblasts, caused by intrinsic and extrinsic aging (Ebling et al., 1992; Geronemus, 2006; Gilchrest, 2007a; Gilchrest, 2007b). Therefore cutaneous aging can be seen as a complex biological phenomenon affecting the different constituents of the skin.

Reducing effects of aging is a biologically beneficial effect of a physiological process, called hormesis, which is represented by mild stress-induced stimulation of protective mechanisms in cells and organisms. In the aging process hormesis is defined as a beneficial rejuvenating mechanism resulting from the cellular responses to single or multiple rounds of mild stress. Single or multiple exposure to low doses of otherwise harmful agents, such as irradiation and heat stress are some of the factors that induce hormetic effects (Rattan, 1998).

The aim of many rejuvenation techniques is to induce thermal stress. Among the rejuvenation methods used, the non-ablative techniques are gaining popularity. These methods claim to induce dermal remodeling without global epidermal injury, using a

thermal approach. Light sources, like lasers and broad band lamps, radio frequency and ultrasound are techniques that can be used as non-ablative rejuvenation methods. The energy is applied as short nanosecond to millisecond pulses or in a continuous wave, resulting in a local temperature increase (Bjerring, 2006; Capon and Mordon, 2006; Geronemus, 2006; Sadick, 2006). In literature it is stated that laser treatment causes two effects. On the one hand, a thermal effect where chromophores absorb the energy of the photons and convert this into heat, which subsequently diffuses throughout the skin. On the other hand a non-thermal photochemical effect on the cells in the skin; photons are absorbed by cytochrome-c proteins, that are located on the membrane of the human dermal fibroblasts, resulting in an increased metabolic activity of the cells (Dinh, 2006; Lubart et al., 2007; Pereira et al., 2007; Rattan, 1998). The present paper focuses on the thermal effect on the fibroblasts in *ex-vivo* skin.

When tissue, such as skin, is exposed to a temperature increase, different effects are observed depending on the temperature and duration of the temperature increase. It is found in literature that denaturation of the enzymes and of the membranes occurs at 40-45°C; coagulation, necrosis and protein denaturation occur at 60°C (Orringer et al., 2005). Among these temperatures, 45°C is a characteristic temperature used frequently in photodynamic therapy (Capon and Mordon, 2006; Verrico et al., 2001; Verrico and Moore, 1997). The temperature range from 57 to 61°C is known to induce shrinkage of collagen. However, the amount of collagen contraction is determined by a combination of time and temperature (Ruiz-Esparza, 2006).

Thermal collagen injury could lead to the complex physiological response of wound healing (Goldberg, 2006; Sadick, 2006), where in the phase of collagen deposition first collagen type III is synthesized and subsequently is substituted by collagen type I up to the ratio of healthy skin (Capon and Mordon, 2006; Stadelmann et al., 2006). It is suggested that dermal fibroblasts react to thermal injury with a heat shock response. Heat shock proteins are produced by fibroblasts to protect the surrounding proteins and the cells from necrosis and apoptosis (Capon and Mordon, 2006). Relevant heat shock proteins for skin regeneration are:

- hsp70; a highly inducible protein that is overproduced when a cell encounters a swift change to a higher temperature (Bowers et al., 2007; Kovalchin et al., 2006; Laszlo, 2007; Ohtsuka and Laszlo, 2007; Snoeckx et al., 2007; Souil et al., 2001; Tandara et al., 2007),
- hsp47; a constitutive protein that binds and transports procollagen from endoplasmic reticulum to the Golgi system and plays an active role in collagen type I synthesis (Brown et al., 2007; Naitoh et al., 2001; Tasab et al., 2000; Verrico and Moore, 1997), and

- hsp27; a constitutive protein that in case of overexpression protects the cell from apoptosis when it encounters a heat shock (Frank et al., 2004; Hirano et al., 2004; Snoeckx et al., 2007).

In our previous study we have shown that these heat shock proteins qualify as biomarkers (Dams et al., 2010). The response of dermal fibroblasts in culture to repeated mild heat shocks has been investigated. These results showed that repeated mild (39°C - 42°C) heat shocks have beneficial effects on aged cells (Geronemus, 2006; Mayes and Holyoak, 2008; Rattan, 1998). However, the duration of the heat shocks applied was between 30 minutes and 1 hour, which is relatively long and could induce thermotolerance (Ohtsuka and Laszlo, 2007). We showed that a pulsed heat shock of two seconds of 45°C as well as 60°C resulted in an increase of procollagen type I synthesis, preceded by an increase of procollagen type I gene expression by human dermal fibroblasts *in-vitro* (Dams et al., 2010).

Although several ablative and non-ablative rejuvenation techniques, based on inducing thermal stimuli, are already used extensively, the processes that are taking place as a result of skin treatment are still not fully understood. A result such as an increase in collagen synthesis is one of the assumed phenomena in skin rejuvenation (Bjerring et al., 2007; Capon and Mordon, 2006; Narurkar, 2006; White et al., 2007). The present research is aimed at answering the question whether thermal shocks lead to an increase of procollagen type I and III gene expression by the fibroblasts in *ex-vivo* skin, being the precursors for more collagen synthesis.

In this paper we heat shock human dermal fibroblasts in their physiological environment, the viable dermis. The aspect of interest is how these cells in the skin respond to the thermal stimulation. For regeneration of the collagen matrix a primary need is stimulation of the dermal fibroblasts to synthesize new collagen. Therefore, in this study we aim to stimulate human dermal fibroblasts in human skin to increase the gene expression of procollagen type I and type III as a precursor for the formation of a new collagen matrix. In addition we use heat shock proteins 27, 47 and 70 as biomarkers for respectively the need for protection from apoptosis, a precursor for collagen I synthesis, and for recognition of the heat shock.

5.2 Materials and Methods

5.2.1 Sample preparation

Excised human skin was obtained from 6 patients undergoing abdominoplasty at the Catharina Hospital Eindhoven. This material was anonymized after the procedure, making tracing back to the patient impossible. The procedure was in conformity with the code of conduct for use of human material as stated by the Dutch Federation of Biomedical Scientific Societies. Sample preparation was carried out quickly after

harvesting of the tissue. The skin was stretched in order to cut slices of 1 mm thickness with a dermatome (Humeca, Enschede, The Netherlands) (figure 5.1). Biopsy needles (Amstel Medical, Amstelveen, The Netherlands) with a diameter of 2 mm were used to cut the samples out of each slice, creating cylindrical samples with thickness of 1 mm. During the puncturing process the samples as well as the slices of skin were moistured with Dulbecco's Modified Eagle Medium (GIBCO, Invitrogen™, Breda, The Netherlands). Approximately 3 hours after surgery the skin samples were ready to be processed.

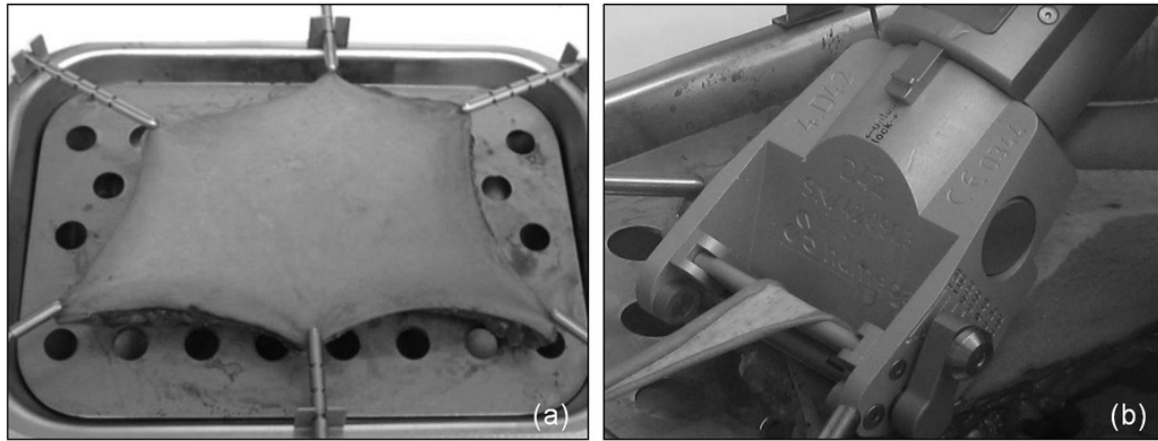


Figure 5.1: Human skin. (a) Stretched abdominal human skin. (b) Dermatomed human skin.

5.2.2 Experimental procedure

All heat shock experiments were performed by immersing the skin samples in heated PBS at 45°C or 60°C to heat the center of the skin samples for 2 seconds. By means of Comsol Multiphysics modeling and simulation it was calculated that immersion times of 8 and 10 seconds were required to achieve a 2 second heat shock at 45°C and 60°C, respectively (Appendix, figure 5.8 and table 5.3).

After the pulsed heat shock, some of the skin samples were snap-frozen in liquid nitrogen at six different time points: 1, 5, 15, 35, 65, and 95 minutes for gene expression analyses. The remaining skin samples were fixed at the same time points in 3,7 % formaldehyde for histology. The viability of the *ex-vivo* skin was measured and visualized before and after the heat shock of 45°C and 60°C.

5.2.3 Calculation of thermal damage

Thermal damage was calculated by the damage integral of Arrhenius (Welch and van Gemert, 1995):

$$\Omega(\tau) = A \int_0^{\tau} e^{-\left(\frac{E_a}{R \cdot T(t)}\right)} dt \quad (5.1)$$

Where $\Omega(\tau)$ is the thermal damage parameter, A is the frequency factor [s^{-1}], τ is the total heating time [s], E_a is the activation energy barrier [J/mole], R is the universal gas constant [$8.32 \text{ J/mole}^{-1}\text{K}^{-1}$], and $T(\tau)$ is the absolute temperature [K].

The heat shocks in the performed experiments have short durations, 8 and 10 seconds, to achieve 45°C and 60°C, respectively. As a result of these pulse durations, the thermal damage calculation can be simplified by calculating the threshold temperature:

$$T_{thresh} = \frac{E_a}{[R \cdot \ln(A \cdot \tau)]} \quad (5.2)$$

T_{thresh} is the threshold temperature [K] above which irreversible damage to proteins will occur (Welch and van Gemert, 1995).

5.2.4 Determination of viability of *ex vivo* skin

The viability of the *ex-vivo* skin samples was determined before and after the heat shocks of 45°C and 60°C by staining with calcein AM (Fluka cat. # 17783) and propidium-iodine (Cat. No. P3566, Invitrogen™). Calcein is well retained within viable cells, producing an intense uniform green fluorescence. The propidium iodide (PI) dye is excluded from the viable cells. This dye will enter necrotic cells and binds DNA, which becomes visible with red fluorescence (Breuls et al., 2003).

Each sample was incubated in calcein at a concentration of 1 µg/ml PBS for 30 minutes after the thermal stimulus. This step was followed by several washings in PBS and subsequently the samples were incubated in 7 µg/ml propidium-iodide concentration for 15 minutes. The skin samples were washed and their viability was visualized with a confocal laser scanning microscope (Carl Zeiss B.V., Sliedrecht, The Netherlands).

5.2.5 Determination of the metabolic activity of the *ex vivo* skin

The metabolic activity was measured before and directly after the heat shock experiment using the 3-[4,5-dimethylthiazol-2-yl]-2,5-diphenyl tetrazolium bromide (MTT) based *in vitro* toxicology assay kit (Sigma, Breda, The Netherlands). The skin samples were placed in a 6-well plate, one sample per well. Per well 250 µl MTT solution (M 5655, Sigma, Breda, The Netherlands) was added immediately and the 6-well plates were placed at 37°C for 3 hours. Subsequently, 250 µl per well isopropanol (Merck, Darmstadt, Germany) was added and the 6-well plates were placed on a shaker (Titramax 1000, Heidl Instruments, Germany) at 300 rpm for another 30 minutes. Metabolically active cells in the tissue cleaved the molecules of the MTT solution resulting in precipitation of formazan crystals. After the 30 minutes of incubation the crystals were dissolved in isopropanol resulting in a purple solution. Absorbance was spectrophotometrically measured at a wavelength of 570 nm (Biotek Synergy, Beun de Ronde, The Netherlands).

5.2.6 Histological and immunohistochemical analyses

The fixed skin samples were embedded in paraffin and cut into sections of 8 µm. The sections were de-waxed and rehydrated before they were incubated with 0.1% PicroSirius Red for one hour to stain collagen. Subsequently, the sections were placed in Weigert's iron Haematoxylin for 10 minutes to visualize the nuclei of the cells. Next, the

sections were washed in running tapwater for 5 minutes and mounted on coverslips with entellan (Merck, Darmstadt, Germany). The stained skin samples were visualized using bright-field and circular cross-polarized microscopy (Axiovert 200M, Zeiss) at room temperature with a 10× objective (Zeiss LD ACHROPLAN) and a NA of 0.4. Haematoxylin stains the nuclei dark blue/black and PicroSirius Red stains the collagen fibers orange/red when visualized with bright-field microscopy. When visualizing the stained tissue sections with circular cross-polarized microscopy, the cells appear black whereas the thin immature collagen fibers appear green and the thick mature collagen bundles are orange (Bancroft and Gamble, 2002).

For heat shock protein 27, immunohistochemical analysis on the paraffin embedded skin sample sections was performed. The sections were de-waxed, rehydrated, washed in PBS for 5 minutes and incubated in Tris-EDTA buffer at room temperature for 20 minutes for epitope retrieval. Subsequently, the sections were incubated in 1% BSA for 30 minutes, to block non-specific binding, and washed for 5 minutes in 0.1% Tween 20, 5 minutes in 1% Triton X-100 and 5 minutes in PBS. After these washing steps the sections were incubated at 4°C overnight with the primary antibody against Hsp27 (1:100) (Abcam, Cambridge, USA). Next, the sections were washed for 5 minutes with 0.1% Tween 20 and 3 times at 5 minutes with PBS. Then, the sections were incubated with horse radish peroxidase-conjugated goat anti rabbit IgG secondary antibody (1:1000) (Abcam, Cambridge, UK). After washing, the sections were visualized with DAB, 3,3'-Diaminobenzidine tetrahydrochloride, (Sigma Aldrich, Breda, The Netherlands) followed by washing in PBS twice for 5 minutes. Then, the sections were counterstained with Weigert's iron Haematoxylin for 10 minutes and mounted with Mowiol. The sections were evaluated using bright-field microscopy (Axiovert 200M, Zeiss) at room temperature with a 20× objective (Zeiss LD ACHROPLAN) at an NA of 0.6. The HRP with DAB reaction results in a dark brown color.

For the histology as well as the immunohistochemistry analyses a Zeiss AxioCam HRM camera was used with Zeiss AxioVision Rel. 4.6 acquisition software.

5.2.7 Determination of gene expression levels of heat shock proteins 27, 47, 70 and procollagen type I and III

The skin samples, used for quantitative PCR, were snap-frozen in liquid nitrogen at six different time points ($t = 1, 5, 15, 35, 65, 95$ min) after the heat shock and stored at -80°C. The skin samples were mashed in lysis buffer (Qiagen, Venlo, The Netherlands) containing 1% β -mercaptoethanol (Merck, Darmstadt, Germany) with an Ultraturrax (IKA, Staufen, Germany), before total RNA could be obtained. Total RNA was isolated using RNeasy kit (Qiagen) in accordance with the manufacturer's protocol. The concentration and purity of the total RNA was determined at OD 260/280 nm measurements (Nanodrop, Isogen, Scotland). RNA integrity was assessed using gel-electrophoresis. 225 ng RNA and random primers were used for cDNA synthesis using

M-MLV reverse transcriptase (Invitrogen™, Carlsbad, USA). Gene expression analysis was performed on an iCycler Real-Time PCR detection system (Biorad, Veenendaal, The Netherlands) using iQ™ SYBR®-Green supermix (Biorad). Primers for hsp27, hsp47, hps70 and procollagen type I and III were used as recently described in chapter 3 (Dams et al., 2010). Results were normalized using reference genes β -Actin and GAPDH, obtained from Primerdesign (South Hampton, U.K.). Fold changes, $2^{-\Delta\Delta Ct}$, were calculated manually.

5.2.8 Statistical analysis

All data are presented as means and their standard deviations for a sample measurement of $n = 6$. Comparisons of gene expression levels between the control and experimental groups were performed by a one-sampled unpaired *t*-test. Comparisons of gene expression levels between the experimental groups were performed by a two-sampled unpaired *t*-test. Differences in both comparisons were considered significant at $p < 0.05$.

5.3 Results

5.3.1 Viability and structure *ex vivo* skin

The effects of the heat shocks on the metabolic activity and the corresponding cellular viability are illustrated in figure 5.2. The absorption levels are proportional to the metabolic activity. As depicted in the figure the absorption levels of the 45°C and the 60°C heat shocked skin samples do not differ significantly from the samples before the heat shock. Therefore, suggesting comparable cell viability between the three samples.

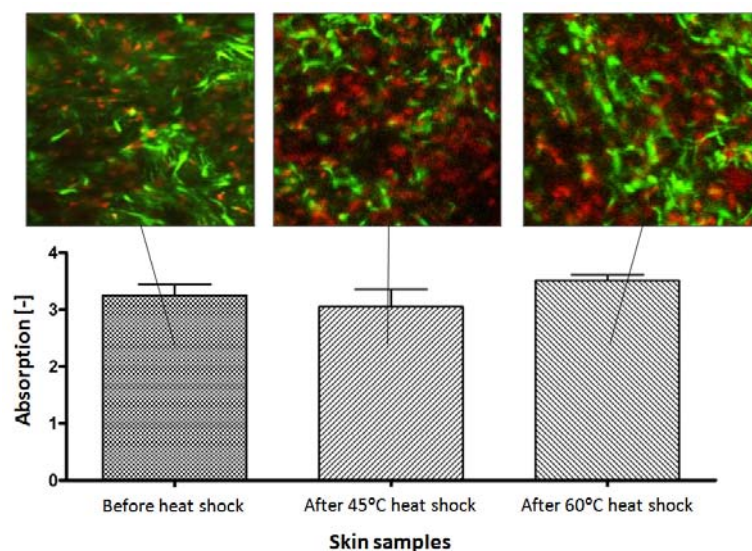


Figure 5.2: Metabolic activity of human dermal fibroblasts in *ex vivo* skin before (referred to as control) and after exposure to the heat shocks. The control was kept at 37°C. The y-axis shows the absorption levels normalized to the control. Note: the absorption is proportional to the metabolic activity. The corresponding confocal images show viable cells appearing green and non-viable cells red.

Figure 5.3(a-d) shows the results of the picosirius red and haematoxylin staining visualized with bright field microscopy. It can be seen in figure 5.3(a-c) that the collagen network, visualized in red, does not show any visible structural change in contrast to the images of the skin sample kept at 60°C for one hour (figure 5.3(d)). In the latter case, changes can be seen, including severe damage of the epidermal cells and disruption of the dermal cells. Furthermore, structural details of the collagen network in the dermal matrix are no longer evident. In figure 5.3(b) and (c) the epidermal cells, visualized in dark blue, stay intact. Furthermore, the dermis shows similar structural details as in the control sample, depicted in figure 5.3(a).

Figures 5.3(e-h) depict the results of identical slices as in figure 5.3(a-d) focused on the same locations visualized with circular cross-polarized microscopy. The mature, thick collagen fibers are depicted in orange and the young, thin collagen fibers are shown in green. Figures 5.3(e-g) demonstrate the intact collagen structure; with no difference in the ratio of orange and green fibers between the heat shocked skin samples and the control samples, indicating an intact collagen matrix. Figure 5.3(h), however, clearly shows a disrupted collagen matrix. The ratio of orange and green fibers in this treated skin sample is changed to predominantly orange compared to the control sample. This result implies destruction of the immature collagen fibers.

5.3.2 Effect of heat shocks on the gene expression of heat shock proteins 27, 47 and 70

The average fold change of hsp70 of the cells in the skin samples over six patients per time point is depicted in figure 5.4(a). It is noticed that the pulsed heat shocks of 45°C as well as the heat shocks of 60°C result in an elevated expression of hsp70 after 15 minutes. The upregulation after the 60°C heat shock, however, shows a more substantial increase after 65 minutes.

Figure 5.4 (b) represents the averaged fold changes per time point of hsp47 in the skin samples of six different patients after the pulsed heat shocks. These data show that the 60°C heat shock resulted in an immediate overall significant increase in hsp47 mRNA, while the heat shock of 45°C caused a delayed upregulation after 65 minutes.

Regarding the mean fold changes of hsp27, figure 5.4 (c) shows an overall significant instantaneous increase in expression after the heat shock of 60°C. Results of the expression of hsp27 in cells in the skin samples heat shocked with 45°C showed no significant upregulation.

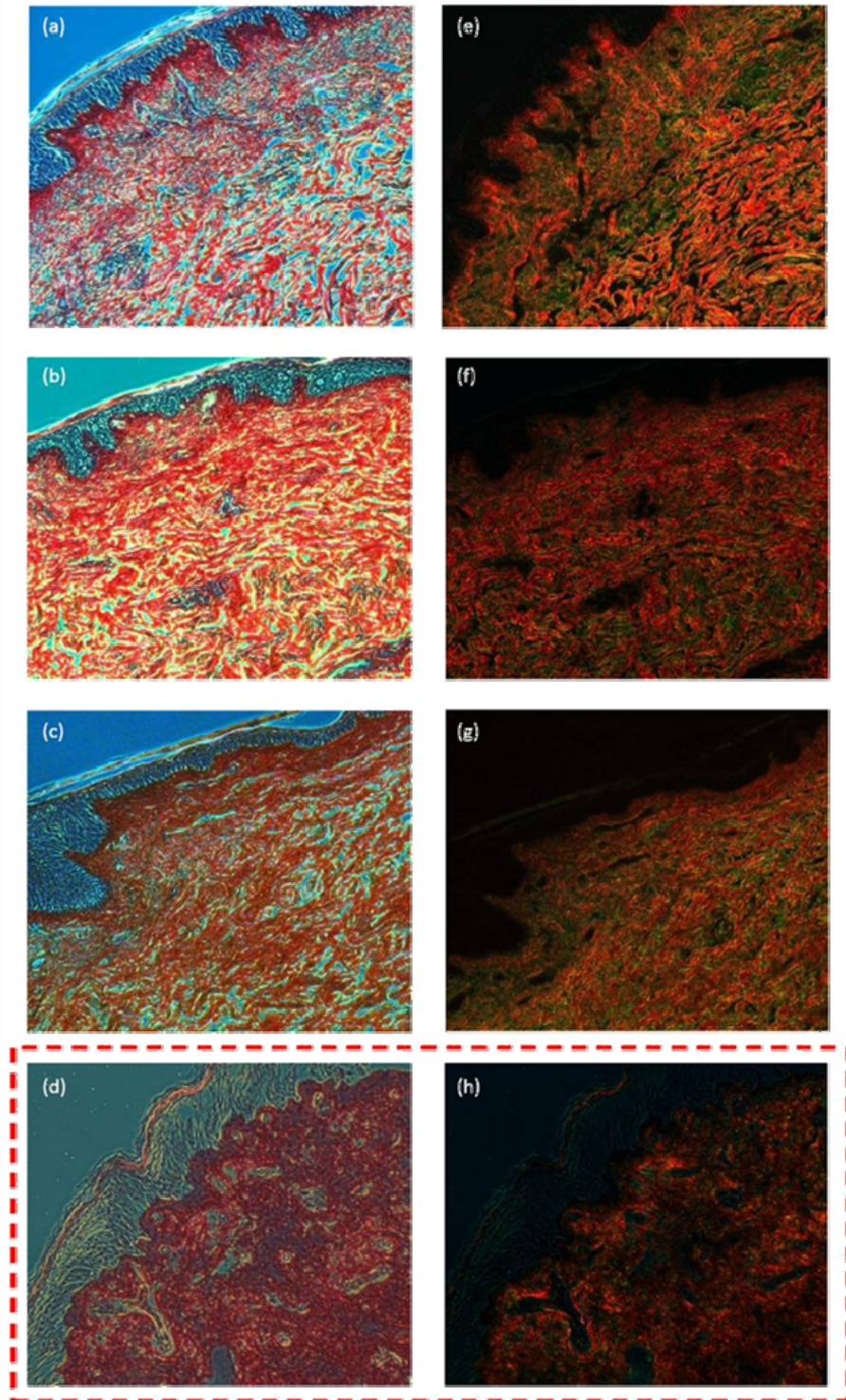


Figure 5.3: Picosirius red with Haematoxylin staining results visualized with bright field (a-d) and cross-polarized (e-h) microscopy. Cells are depicted in dark blue and the collagen bundles are colored red. Figures 3(a) and 3(e) depict the control samples fixated after 95 minutes after treatment. In figures 3(b) and 3(f) the staining on the fixated tissue samples of 95 minutes after the 45°C heat shock are shown. The skin samples heat shocked at 60°C and fixated at $t = 95$ after the pulsed heat shock is depicted in figures 3(c) and 3(g). In figures 3(d) and 3(h) results are demonstrated of a skin sample 95 minutes after treatment with 60°C for one hour.

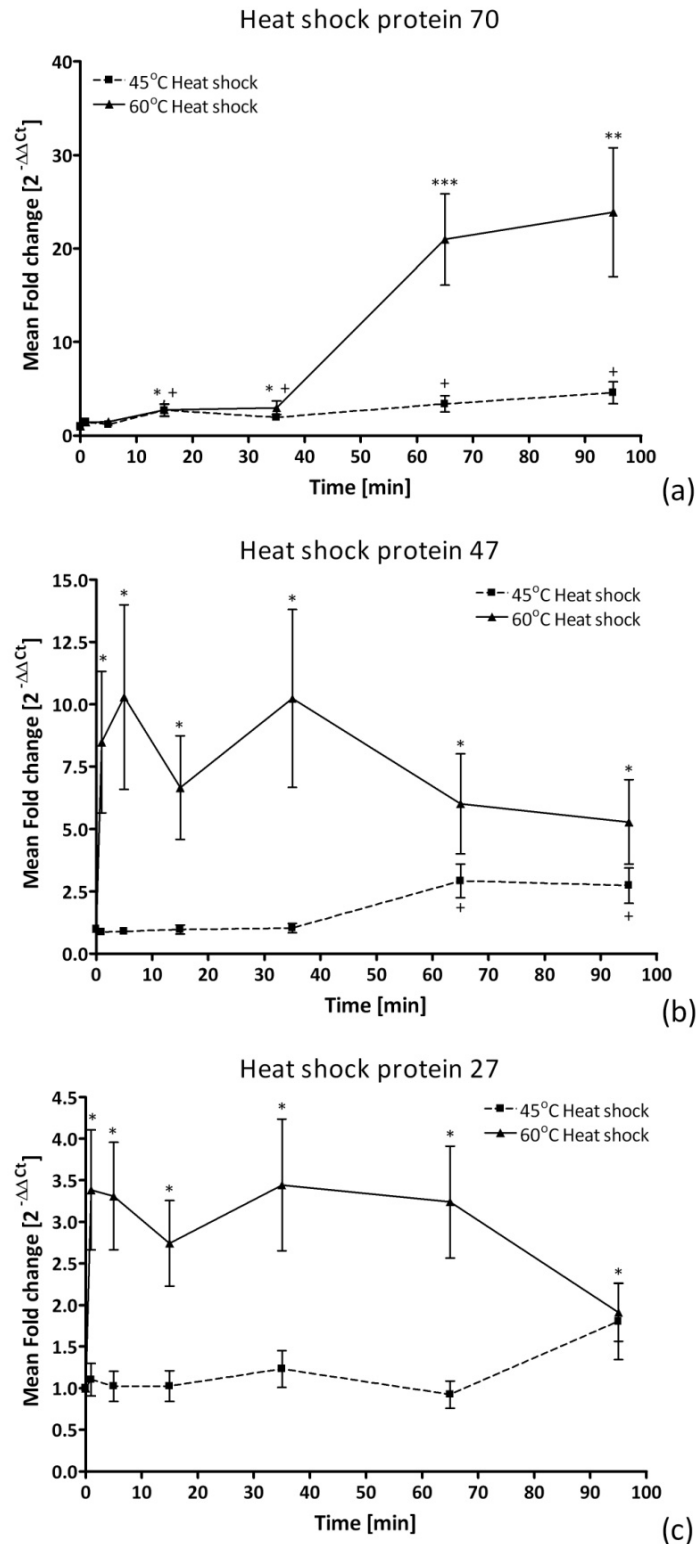


Figure 5.4: Mean fold changes, $2^{-\Delta\Delta Ct}$ of heat shock protein 70 (a), heat shock protein 47 (b) and heat shock protein 27 (c) at the different time points after exposure to the heat shock. The data are relative to the control and the reference genes β -Actin and GAPDH. The x-axis depicts the time given in minutes. The y-axis shows the mean fold changes of the cells in the skin samples heat shocked at 45°C and 60°C, dashed and solid line, respectively. Data are shown as the mean \pm SD for 6 independent experiments each run in duplicate with significant differences compared to control for 45°C heat shocked samples at $^+ p < 0.05$, $^{++} p < 0.01$ and $^{+++} p < 0.001$ and for 60°C heat shocked samples at $^* p < 0.05$, $^{**} p < 0.01$ and $^{***} p < 0.001$.

5.3.3 Effect of heat shocks on the gene expression of procollagen type I and III

The results of both 45°C and 60°C heat shock on the expression of procollagen type I and type III are shown in figure 5.5. The figure indicates the mean fold changes over 6 patients per time point. An overall significant increase in expression for procollagen type I can be seen for heat shocks at 45°C and, more substantially at 60°C (figure 5.5(a)).

As demonstrated in 5.5(b) both 45°C and 60°C heat shock resulted in an overall significant increase in expression of procollagen type III instantaneously. However, the 60°C heat shock appeared to result in a higher upregulation compared to the 45°C heat shock.

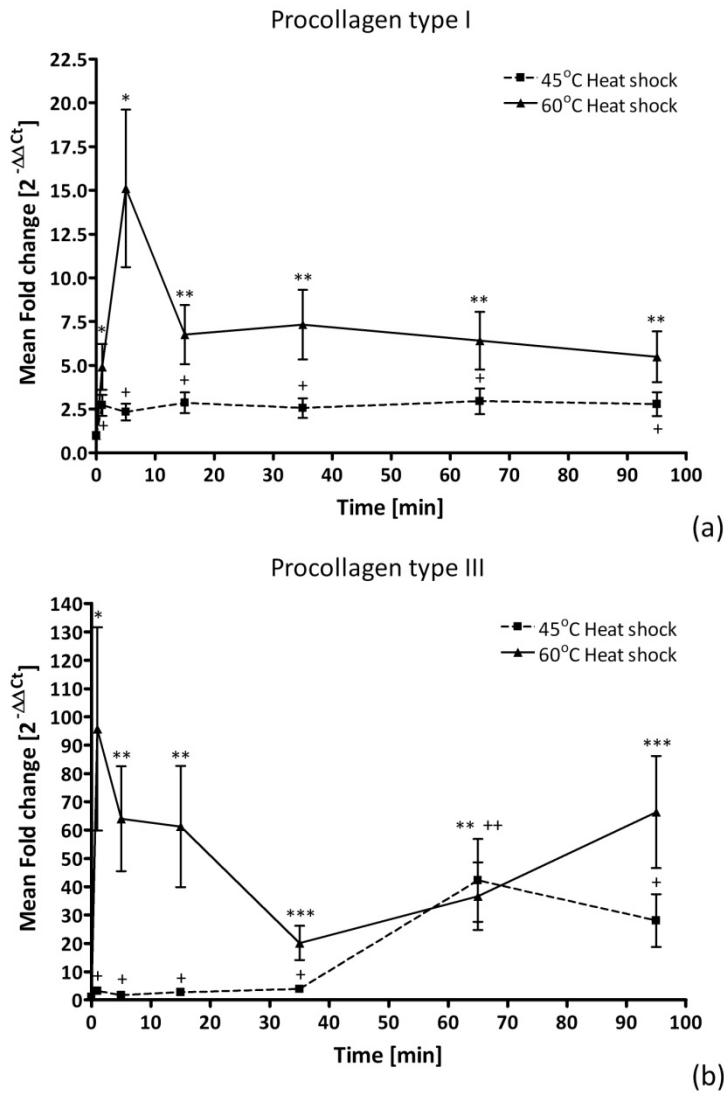


Figure 5.5: Mean fold changes, $2^{-\Delta\Delta Ct}$, of procollagen type I (a) and procollagen type III (b) at the different time points after exposure to the heat shock. The data are relative to the control and to the reference genes β -Actin and GAPDH. The x-axis depicts the time given in minutes. The y-axis shows the mean fold changes of procollagen type III and procollagen type I of the cells in the skin samples heat shocked at 45°C and 60°C, dashed and solid line, respectively. Data are shown as the mean \pm SD for 6 independent experiments each run in duplicate with significant differences compared to control for 45°C heat shocked samples at + p < 0.05, ** p < 0.01 and *** p < 0.001 and for 60°C heat shocked samples at * p < 0.05, ** p < 0.01 and *** p < 0.001.

However, the 60°C heat shock appeared to result in a higher upregulation compared to the 45°C heat shock. A different tendency over time can be observed: The heat shock of 60°C shows a consistent upregulation over time over the population, while the effect of the 45°C heat shock appears to be more substantial after 65 minutes.

5.3.4 Thermal damage

As explained in the introduction heat shock protein 27 is a biomarker to indicate early damage response by fibroblasts. In figure 5.6 the results of the immunohistochemical staining for hsp27 are shown. The stained skin samples heat shocked at 60°C appear to show brown coloration around the cells, suggesting deposition of hsp27, indicated by the arrows (figure 5.6(c)). By contrast the 45°C heat shock results in much less brown coloration around the cells, as shown in figure 5.6(b), and cannot be distinguished from the control, figure 5.6(a). The brown coloration in the epidermis, seen in all images, is a result of the reaction of endogenous peroxidases in the epidermis with DAB (Shindo et al., 1994).

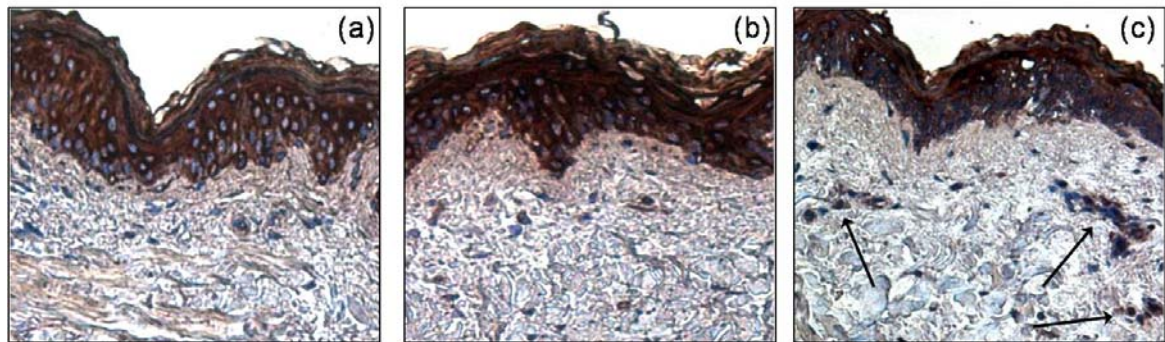


Figure 5.6: Immunohistochemical staining for hsp27 after 95 minutes of the control skin sample kept at 37°C (a), 45°C heat shocked skin sample (b), and 60°C heat shocked skin sample (c). The dark brown region around the cells in the dermis (arrows) suggests the presence of hsp27. The nuclei of the cells are depicted in blue. Note: the brown coloration in the epidermis is a result of the reaction of endogenous peroxidases with DAB (Shindo et al., 1994).

The parameters for the calculation of the thermal damage according to the Arrhenius integral are listed in table 5.1 in the Appendix. It follows from figure 5.7 that exposing the sample for 10 seconds at 60°C likely causes irreversible damage to the proteins, whereas following an exposure of 8 seconds at 45°C areas of damage are likely to be reversible. However, it should be noticed that only the outer layer of the skin sample is exposed to 60°C for the full 10 seconds.

5.4 Discussion

This study has demonstrated that heat shocks stimulate cells in *ex-vivo* skin to upregulate gene expression of procollagen type I and procollagen type III as an initial response. The heat shocks at both 45°C and 60°C cause an upregulation of procollagen type I and type III directly after the stimulus. In the case of the expression of procollagen

type III a difference can be noticed. The 45°C heat shock caused a more substantial upregulation after 65 minutes, while the heat shock of 60°C results in an instantaneous extensive upregulation.

The expression of procollagen type I in cultured monolayers of human dermal fibroblasts has recently been demonstrated to be upregulated after 35 minutes by human dermal fibroblasts in culture treated with short pulsed heat shocks of 2 seconds at 45 and 60°C (Dams et al., 2010). The results shown here are from cells in viable *ex-vivo* skin samples. To achieve the desired temperatures of 45°C and 60°C for 2 seconds in the center of the skin samples, simulations were performed (appendix). The simulations pertain to the experimental procedure where skin samples were immersed in heated PBS, causing a heterogeneous heat distribution; the outer layers were exposed to temperatures of 45°C and 60°C for, respectively, 8 and 10 seconds, while the centers were heat shocked for 2 seconds. In this study it is shown that heat shocks of 45°C and 60°C, for 8 and 10 seconds respectively, result in a significant increase in gene expression of procollagen type I by fibroblasts in skin samples directly after the heat shock. We also found that the early response in upregulation of hsp47 by the cells in the skin samples heat shocked at 60°C and the delayed upregulation by the cells in the skin samples heat shocked at 45°C correlate with the trend that we found for procollagen type I expression. There is a clear relevance of the correlation between the significant upregulation of procollagen type I and the upregulation of hsp47 for both heat shock temperatures, because hsp47 has the ability to bind procollagen I for transportation to the Golgi system (Tasab et al., 2000; Tasab et al., 2002). Furthermore, it is stated that hsp47 takes an active role in the collagen type I synthesis (Naitoh et al., 2001; Tasab et al., 2000; Verrico et al., 2001). Our results support that these physiological processes are also initiated in fibroblast in viable *ex-vivo* skin.

The upregulation of hsp70 (figure 5.4(b)) indicates that the cells in the skin samples are sensitive to the heat shock (Mayes and Holyoak, 2008; Rattan, 1998; Verbeke et al., 2007). It is well established that hsp70 upregulates under various stress conditions, including mechanical stress (Snoeckx et al., 2007). Therefore, if any upregulation would have occurred in the cells of the experimental samples, due to mechanical or other stress factors induced by the sample preparation, it would also have occurred in the control samples. However, our results are displayed in fold changes, meaning that the experimental data are normalized to reference genes and to the control data. Thus the increased levels of hsp70 mRNA suggest that both heat shock temperatures have evidently stimulated the cells in the *ex-vivo* skin, which is in accordance with *in-vitro* cell studies (Snoeckx et al., 2007; Verbeke et al., 2007).

Heat shock protein 27 plays an important role in protecting cells against apoptosis and can be elevated under stress (Snoeckx et al., 2007). We have observed an upregulation of hsp27 in cells of the skin samples heat shocked at 60°C, but no upregulation in the

cells heat shocked at 45°C. It is interesting to compare these results with the predictions of the calculated thermal damage using the model of Arrhenius (Welch and van Gemert, 1995). According to this model the threshold temperature predicts that irreversible damage occurs at 60°C after roughly 1 second (figure 5.7). Hence, an upregulation of hsp27 can be expected. Additionally, we suggest by means of immunohistochemical analysis for hsp27 that this protein is notably present in the dermis after the heat shock of 60°C (figure 5.6(c)).

Although several studies have shown that 60°C heat would destroy living tissue (Mertyna et al., 2009), it can be concluded from our data that 45°C and 60°C heat shocks do not compromise the structure nor the viability of skin in the time range of 8 and 10 seconds, respectively (figure 5.2 and figure 5.3). However, this is not in accordance with the calculation of the thermal damage with the Arrhenius equation. This contradiction can be explained by the fact that only the outer layers of the skin samples are exposed to 60°C for 10 seconds. Furthermore, the parameters used, A and E_a , are based on values for porcine skin, whereas in this study human skin is used.

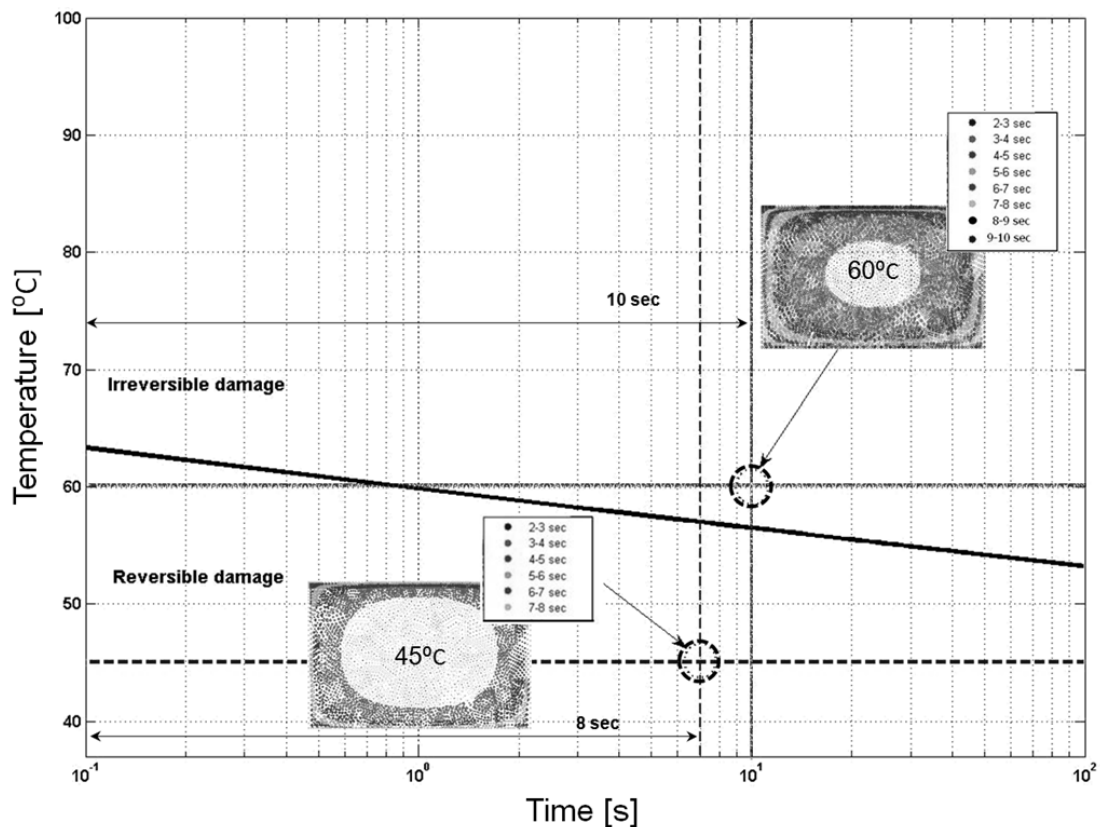


Figure 5.7: Threshold temperature versus exposure duration for skin according the Arrhenius equation indicating the border between irreversible and reversible damage zones (black line). Within the graph schematic representations are depicted of the different time zones within the skin samples heat shocked at 45°C (left) and 60°C (right). The cross-sections of the blue dashed and the solid red lines depict the final situations of the 45°C and 60°C heat shock skin samples, respectively.

In literature a large number of clinical studies on laser skin rejuvenation treatments is described (Bjerring, 2006; Capon and Mordon, 2006; Goldberg, 2006; Sadick, 2006). In this study, we wanted to isolate the thermal effects from the photochemical effects. To approach the pulse duration of the heat shock of rejuvenation methods like non-ablative laser treatments, we have chosen to apply heat shocks through conductive heating over a short duration. However, the heterogeneous heat distribution caused by immersing the skin samples results in different exposure times of the cells located in the center of the skin sample versus the cells located at the edges of the sample. We expect that this difference in exposure time reflects on the response of the fibroblasts, as has been noticed in the thermal damage calculation. The temperature of 45°C was chosen in the present study, because the temperature reached in the dermis after laser treatment is between 42 and 45°C (Verrico et al., 2001). In addition, the 60°C heat shock temperature was chosen, because it is known that this is a threshold temperature for protein denaturation (Ebling et al., 1992; Farber and Rubin, 1998; Mitchell et al., 1999). However, it needs to be considered that changes in the pulse duration and temperature could result in a different response of human dermal fibroblasts in *ex vivo* skin (Altshuler et al., 2007; Watanabe, 2008).

Heat shock response of human dermal fibroblasts induced by either laser treatments or pulsed heat shocks is poorly understood. In this study we have shown that the thermally induced heat shocks stimulate the cells in *ex-vivo* skin. With regard to our findings, it can be suggested that the 60°C heat shock leads to a more pronounced effect on the stimulation of fibroblasts in *ex-vivo* skin than the 45°C heat shock in the complex process of regeneration of the collagen matrix. Moreover, the heat shock resulted in a temperature gradient over the skin samples resulting in heat shocking fibroblasts from 2 up to 8 and 10 seconds to achieve 45°C and 60°C, respectively. In order to identify the actual process of collagen synthesis in the skin this research has to be extended to investigating the effect of the pulse duration of the heat shocks on the human dermal fibroblasts. Furthermore, to enable quantitative protein measurements a more suitable skin model should be developed.

5.5 Acknowledgements

The authors would like to thank Sarita Soekhradj-Soechit for the immunohistological analysis of the paraffinized skin samples. Furthermore, they would like to thank the Catharina hospital for providing the human tissue.

5.6 Appendix

5.6.1 Numerical modeling and simulation of the experimental procedure

For modeling and simulation COMSOL Multiphysics®3.5 (COMSOL BV, Zoetermeer, The Netherlands) is used. A 3D skin model is built up for simulating the skin heating and

cooling process in a constant temperature bath. This skin model enables exploration of several factors beneficial for controlling the experiment. Because of the shape and the size of the samples it is a priori not clear how the temperature field within the skin will evolve in place and time. A theoretical model was developed to estimate the temperature profiles as a function of time.

Table 5.1: Input constants thermal damage (Welch and van Gemert, 1995).

Desired temperature [°C]	Activation energy barrier, E_a [J/mole]	Frequency factor, A [s^{-1}]	Total heating time [s]
45	$6.28 \cdot 10^5$	$3.1 \cdot 10^{98}$	8
60			10

As required by the experiment, a cylindrical mesh is created with a diameter of 2 mm and thickness of 1 mm (figure 5.8). The initial temperature is set to 37 °C. Boundary conditions are varied to simulate the water bath conditions.

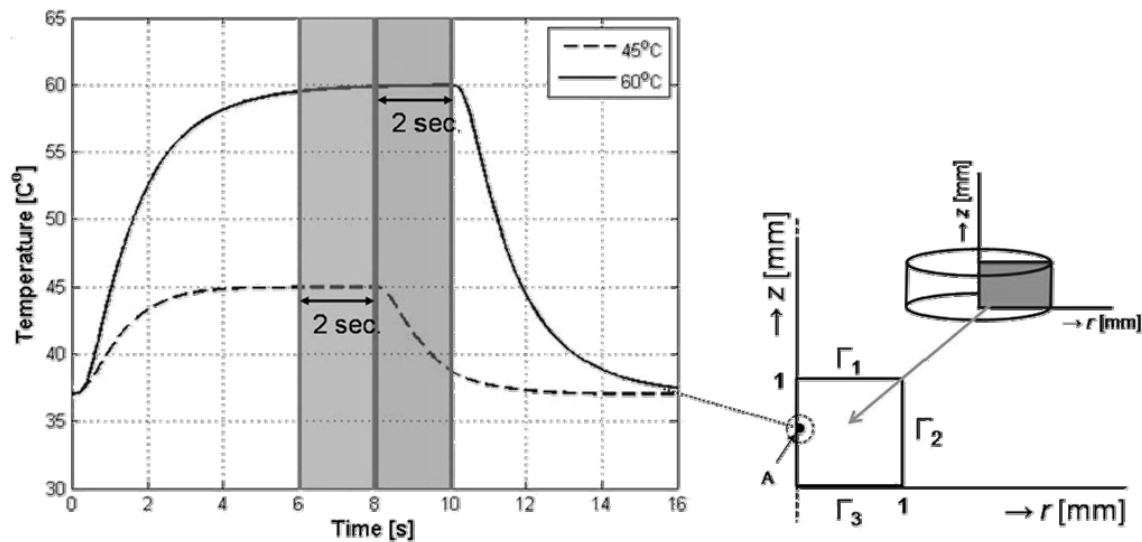


Figure 5.8: Schematic cylindrical mesh of the skin sample (right), $z = 1$ mm and $\varnothing = 2$ mm. A 2D cross-section is depicted to point out the boundary conditions. The graph (left) depicts the results of the simulation of the heating process in the center of the mesh (depicted by the black bullet). It demonstrates the temperature, y-axis, versus time, x-axis, for a skin sample heating up to 45°C or 60°C, dashed and solid line respectively. The blue and the red zone indicate the 2 second interval of the final temperature.

Skin thermal properties, as listed in table 5.1, are set in sub-domain conditions in COMSOL Multiphysics®. The following diffusion equation is solved:

$$\nabla^2 T + \dot{q} = \frac{\rho c}{k} \frac{\partial T}{\partial t} \tag{5.3}$$

Were T is temperature, \dot{q} is heat generation rate in each element, k thermal conductivity of the skin, ρ density of skin, c specific heat of skin and t is time (Table 5.2). The metabolism of the cells is neglected; hence this heat generation rate is set to zero.

Table 5.2: Thermal properties of human skin (Humbert and Agache, 2004; Tuchin et al., 2010).

Tissue	Density, ρ [kg/ m ³]	Thermal conductivity , k [W/(m*K)]	Specific heat, c [J/(kg*K)]	Initial temperature, T [°C]
Epidermis	1200	0.24	3590	37
Dermis	1200	0.45	3300	37

The procedure is based on our previous cell research where we heat shocked monolayers of human dermal fibroblasts for 2 seconds with 45°C and 60°C (Dams et al., 2010). This procedure runs a simulation where the skin sample is initially kept at 37°C, followed by a heat shock where it is heated up to 45°C and 60°C using heated PBS, subsequently kept at the highest temperature for 2 seconds, then cooled down to 37 °C.

5.6.2 Numerical modeling and simulation results

Figure 5.8 shows a schematical representation of the cylindrical mesh of the skin sample, with height, $h = 1$ mm and diameter, $\varnothing = 2$ mm. Next to the mesh a 2D slice is shown where the boundary conditions, Γ_1 , Γ_2 and Γ_3 are depicted. The graph in figure 5.8 depicts the results of the simulation of the heating process in the center of the mesh in point A. It demonstrates the temperature versus time for a skin sample immersed in 45°C and 60°C, dashed line and solid line respectively. The grey zones indicate the 2 seconds of the pulse durations.

Table 5.3: Results simulation heat shock experiment.

Desired Temp. [°C]	Threshold [°C]	Time to final temp. [s]	Time to begin cooling [s]	Time to cool down to 37 °C [s]
45	44.5	6	8	3
60	59.5	8	10	4

In this graph and in table 5.3 it is demonstrated that it takes roughly 8 seconds and 10 seconds to heat shock the center of a skin sample for two seconds with thickness of 1.0 mm and a diameter of 2 mm at 45°C and 60°C, respectively. The accuracy of the immersion times were set at 0.5°C. Therefore the cutoff was at 44.5°C in case of the 45°C heat shock simulation. In case of the 60°C heat shock this was 59.5°C.

Chapter 6

Procollagen gene upregulation in *ex-vivo*
human skin after laser irradiation:

A pilot study

6.1 Introduction

To rejuvenate the skin is to stop or reverse the aging effects of the skin. Some of these effects, such as loosening and unraveling of the dermis, cause visible changes like sagging skin and wrinkles (Gilchrest, 2007a; Kurban and Bhawan, 2007). It is believed that injury of the skin and the subsequent wound healing response is one of the mechanisms that results in a younger looking skin (Capon and Mordon, 2006; Geronemus, 2006; Manstein et al., 2006).

The development of rejuvenation treatments for aged skin is booming, especially the area of the laser-based techniques, consisting of ablative and non-ablative laser cosmetic surgery (Eze and Kumar, 2010). In this chapter we focus on the non-ablative laser treatments that traumatize the dermis (Capon and Mordon, 2006; Laubach et al., 2006; Weiss et al., 2006).

An induced thermal trauma by laser therapy leads to stimulation of collagen synthesis (Capon and Mordon, 2006; Laubach et al., 2006; Narurkar, 2007; Weiss et al., 2006). The result is skin thickening and tightening. Typical lasers that are used for non-ablative rejuvenation are lasers that emit in the 676 – 1540 nm region where absorption by water is not so strong (Narurkar, 2006; Pearlman, 2006). In this chapter we will use a laser diode of 976 nm.

It was shown in chapter 3 that pulsed heat shocks of two seconds of 45°C as well as 60°C resulted in an increase of procollagen type I synthesis, preceded by an increase of procollagen type I gene expression in human dermal fibroblasts *in-vitro*. Furthermore, in chapter 5 a heat shock of 45°C as well as 60°C on *ex-vivo* human skin demonstrated upregulated procollagen type I and type III expression. The aim in this chapter is to investigate the effect of laser treatment that induces temperatures of 45°C and 60°C in the dermis.

We have performed a pilot study on the effect of a laser induced heat shock applied to human dermal fibroblasts in their physiological environment, the viable dermis. Simulations are performed to establish the irradiation time of the laser diode to the *ex-vivo* skin samples to achieve 45°C as well as 60°C for approximately 2 seconds in the center of the skin samples. Additionally, experiments were performed in which *ex-vivo* skin samples were exposed to the laser in order to stimulate the cells in the skin to increase the gene expression of procollagen type I and type III as a precursor for the formation of a new collagen matrix (chapter 3 and 4). Gene expressions of heat shock proteins 27, 47 and 70 were used as biomarkers.

6.2 Materials and methods

6.2.1 Sample preparation

Excised human skin was obtained from 6 patients undergoing abdominoplasty at the Catharina Hospital Eindhoven. This material was anonymized after the procedure. The procedure is in conformity with the code of conduct for use of secondary human material as stated by the Dutch Federation of Biomedical Scientific Societies. Sample preparation was carried out quickly after harvesting of the tissue, conform the protocol used in chapter 5.

6.2.2 Simulation laser irradiation

Heat distribution was calculated with the skin model used in chapter 2. The geometrical configuration used in the simulations is similar to the geometry of the *ex-vivo* skin samples (diameter = 2 mm, h = 1 mm).

6.2.3 Experimental procedure

All heat shock experiments were performed by exposing the skin samples to a 976 nm laser diode. Based on the simulations the skin samples were exposed to the laser diode for approximately 8 and 23 seconds, resulting in a temperature rise to a maximum of 45°C and 60°C, respectively. This maximum temperature was maintained for a period of 2 seconds. For positive control to verify structural damage, a few samples were heated for approximately 35 seconds to achieve 75°C in the skin samples.

After the heat shock, some skin samples were snap-frozen in liquid nitrogen at six different time points: 1, 1.5, 3, 6, 12 and 24 hours for gene expression analyses. Some skin samples were fixed at the same time points after treatment in 10% formalin for histology. Metabolic activity and gene expression levels were measured and histology, immuno-histochemical staining were performed conform the protocols used in chapter 5. The immuno staining of hsp 27, however, contains one exception. An extra incubation step in 3% hydrogen peroxide in methanol for 20 minutes was performed in order to block the endogeneous peroxidases in the epidermis.

6.2.4 Statistical analysis

All data are presented as the mean and standard deviation for a sample measurement of $n = 6$. Comparisons of gene expression levels between the control and experimental groups were performed by a one-tailed unpaired *t*-test. Comparisons of gene expression levels between the experimental groups were performed by a two-tailed unpaired *t*-test. Differences in both comparisons were considered significant at $p < 0.05$

6.3 Results

6.3.1 Calculation exposure time

The test conditions relate to the experimental conditions. To mimic the experimental situation, the initial temperature at all sides was set at 37°C. The simulations were run using the laser parameters determined in chapter 2; a wavelength of 976 nm, 4 mm in diameter and a power of 1 W.

Figure 6.1 depicts the results of the simulations. The heat distribution in the center of the skin sample along the longitudinal axis is shown. According to our simulations the surface of the skin is heated to 45°C in the dermis within 8.4 seconds (figure 6.1(a)). To achieve 60°C at the surface of the skin, it needs to be exposed to the laser for approximately 23 seconds (figure 6.1(b)). The skin samples remained at 45°C and 60°C for approximately 2 seconds after the laser was turned off. The sample was cooled after 2 seconds to 37°C, by placing the sample in 37°C medium.

The temperature at the epidermis, the surface of the skin sample, is approximately 1°C higher than 1 mm into the dermis, the bottom of the skin sample. In contrast to the heterogeneous heat distribution with time that is obtained with the immersion procedure in chapter 5, laser treatment results in a more homogeneous distribution.

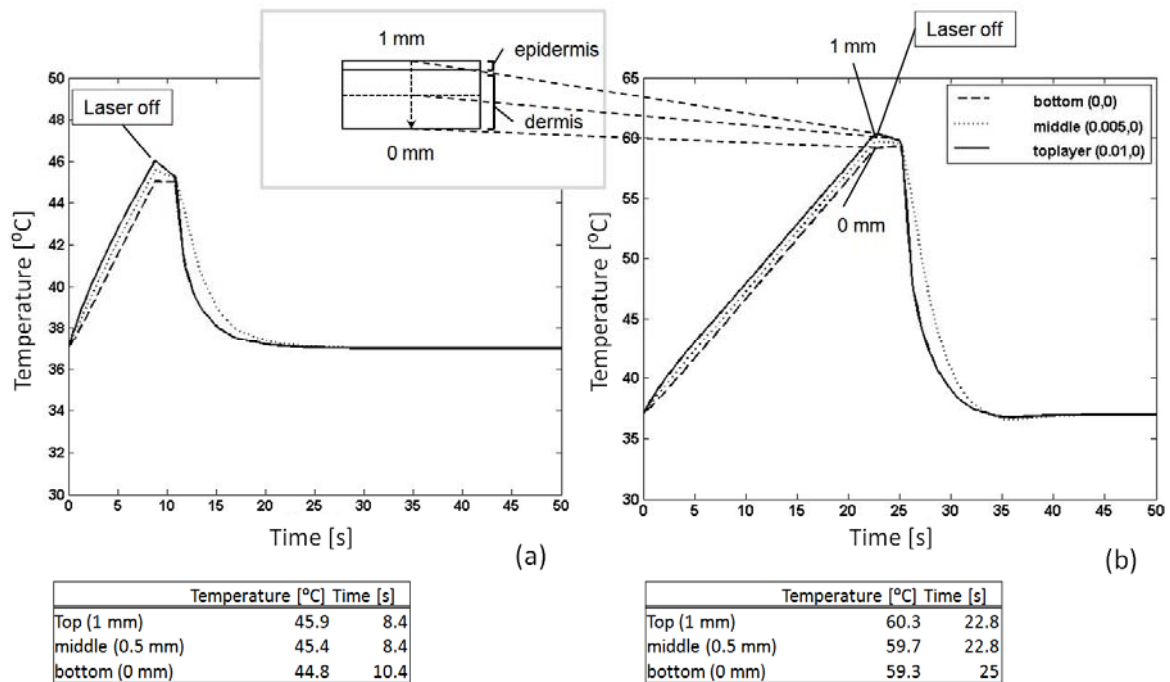


Figure 6.1: Simulation results of heating and cooling process of the skin samples with diameter 2 mm and height 1 mm exposed to a 976 nm laser diode with beam diameter of 4 mm and a power of 1W. The heating process in the skin due to laser irradiation and the recovery process to 37°C. (a) 45°C laser induced heat shock (b) 60°C laser induced heat shock.

6.3.2 Metabolic activity, structure, and damage of ex-vivo skin

The effects of the laser heat shocks on the metabolic activity are illustrated in figure 6.2. The absorption levels of the 45°C heat shocked skin samples do not differ significantly from the samples before the heat shock. The 60°C heat shocked skin samples, on the other hand, differ significantly from the control.

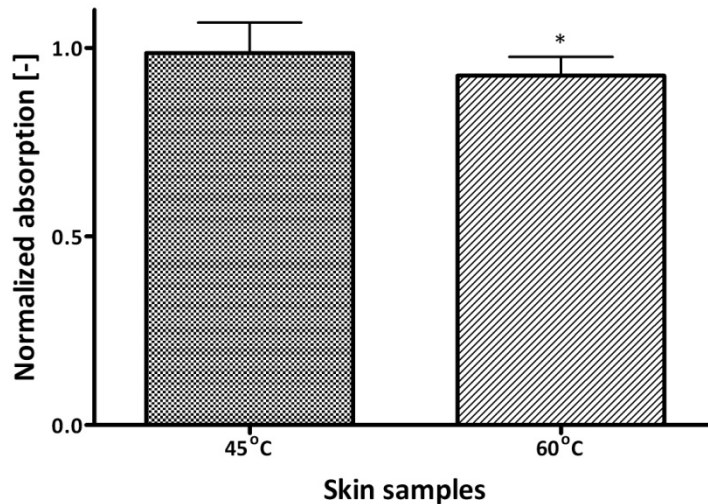


Figure 6.2: Metabolic activity 1.5 hours after the heat shock. The absorption levels are proportional to the metabolic activity. The values are normalized to the control value. The x-axis depicts the two heat shock temperatures and the y-axis the normalized absorption.

Figure 6.3 shows the results of the picosirius red and haematoxylin staining visualized with bright field microscopy (left images) and circular cross-polarized microscopy (images on the right). The collagen network of the skin samples exposed to 45°C and 60°C (figure 6.3(c-f)) visualized with the bright-field microscopy, depicted in red, does not show any visible structural change compared to the control (figure 6.3(a-b)) in contrast to the collagen network that was subjected to 75°C, figure 6.3(g-h). Structural changes can be seen, the epidermal cells are severely damaged and dermal cells are disrupted. Furthermore, structural details of the collagen network in the dermal matrix are not clearly noticeable anymore, in contrast to the 45°C and 60°C heat shock skin samples. In the figures 6.3(c) and (e) the epidermal cells, visualized in dark blue, stay intact. Furthermore, the dermis shows similar structural details as in the control sample, depicted in figure 6.3(a).

Circular cross-polarized microscopy reveals differences in fiber thickness. The mature, thick collagen fibers are colored in orange and the young, thin collagen fibers are shown in green. It is demonstrated in figures 6.3(d) and (f) that the heat shocks of 45°C and 60°C leave the collagen structure intact. Figure 6.3(h), clearly shows that heating to 75°C resulted in a disrupted collagen matrix. The ratio of orange and green fibers in this treated skin sample is changed to predominantly orange compared to the control sample.

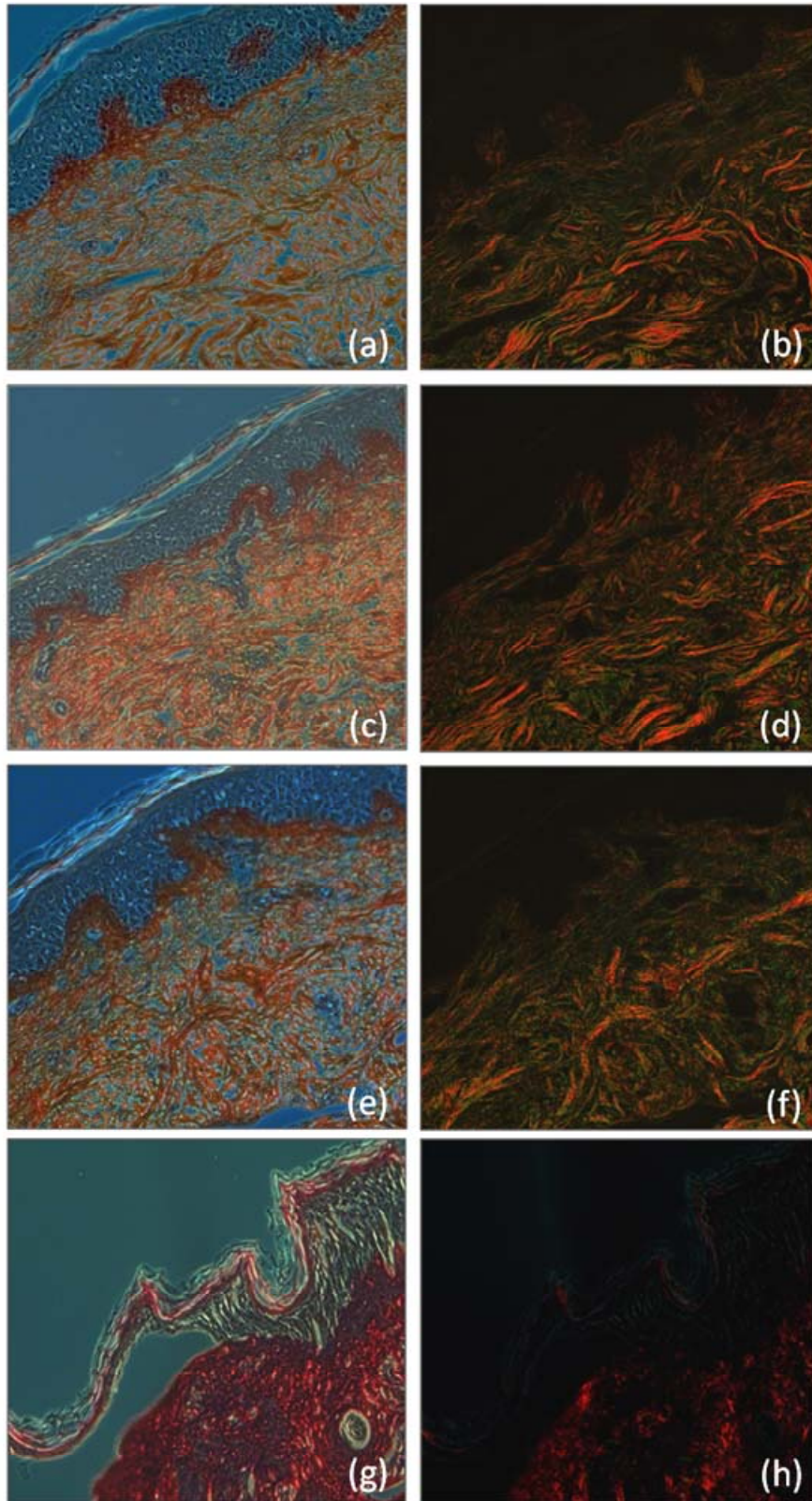


Figure 6.3: Picrosirius red with Haematoxylin staining results visualized with bright field (a, c, e, g) and cross-polarized (b, d, f, h) microscopy. Cells are depicted in dark blue and the collagen bundles are colored red. Figures 3(a) and 3(b) depict the control samples fixated after 6 hours after treatment. In figures 3(c) and 3(d) the staining on the fixated tissue samples of 6 hours after the 45°C heat shock are shown. The skin samples heat shocked at 60°C and fixated at $t = 6\text{h}$ after the pulsed heat shock is depicted in figures 3(e) and 3(f). In figures 3(g) and 3(h) results are demonstrated of a skin sample 6 hours after heating to 75°C.

In figure 6.4 the results of the immunohistochemical staining for hsp27 are shown. Heat shock protein 27 serves as a biomarker to indicate early damage response by fibroblasts.

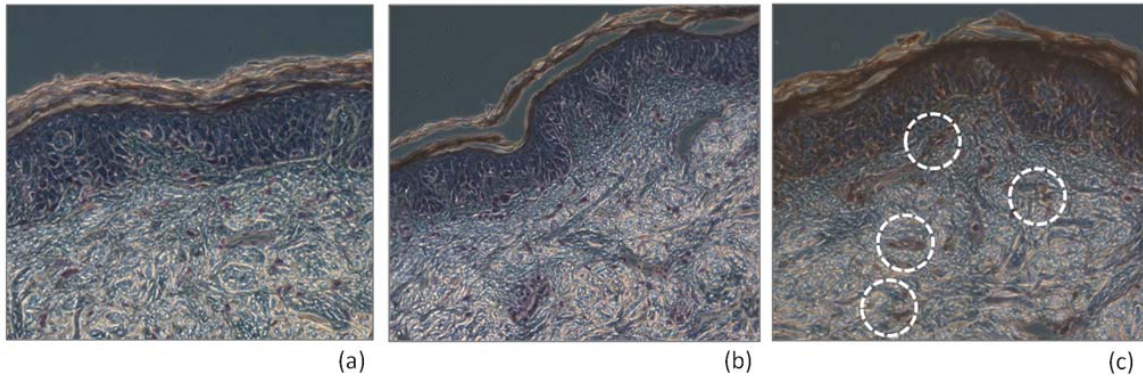


Figure 6.4: Immunohistochemical staining for hsp27 after 1.5 hours of the control skin sample kept at 37°C (a), 45°C heat shocked skin sample (b), and 60°C heat shocked skin sample (c). The dark brown region around the cells in the dermis (dashed circles) suggests the presence of hsp27. The nuclei of the cells are depicted in blue.

Expression of this protein suggests an initial response to damage. It can be seen that the laser induced heat shock of 60°C results in deposition of hsp27 around the fibroblasts, indicated by the dashed circles (figure 6.4 (c)). As shown in figure 6.4 (b), the laser induced heat shock of 45°C resulted in very little deposition of hsp27, and cannot be distinguished from the control, figure 6.4(a). Although we do not address the epidermis and therefore hsp27 synthesis by keratinocytes (Gloaguen et al., 2008) in this thesis, we would like to point out the brown coloration of the epidermis in the 60°C heat shocked sample (figure 6.4(c)), showing a clear difference compared to the 45°C heat shocked and the control samples (figures 6.4(a) and (b)).

6.3.3 Effect of the laser irradiation on the gene expression of heat shock proteins 70, 47 and 27

The average fold change of hsp70 of the cells in the skin samples over six patients per time point is shown in figure 6.5(a). It is noticed that the laser induced heat shocks of 60°C result in an elevated expression of hsp70 after 1.5 - 3 hours. Beyond three hours after the heat shock downregulation of hsp70 is noticed. The gene expression of hsp70 after the 45°C laser induced heat shocks, however, does not show any upregulation, albeit after 6 hours a downregulation of the gene can be seen.

Hsp47 gene expression is depicted in figure 6.5(b). These data show that the 60°C as well as the 45°C laser induced heat shocks resulted in an immediate overall significant increase in hsp47 mRNA. After 24 hours no significant up- or downregulation is noticed.

Regarding the mean fold changes of hsp27, figure 6.5(c) shows an overall significant instantaneous increase in expression after the laser induced heat shock of 60°C. The gene expression of hsp27 in cells in the skin samples after the laser induced heat shock of 45°C showed no significant upregulation. This seems to be consistent with histology.

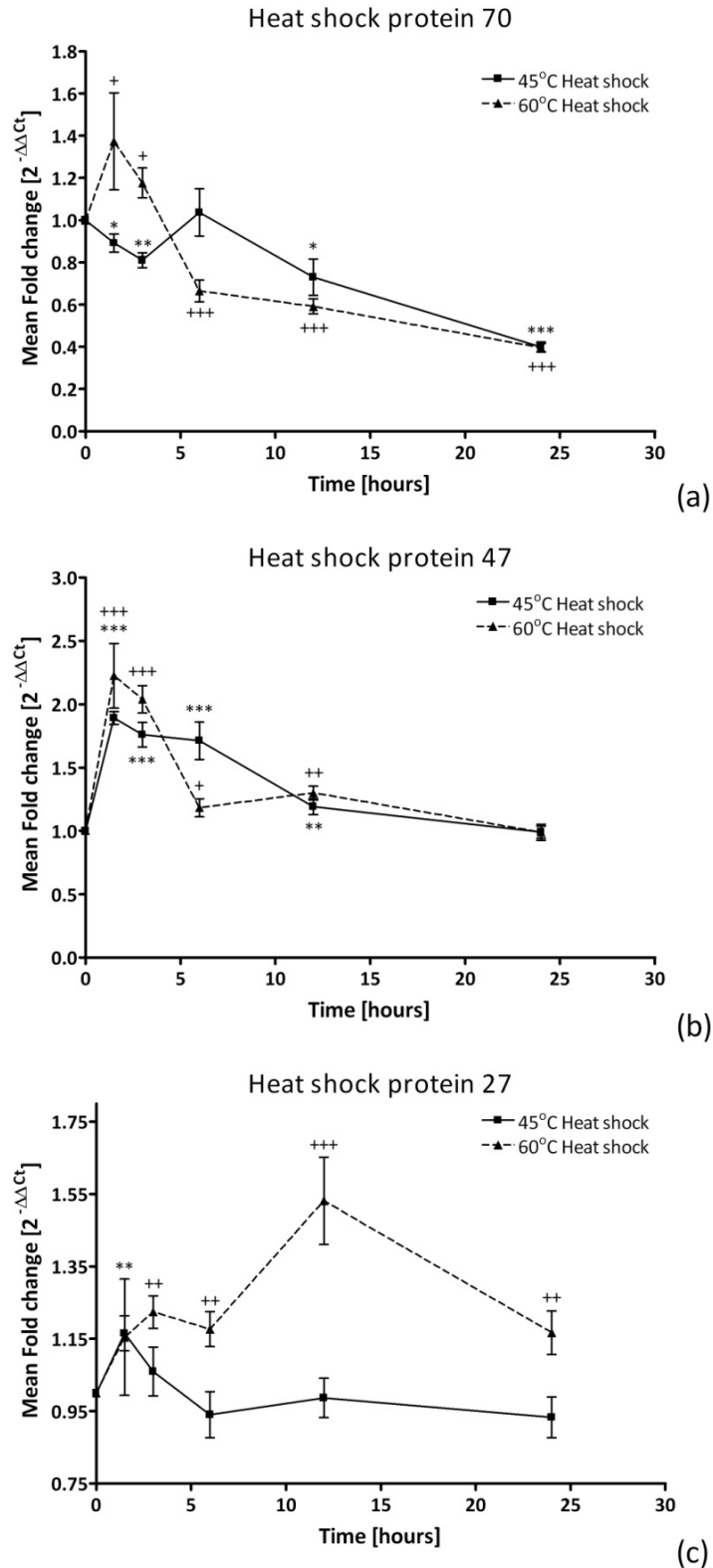


Figure 6.5: Mean fold changes, $2^{-\Delta\Delta Ct}$ of heat shock protein 70 (a), heat shock protein 47 (b) and heat shock protein 27 (c) at the different time points after exposure to the heat shock. The data are relative to the control and the reference genes β -Actin and GAPDH. The x-axis depicts the time given in hours. The y-axis shows the mean fold changes of the cells in the skin samples heat shocked at 45°C and 60°C, solid and dashed line, respectively. Data are shown as the mean \pm SD for 6 independent experiments each run in duplo with significant differences compared to control for 45°C heat shocked samples at * $p < 0.05$, ** $p < 0.01$ and *** $p < 0.001$ and for 60°C heat shocked samples at + $p < 0.05$, ++ $p < 0.01$ and *** $p < 0.001$.

6.3.4 Effect of laser irradiation on the gene expression of procollagen type I and type III

The results of the 45°C and 60°C heat shock on the expression of procollagen type I and type III are shown in figure 6.6. The figure shows the average of the fold changes over 6 patients per time point. Figure 6.6(a) depicts the fold changes of procollagen type I. A significant increase in expression can be seen after both the 45°C and the 60°C laser induced heat shocks after 1.5 hours.

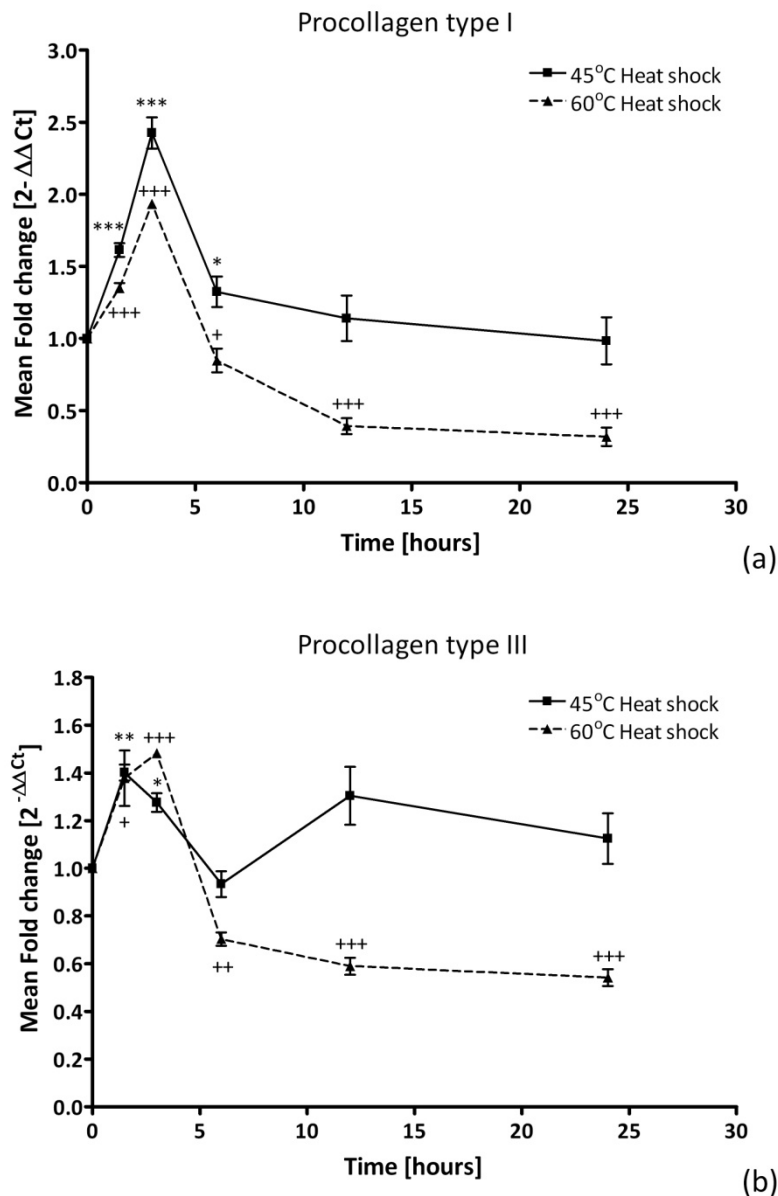


Figure 6.6: Mean fold changes, $2^{-\Delta\Delta Ct}$, of procollagen type I (a) and procollagen type III (b) at the different time points after exposure to the heat shock. The data are relative to the control and to the reference genes β -Actin and GAPDH. The x-axis depicts the time given in minutes. The y-axis shows the mean fold changes of procollagen type III and procollagen type I of the cells in the skin samples heat shocked at 45°C and 60°C, solid and dashed line, respectively. Data are shown as the mean \pm SD for 6 independent experiments each run in duplo with significant differences compared to control for 45°C heat shocked samples at * $p < 0.05$, ** $p < 0.01$ and *** $p < 0.001$ and for 60°C heat shocked samples at + $p < 0.05$, ++ $p < 0.01$ and +++ $p < 0.001$.

The 45°C laser induced heat shock results in an upregulation of procollagen type I up to 6 hours. Beyond 6 hours the gene expression does not differ from the control level. The 60°C laser induced heat shock results in an upregulation of procollagen type I the first three hours. Beyond 3 hours, procollagen type I is downregulated.

As shown in figure 6.6(b) the 45°C and 60°C laser induced heat shocks resulted in an overall significant increase in expression of procollagen type III up to 3 hours after the heat shock. Beyond three hours, the gene expression of procollagen type III, after the 45°C laser induced heat shock, returns to the level of the control, while the gene expression after the 60°C laser induced heat shock is downregulated.

6.4 Discussion

In this chapter we have shown that the laser induced heat shocks stimulate *ex-vivo* skin to upregulate gene expression of procollagen type I and procollagen type III as an initial response. The heat shocks of 45°C as well as the heat shocks of 60°C caused an upregulation of procollagen type I and type III within 1.5 hours after the stimulus.

Although the upregulation was significantly relevant, the experiments were performed on *ex-vivo* human skin. Here several other factors could play a role in up- or downregulation of a gene and the cells are not so well controlled as *in-vitro* in chapter 3. In literature fold change values between 0.5 and 2 are considered not to be biologically relevant (Zeller et al., 2010). Taking this into account, only after the heat shocks of 45°C the gene expression of procollagen type I is upregulated, while the heat shock of 60°C results in a significant downregulation after 12 hours. Additionally, it can be concluded that the up- and downregulated gene expression of procollagen type III and the heat shock proteins 70, 47 and 27 will be considered as not biologically relevant.

Gene expression analysis of hsp27 showed not to be biologically relevant, while immunohistological analysis nonetheless appeared to demonstrate an elevated brown coloration, suggesting the presence of heat shock protein 27 around the cells in skin samples exposed to the 60°C laser induced heat shock (figure 6.4). Since hsp27 plays an important role in protecting cells against apoptosis (Snoeckx *et al.*, 2007), it is tempting to suggest that a 60°C heat shock causes damage to the cells. The upregulation was not visible on genetic level, but evidently hsp27, as a constitutive protein, can be upregulated at protein level as well.

A major problem for the interpretation of the results of chapter 5 as well as chapter 6 is that the “heat shock” is not a step function in time. In the mono-layer experiments in chapters 3 and 4 the temperature increase and decrease can be achieved very fast, so the exposure times to the different temperatures are fairly accurate. In the *ex-vivo* skin samples it takes much longer to reach the required temperatures of 45°C and 60°C (for the immersion experiments up to 10 seconds in the laser irradiation experiments up to

23 seconds). In addition, the immersion experiments of *ex-vivo* skin samples lead to a non-uniform temperature distribution in the skin with the longest exposure times to high temperatures at the skin surface, while the laser treatment leads to a more homogeneous distribution.

We have shown previously that thermal shocks stimulate the cells in *ex-vivo* skin (chapter 5). With this pilot study, we have shown that laser induced heat shocks of 45°C also result in an upregulation of procollagen type I. However, more studies have to be performed to unravel the exact results of laser induced heating of the skin.

6.5 Acknowledgements

The authors would like to thank the Catharina Hospital in Eindhoven for providing the tissue. Furthermore, they would like to thank Sarita Soekhradj-Soechit for the immunohistological analysis of the paraffinized skin samples.

Chapter 7

General discussion

7.1 Introductory remarks

Skin rejuvenation is defined as stopping or reversing the characteristics of skin aging (Gilchrest, 2007b; Gilchrest and Bohr, 2006; Rattan, 1998). Skin aging is a natural process. In recent years this subject has led to an increased research interest, fueled by the cosmetic industry (Capon and Mordon, 2006; Goldberg, 2006; Sadick, 2006). However, fundamental knowledge on the underlying physiological processes is still scarce. Despite this, many skin rejuvenation techniques are available in practice and, as a consequence, some are successful and some are not (chapter 1). The non-ablative treatments, specifically non-ablative laser techniques, are of interest as these optical techniques enable selective heating without compromising the integrity of the skin.

Laser irradiation is said to stimulate human dermal fibroblasts via two distinct mechanisms. The first mechanism is thermal stimulation, in which the energy of a photon is converted into by chromophores present in the skin. The second mechanism is photochemical stimulation of the human dermal fibroblasts. Hereby, photons are absorbed by cytochrome-c on the membranes of the cells. By doing so, the metabolic activity of the HDFs, and therefore their protein synthesis, is said to be stimulated (Dinh, 2006). In this thesis, we have chosen to primarily focus on the first mechanism, the thermal effect.

As a consequence of a heat shock at a certain temperature and exposure time, skin can either be stimulated or damaged (Watanabe, 2008). As a result, upregulation of the production of constructive proteins, (e.g. collagen, elastin and proteoglycans) and heat shock proteins can be achieved (Snoeckx et al., 2007).

The goal of this research is to elucidate the effect of heat shocks on both fibroblasts in culture and skin explants. This knowledge can be used for improvement of existing rejuvenation techniques or in other areas of (bio-) medical research, such as tissue engineering and cancer treatment (Lecomte et al., 2010).

In the following sections the adopted methodologies are analysed, namely, the experimental and numerical models, the application of the heat shocks and biomarker panel (section 7.2). The main results of the presented studies will be summarized in section 7.3. Directions for future perspectives are indicated in section 7.4.

7.2 Model systems

The research methods used to study viability, metabolic activity, gene expression and protein production are all destructive in nature. This makes *in-vivo* studies difficult or impossible to perform. Animal studies are not an option because of ethical reasons. Studies involving human volunteers are also problematic, because of the invasive nature

of collection skin biopsies. These issues motivated the use of *in-vitro* cell studies and *ex-vivo* skin, as first attempts to study the reaction of cells in skin to heat stimulation.

It is known that many rejuvenation methods are based on a wound healing response of the skin and evidently our used model systems are not suitable for this. Our focus has been on non-ablative techniques. However, it has been shown that 60°C pulses longer than 2 seconds lead to considerable cell damage (chapter 4). This does not mean that these settings cannot be used in practice, but it is clear that a wound healing model is required to further investigate this.

7.2.1 Experimental model system

Any heat pulse method that is used will inevitably result in a heterogeneous temperature distribution in the skin, so different parts of the skin “feel” different heat shocks. Thus, to be able to predict the response of skin after exposure to a laser pulse, it is important to clarify how skin behaves to various heat pulses. Important parameters are the temperature, as well as the pulse duration. This motivated the initial experiments involving cell cultures, where temperature and time could be controlled accurately and independently. For this an adult cell line of HDFs was used, since these cells are representative of aging skin.

The cell culture system and the technique to apply the heat shocks have led to reproducible results. The developed experimental set up enabled large scale studies, where many variables can be introduced. We would have liked to determine from these studies a theoretical model that could predict collagen production as a function of temperature and pulse duration. However, to develop such a model more variables, such as the measurement of different MMPs must also be investigated. Furthermore, these tests are performed in a 2D cell culture, which does not physiologically relate to the 3D matrix of human dermis.

For *ex-vivo* studies skin obtained from abdominoplastic surgery was used (chapter 5 and 6). The advantage of this experimental setup is that it approaches the physiological relevance for investigation skin rejuvenation. However, our METC (“medisch etische toetsings commissie”) approval required that this material was anonymized after the surgical procedure. This is a severe disadvantage, because variations found in the results cannot be related to possible characteristic features of individual patients. Indeed, it would be interesting and quite relevant to investigate the correlation of the cellular response with the age of the skin. The latter would require a different protocol for including patients, and thus a more extensive medical ethical approval, and a multi-center trial to get enough samples in a reasonable time period.

7.2.2 Numerical model system

Different model systems were used to describe the heat distribution of the skin samples heated by laser irradiation and of the skin samples that were immersed in heated PBS. Both models were designed for *in-vitro* settings.

In chapters 2 and 6, the probability of photon absorption in the skin was estimated, which was multiplied by the laser power. This provided heat sources to calculate the diffusion process throughout the skin. The advantage of using Monte Carlo simulation is two-fold: First, it is three dimensional, which approaches the experimental studies more accurately. Secondly, it predicts the absorption of photons by the skin using the different skin properties of the skin layers.

Settings to simulate the temperature distribution in the *ex-vivo* skin studies in chapter 5 and 6 were chosen in such a way that the center or the bottom of the dermis of the skin sample was heated for 2 seconds, respectively. In the case of the immersion experiment (chapter 5), this led to a temperature gradient from the edges to the center of the skin sample, leaving the cells in the outer region exposed longer to the heat shock temperatures than the inner cells (chapter 5). In the case of the laser heated skin samples, this led to a relatively long exposure time to reach 60°C in the dermal layer.

Therefore, the investigation of different exposure times of 45°C and 60°C is highly relevant in acquiring more understanding of the response of HDFs to the thermal stimuli in the skin.

7.2.3 Heat shock application

As stated above laser methods can have a thermal as well as a photo-chemical effect. To be able to separate those we have chosen to use immersion experiments for the *in-vitro* cell cultures. The method was simple, reproducible and accurate.

To thoroughly investigate the effect of specific temperatures on HDFs either in *in-vitro* or in *ex-vivo* skin, the immersion protocol was most accurate. The temperature reached with the laser induced heating process was difficult to measure. Some preliminary experiments for validation of the skin model were performed (chapter 2). However, more extensive research is necessary to accurately validate the model.

Furthermore, it should be taken into account that the two heating processes differ in the way they “deliver” the heat in the skin. The temperature increase generated by the laser is predominantly induced by the energy of the photons that has been absorbed and converted into heat by chromophores in the skin, while the temperature increase caused by the immersion procedure is purely a conduction process of heat. For comparison of the two heating procedures further extensive research is required.

7.2.4 Biomarker panel

Gene expression analysis is widely used to determine early synthesis of a protein. However, the method is based on the amount of RNA present within the cells. It should therefore be taken into account that an upregulation in gene expression does not necessarily result in an upregulation of the translated protein.

Upregulation of a gene can be measured accurately over time with qPCR techniques. Therefore, many papers report statistically significant differences in fold changes which are just above 1. In literature fold change values between 0.5 and 2 are considered not to be biologically relevant (Zeller et al., 2010). Because of the biological diversity of human tissue, this is taken into account in the interpretation of the gene expression results of the *ex-vivo* skin sample studies (chapter 5 and 6).

The use of heat shock proteins as biomarkers was shown to be useful. Our results demonstrated the response to the heat shock by elevated levels of hsp70. Furthermore, hsp27 has shown to be a relevant marker for damage at cellular level, although the staining procedure for hsp27 must be further improved. Additionally, measuring the hsp47 RNA levels has indicated their relevance in collagen type I synthesis, since the data sets of procollagen type I and hsp47 correlated (chapters 3-6).

One of the most dominant and important building blocks of the the structure of the dermal matrix is collagen type I. However, skin rejuvenation comprises much more than collagen type I synthesis. Other important structural dermal proteins that are worthwhile investigating are elastin and proteoglycans. The production of collagen type III is also an interesting research area that should be adressed, since the ration of collagen type I and collagen type III indicates whether the newly formed skin is healthy or that scar formation has taken place. Therefore, correct remodeling of the extracellular matrix of the dermis is important for development of new skin. In this thesis we look at remodeling markers for collagen type I: procollagen type I carboxy-terminal propeptide, P1P, and carboxy-terminal telopeptide of type I, ICTP, since our focus is on the synthesis of collagen type I. However, the process of dermal remodeling comprises a far more complex physiological process. Besides P1P and ICTP it also involves, among others, the ration of collagen type I and collagen type III synthesis, matrix metalloproteinases, MMPs, and tissue inhibitors of metalloproteinases, TIMPs (Madlener et al., 2006; Park et al., 2007; Vaalamo et al., 2006). Using them as biomarkers would be beneficial for further understanding of the dermal remodeling process.

7.3 Main findings

The effect of non-ablative laser treatment was investigated in this thesis. The heat distribution, caused by laser irradiation, was simulated and examined in chapter 2. Furthermore, the model was used to perform parametric studies to obtain the required

laser parameter settings; wavelength, beam diameter and output power. It was demonstrated that a 976 nm laser with a beam diameter of 4 mm and a power of 1 W matched the requirements of the design best (table 2.6). Further simulations revealed that the exposure times to achieve 45°C and 60°C were 8.4 seconds and 22.6 seconds, respectively (fig 2.4).

The calculated heat distribution and the estimated exposure times in chapter 2, provided more insight in the thermal gradient in which the skin would be exposed to in an *in-vivo* situation.

In table 7.1 the effect of the thermal heat shocks on the gene and protein expression of collagen type I and heat shock protein 27 is summarized. It also provides an overview of the correlation between gene and protein expression. Collagen type I is depicted as one of the most important constituents of young skin and heat shock protein 27 is chosen, because of its relevance to thermal damage that is induced by the applied heat shocks.

It was demonstrated that HDFs *in-vitro* produced more collagen type I after being exposed to a 2 seconds pulsed heat shock (figure 3.6). As can be seen in table 7.1, this increase in protein expression was preceded by an increase in procollagen type I gene expression.

Table 7.1: Summary of the effects of the thermal stimuli of 45°C and 60°C to HDFs *in-vitro* and in *ex-vivo* skin. The influence of the heat shock is indicated with – (decrease) or with + and ++ (increase). No change is indicated with ‘o’ and not available with N.A.

Chapter	Applied heat shock [s]	Collagen type I				Heat shock protein 27			
		Gene expression		Protein synthesis		Gene expression		Protein expression	
		45°C	60°C	45°C	60°C	45°C	60°C	45°C	60°C
3 & 4	2	+	+	+	++	-	++	N.A.	N.A.
	4	+		+		+			
	8	++		++		+			
4	10	+	N.A.	++	N.A.	+	N.A.	N.A.	N.A.
	16	+		-		++			
	21	+		-		++			
5	8 and 10	+	+	N.A.	N.A.	o	+	o	+
6	8 and 21	+	+	N.A.	N.A.	o	+	o	+

Results of hsp27 gene expression revealed that the 60°C heat shock caused an upregulation of this gene; a first indication that the HDFs are compromised after a 60°C heat shock.

Since our simulations indicated that heating of skin causes a temperature gradient, investigation of the combination of temperature and exposure time is essential. In

chapter 4 the effect of different exposure times in combination with the chosen heat shock temperatures, 45°C and 60°C, is demonstrated. Findings suggest, as can be seen in table 7.1 and figure 4.4, that the optimal exposure time range for the 45°C heat shock temperature to produce the highest amount of net collagen content is 8 to 10 seconds. Furthermore, after 48 hours the gene expression levels returned to control levels, which indicate the end of the effect of the stimulus. Additionally, the 60°C heat shock used with an exposure time beyond 2 seconds has evidently been shown to be harmful for the cultured HDFs (figure 4.1).

The question of how fibroblasts in the skin are influenced by the heat shocks is still to be answered. Therefore, the influence of the thermal stimuli on HDFs in *ex-vivo* human skin was investigated (chapter 5). Both heat shock temperatures showed an upregulation of procollagen type I (table 7.1 and figure 5.5). However, in conjuncture with the calculated prediction of thermal damage, visualizing the early damage marker hsp27 appeared to reveal that the 60°C heat shock, in contrast to the 45°C, might have induced damage (figure 5.6).

As mentioned in the general introduction, the present thesis focuses on the thermal stimulus of the non-ablative laser treatments. Therefore, a pilot study was performed to study the effect of the heat shocks of the same temperature, as used in chapter 5, only induced by a laser. The effect of a laser induced heat shock of 45°C has also been shown to stimulate the gene expression of collagen type I. Furthermore, it demonstrated that the 60°C laser induced heat shock also compromised the HDFs in the skin, because gene upregulation (table 7.1) as well as supposed protein expression of hsp27 was noticed (figure 6.4).

Results of chapters 5 and 6 demonstrated that the heating process of laser irradiation differed from the heating process by immersion of the skin sample. The irradiated skin samples are heated for approximately 2 seconds at 45°C and 60°C, while the immersed skin samples were heated for 8 and 10 seconds at 45°C and 60°C, respectively.

7.4 Recommendations for future perspectives

The present thesis demonstrates that heat shocks of 45°C have resulted in an increase in collagen type I synthesis and that 60°C heat shocks beyond 2 seconds are harmful for cell cultures. However, as mentioned in this chapter, skin rejuvenation is far more complex. Therefore, to fully unravel the physiological implications of skin rejuvenation upon thermal stimuli several recommendations for future work can be provided.

For example *in-vitro* studies, that address stimulation rather than injury, should aim at different temperatures between 45°C and 60°C. Since the present thesis has shown that heating the dermis is not a step function in time, it is of interest to investigate different temperatures between 45°C and 60°C with different exposure times. For the

investigation of combinations of exposure time and temperature that induce thermal damage, it is recommended to use a different model, such as a wound healing model.

Recommendations for investigation of the physiological process, the question whether production of proteoglycans and elastin will be stimulated by thermal stimuli also needs to be addressed. For regeneration of skin these proteins play an important role as “filling moisturizers” and “elasticity providers”, respectively. Without these proteins the skin would become stiff and “scar-like”.

Another recommendation is extending the *in-vitro* cell studies to cells seeded in three dimensional matrices, for the purpose of quantifying the amount of synthesized proteins.

The present work involves two extreme model systems, one encompassing cells alone and the other employing *ex-vivo* skin. The use of full thickness skin equivalents, incorporating keratinocytes and fibroblasts, could be argued, because such an approach would be necessarily costly. However, it is an important step for enabling similar test conditions for the fibroblasts. Furthermore, for future *ex-vivo* skin research it is also relevant to investigate the correlation between the age of the skin and the subsequent response of the cells in the skin.

Before testing *in-vivo* a non-invasive method for measuring newly formed dermal components should be developed, to obviate the need for taking a biopsy. Consequently, well-defined *in-vivo* studies should be performed as well. Here, it should be taken into account that such studies are time consuming and are difficult to interpret without proper background information that can be obtained as mentioned above.

The development of a skin model (as in chapter 2) is helpful for the prediction of the heat distribution or even for the prediction of collagen remodeling. It should be taken into account that extensive validation is necessary. Furthermore, more detailed data about exposure time and heat shock temperature would be beneficial for the development of such a model.

Ultimately, the combination of a well-validated skin model and experimental data obtained from *in-vivo* studies could lead to a tool that can be used in multiple areas of skin rejuvenation research, such as wound healing, scar formation and the development of preventative or treatment strategies.

Bibliography

Agache, P. G., Monneur, C., Leveque, J. L., De Rigal, J., (2007). Mechanical properties and Young's modulus of human skin *in vivo*. Archives of Dermatologic Restoration 269, 221-232.

Altshuler, G. B., Anderson, R. R., Manstein, D., Zenzie, H. H., Smirnov, M. Z., (2007). Extended theory of selective photothermolysis. Lasers in Surgery and Medicine 29, 416-432.

Anderson, R. R., Parrish, J. A., (2007). The optics of human skin. Journal of Investigative Dermatology 77, 13-19.

Atiyeh, B. S., Dibo, S. A., (2009). Nonsurgical nonablative treatment of aging skin: radiofrequency technologies between aggressive marketing and evidence-based efficacy. Aesthetic Plast.Surg. 33, 283-294.

Bailey, A. J., (2007). Review: Molecular mechanisms of ageing in connective tissues. Mechanisms of Ageing and Development 122, 735-755.

Bailey, A. J., Paul, R. G., Knott, L., (2007). Review: Mechanisms of maturation and ageing of collagen. Mechanisms of Ageing and Development 106, 1-56.

Bancroft, J. D., Gamble, M., (2002). Theory and Practice of Histological Techniques. Harcourt Publishers.

Bashkatov, A. N., Genina, E. A., Kochubey, V. I., Tuchin, V. V., (2005). Optical properties of human skin, subcutaneous and mucous tissues in the wavelength range from 400-2000 nm. Journal of Physics section D: Applied Physics 35, 2543-2555.

Bernerd, F., Asselineau, D., (2006). UVA exposure of human skin reconstructed *in vitro* induces apoptosis of dermal fibroblasts: subsequent connective tissue repair and implications in photoaging. Cell Death and Differentiation 5, 792-802.

Biesman, B. S., (2007). Non-invasive skin tightening. Aesthetic Dermatology Phototherapy 38-40.

Bjerring, P., (2006). Photorejuvenation - An Overview. Medical Laser Application 19, 186-195.

Bjerring, P., Christiansen, K., Troilius, A., Dierickx, C., (2006). Facial Photo Rejuvenation Using Two different Intense Pulsed Light (IPL) Wavelength Bands. Lasers in Surgery and Medicine 34, 120-126.

Bjerring, P., Clement, M., Heickendorff, L., Hybecker, H., Kiernan, M., (2007). Dermal collagen production following irradiation by dye laser and broadband light source. *Journal of Cosmetic & Laser Therapy* 4, 39-43.

Bonelli, M. A., Alfieri, R. R., Petronini, P. G., Brigotti, M., Campanini, C., Borghetti, A. F., (1999). Attenuated expression of 70-kDa heat shock protein in WI-38 human fibroblasts during aging in vitro. *Exp.Cell Res.* 252, 20-32.

Bowers, W., Blaha, M., Alkhyat, A., Sankovich, J., Kohl.J., Wong, G., Patterson, D., (2007). Artificial human skin: cytokine, prostaglandin, HSP70 and histological responses to heat exposure. *Journal of Dermatological Science* 20, 172-182.

Bowler, P., (2007). Radio Frequency: A Real Non-Surgical Face-Lift? *Aesthetic Medicine* 49-52.

Branchet, M. C., Boisinic, S., Frances, C., Robert, A. M., (2007). Skin thickness changes in normal aging skin. *Gerontology* 36, 28-35.

Breuls, R. G., Mol, A., Petterson, R., Oomens, C. W., Baaijens, F. P., Bouten, C. V., (2003). Monitoring local cell viability in engineered tissues: a fast, quantitative, and nondestructive approach. *Tissue Eng* 9, 269-281.

Brown, S. A., Farkas, J. P., Arnold, C., Hatef, D. A., Kim, J., Hoopman, J., Kenkel, J. M., (2007). Heat shock proteins 47 and 70 expression in rodent skin model as a function of contact cooling temperature: Are we overcooling our target? *Lasers Surg.Med.* 39, 504-512.

Capon, A., Mordon, S., (2006). Can Thermal Lasers Promote Skin Wound Healing? *American Journal of Clinical Dermatology* 4, 1-12.

Crochet, J. J., Gnyawali, S. C., Chen, Y., Lemley, E. C., Wang, L. V., Chen, W. R., (2006). Temperature distribution in selective laser-tissue interaction. *J.Biomed.Opt.* 11, 34031.

Daamen, W. F., Veerkamp, J. H., van Hest, J. C., van Kuppevelt, T. H., (2007). Elastin as a biomaterial for tissue engineering. *Biomaterials* 28, 4378-4398.

Dams, S. D., de Liefde-van Beest, M., Nuijs, A. M., Oomens, C. W. J., Baaijens, F. P. T., (2010). Pulsed heat shocks enhance procollagen type I and procollagen type III expression in human dermal fibroblasts.

Dierickx, C. C., (2007). The role of deep heating for noninvasive skin rejuvenation. *Lasers in Surgery and Medicine* 38, 799-807.

Dierickx, C. C., Anderson, R. R., (2007). Visible light treatment of photoaging. *Dermatologic Therapy* 18, 191-208.

Dimri, G. P., Lee, X., Basile, G., Acosta, M., Scott, G., Roskelley, C., Medrano, E. E., Linskens, M., Rubelj, I., Pereira-Smith, O., Peacocke, M., Campisi, J., (2007). A biomarker

that identifies senescent human cells in culture and in aging skin in vivo. *Cell Biology* 92, 9363-9367.

Dinh, V., (2006). Low-Power Laser Therapy. *Biomedical Photonics Handbook*. CRC Press, pp. 48-1-48-25.

Diridollou, S., Vabre, V., Berson, M., Vaillant, L., Black, D., Lagarde, J. M., Grégoire, J. M., Gall, Y., Patat, F., (2007). Skin ageing: Changes of physical properties of human skin in vivo. *International Journal of Cosmetic Science* 23, 353-362.

Duval, C., Smit, N. P., Kolb, A. M., Regnier, M., Pavel, S., Schmidt, R., (2002). Keratinocytes control the pheo/eumelanin ratio in cultured normal human melanocytes. *Pigment Cell Res.* 15, 440-446.

Ebling, Rook, Wilkinson, (1992). *Textbook of Dermatology*. Blackwell Scientific Publications.

Eze, R., Kumar, S., (2010). Laser transport through thin scattering layers. *Appl.Opt.* 49, 358-368.

Farber, J. L., Rubin, E., (1998). *Pathology*. Lippincott Williams & Wilkins.

Fitzpatrick, T. B., (1988). The validity and practicality of sun-reactive skin types I through VI. *Arch.Dermatol.* 124, 869-871.

Fitzpatrick, T. B., SEIJI, M., McGUGAN, A. D., (1961). Melanin pigmentation. *N.Engl.J.Med.* 265, 430-434.

Frank, S., Oliver, L., Lebreton-De Coster, C., Moreau, C., Lecabellec, M. T., Michel, L., Vallette, F. M., Dubertret, L., Coulomb, B., (2004). Infrared radiation affects the mitochondrial pathway of apoptosis in human fibroblasts. *J.Invest Dermatol.* 123, 823-831.

Gamborg Andersen, G., Petrunin, V. V., Baurichter, A., (2010). Numerical calculations of pulsed laser heating of non-isotropic materials. *Proceedings COMSOL Multiphysics User's Conference 2005*.

Geronemus, R. G., (2006). Fractional Photothermolysis: Current and Future Applications. *Lasers in Surgery and Medicine* 38, 169-176.

Giacomoni, P. U., D'Alessio, P., (2007). Open questions in photobiology IV. Photoaging of the skin. *Journal of Photochemistry and Photobiology* 33, 267-272.

Giacomoni, P. U., Rein, G., (2007). Review: A mechanistic model for the aging of human skin. *Micron* 35, 179-184.

Gilchrest, B. A., (2007a). A review of skin ageing and its medical therapy. *British Journal of Dermatology* 135, 867-875.

Gilchrest, B. A., (2007b). Clinical features of photageing differ from those of intrinsic ageing. *Journal of Dermatological Treatment* 7, S5-S6.

Gilchrest, B. A., (2007c). The spectrum of photodamage and its treatment. *Dermatology* 190, 260-264.

Gilchrest, B. A., (2007d). The variable face of photoaging: Influence of skin type. *Cosmetics & Toiletries* 107, 41-42.

Gilchrest, B. A., Bohr, V. A., (2006). Aging processes, DNA damage, and repair. *Federation of American Societies for Experimental Biology Journal* 11, 322-330.

Gilchrest, B. A., Garmyn, M., Yaar, M., (2007). Aging and photoaging affect gene expression in cultured human keratinocytes. *Archives of Dermatology* 130, 82-86.

Gloaguen, V., Krausz, P., Brudieux, V., Closs, B., Leroy, Y., Guerardel, Y., (2008). Structural patterns of rhamnogalacturonans modulating Hsp-27 expression in cultured human keratinocytes. *Molecules*. 13, 1207-1218.

Goldberg, D. J., (2006). Lasers for Facial Rejuvenation. *American Journal of Clinical Dermatology* 4, 225-234.

Groff, W. F., Fitzpatrick, R. E., Uebelhoer, N. S., (2008). Fractional carbon dioxide laser and plasmakinetic skin resurfacing. *Semin.Cutan.Med.Surg.* 27, 239-251.

Hamblin, M. R., Demidova, T. N., (2007). Mechanisms of Low Level Light Therapy. *Proceedings of the Society for Photo-optical Instruments and Engineering* 6140.

Hantash, B. M., Bedi, V. P., Chan, K. F., Zachary, C. B., (2007). Ex vivo histological characterization of a novel ablative fractional resurfacing device. *Lasers Surg.Med.* 39, 87-95.

Hirano, S., Shelden, E. A., Gilmont, R. R., (2004). HSP27 regulates fibroblast adhesion, motility, and matrix contraction. *Cell Stress.Chaperones*. 9, 29-37.

Humbert, P., Agache, P. G., (2004). *Measuring the Skin*. Springer.

Kameyama, K., (2008). Histological and clinical studies on the effects of low to medium level infrared light therapy on human and mouse skin. *J.Drugs Dermatol.* 7, 230-235.

Kim, K., Guo, Z., (2007). Multi-time-scale heat transfer modeling of turbid tissues exposed to short-pulsed irradiations. *Comput.Methods Programs Biomed.* 86, 112-123.

Knott, L., Bailey, A. J., (2007). Collagen Cross-Links in Mineralizing Tissues: A Review of Their Chemistry, Function, and Clinical Relevance. *Bone* 22, 181-187.

Kovalchin, J. T., Wang, R., Wagh, M. S., Azoulay, J., Sanders, M., Chandawarkar, R. Y., (2006). In vivo delivery of heat shock protein 70 accelerates wound healing by up-regulating macrophage-mediated phagocytosis. *Wound.Repair Regen.* 14, 129-137.

- Krutmann, J., (2007). Skin aging. *Hautarzt* 54, 809-817.
- Kurban, R. S., Bhawan, J., (2007). Histologic changes in skin associated with aging. *Journal of Dermatology, Surgery & Oncology* 16, 908-914.
- Kuroda, K., Tsukifuji, R., Shinkai, H., (1998). Increased expression of heat-shock protein 47 is associated with overproduction of type I procollagen in systemic sclerosis skin fibroblasts. *J.Invest Dermatol.* 111, 1023-1028.
- Labat-Robert, J., Robert, L., (2007). Mini-Review: Aging of the extracellular matrix and its pathology. *Experimental Gerontology* 23, 5-18.
- Laszlo, A., (2007). The relationship of heat-shock proteins, Thermotolerance, and Protein Synthesis. *Experimental Cell Research* 178, 401-414.
- Laubach, H. J., Tannous, Z., Anderson, R. R., Manstein, D., (2006). Skin responses to fractional photothermolysis. *Lasers Surg.Med.* 38, 142-149.
- Lecomte, S., Desmots, F., Le, M. F., Le, G. P., Michel, D., Christians, E. S., Le, D. Y., (2010). Roles of heat shock factor 1 and 2 in response to proteasome inhibition: consequence on p53 stability. *Oncogene*.
- Leveque, J. L., Corcuff, P., De Rigal, J., Agache, P. G., (2007a). In vivo studies of the evolution of physical properties of the human skin with age. *International journal of dermatology* 23, 322-329.
- Leveque, J. L., De Rigal, J., Agache, P. G., Monneur, C., (2007b). Influence of ageing on the in vivo extensibility of human skin at low stress. *Archives of Dermatologic Research* 269, 127-135.
- Lewis, J., Raff, M., Roberts, K., Watson, J. D., Alberts, B., Bray, D., (1994). *Molecular Biology of the Cell*. Garland Publisher.
- Longo, L., Lubart, R., Friedmann, H., Lavie, R., (2007). A possible mechanism for visible-light-induced skin rejuvenation. *Proceedings of the Society for Photo-optical Instruments and Engineering* 5610, 158-164.
- Lu, H., Edwards, C., Gaskell, S., Pearse, A., Marks, R., (1996). Melanin content and distribution in the surface corneocyte with skin phototypes. *Br.J.Dermatol.* 135, 263-267.
- Lubart, R., Friedmann, H., Lavie, R., Longo, L., Krutmann, J., Baruchin, O., Baruchin, A. M., (2007). A reasonable mechanism for visible light-induced skin rejuvenation. *Lasers in Medicine and Science* 22, 1-3.
- Madlener, M., Parks, W. C., Werner, Sa., (2006). Matrix Metalloproteinases (MMPs) and Their Physiological Inhibitors (TIMPs) Are Differentially Expressed during Excisional Skin Wound Repair. *Experimental Cell Research* 242, 201-210.

Manstein, D., Herron, G. S., Sink, R. K., Tanner, H., Anderson, R. R., (2006). Fractional Photothermolysis: A New Concept for Cutaneous Remodeling Using Microscopic Patterns of Thermal Injury. *Lasers in Surgery and Medicine* 34, 426-438.

Marshall, H., Kind, C. N., (2007). Detection and cellular localization of stress-induced 72kD heat shock protein in cultured swiss 3T3 mouse fibroblasts. *Toxicology in Vitro* 8, 545-548.

Mayes, A. E., Holyoak, C. D., (2008). Repeat mild heat shock increases dermal fibroblast activity and collagen production. *Rejuvenation.Res.* 11, 461-465.

Mertyna, P., Goldberg, W., Yang, W., Goldberg, S. N., (2009). Thermal ablation a comparison of thermal dose required for radiofrequency-, microwave-, and laser-induced coagulation in an ex vivo bovine liver model. *Acad.Radiol.* 16, 1539-1548.

Mitchell, L. G., Campbell, N. A., Reece, J. B., (1999). *Biology*. Adison-Wesley.

Naitoh, M., Hosokawa, N., Kubota, H., Tanaka, T., Shirane, H., Sawada, M., Nishimura, Y., Nagata, K., (2001). Upregulation of HSP47 and collagen type III in the dermal fibrotic disease, keloid. *Biochem.Biophys.Res.Comm.* 280, 1316-1322.

Narurkar, V. A., (2006). Lasers, light sources, and radiofrequency devices for skin rejuvenation. *Semin.Cutan.Med.Surg.* 25, 145-150.

Narurkar, V. A., (2007). Skin rejuvenationwith microthermal fractional photothermolysis. *Dermatologic Therapy* 20, S10-S13.

Ohtsuka, K., Laszlo, A., (2007). The relationship between hsp70 localization and heat resistance. *Experimental Cell Research* 202, 507-518.

Orringer, J. S., Voorhees, J. J., Hamilton, T., Hammerberg, C., Kang, S., Johnson, T. M., Karimipour, D. J., Fisher, G., (2005). Dermal matrix remodeling after nonablative laser therapy. *J.Am.Acad.Dermatol.* 53, 775-782.

P.Bjerring, K.Christiansen, A.Troilius, C.Dierickx, (2006). Facial Photo Rejuvenation Using Two different Intense Pulsed Light (IPL) Wavelength Bands. *Lasers in Surgery and Medicine* 34, 120-126.

Park, C. H., Lee, M. J., Ahn, J., Kim, S., Kim, H. H., Kim, K. H., Eun, H. C., Chung, J. H., (2007). Heat shock-induced matrix metalloproteinase (MMP)-1 and MMP-3 are mediated through ERK and JNK activation and via an autocrine interleukin-6 loop. *Journal of Investigative Dermatology* 123, 1012-1019.

Pasquali-Ronchetti, I., Baccarani-Contri, M., (1997). Elastic fiber during development and aging. *Microsc.Res.Tech.* 38, 428-435.

Pearlman, S. J., (2006). Surgical treatment of the nasolabial angle in balanced rhinoplasty. *Facial.Plast.Surg.* 22, 28-35.

Pereira, A. N., Eduardo, C. P., Matson, E., Marques, M. M., (2007). Effect of low-power laser irradiation on cell growth and procollagen synthesis of cultured fibroblasts. *Lasers in Surgery and Medicine* 31, 263-267.

Prydz, K., Dalen, K. T., (2007). Synthesis and sorting of proteoglycans. *Journal of Cell Science* 113, 193-205.

R.R.Anderson, J.A.Parrish, (2007). The optics of human skin. *Journal of Investigative Dermatology* 77, 13-19.

Ramos-e-Silva, M., da Silva Carneiro, S. C., (2007). Elderly skin and its rejuvenation: products and procedures for the aging skin . *Journal of Cosmetic Dermatology* 6, 40-50.

Rattan, S. I., (1998). Repeated mild heat shock delays ageing in cultured human skin fibroblasts. *Biochem.Mol.Biol.Int.* 45, 753-759.

Roberts, W. E., (2009). Skin type classification systems old and new. *Dermatol.Clin.* 27, 529-33, viii.

Ruiz-Esparza, J., (2006). Near [corrected] painless, nonablative, immediate skin contraction induced by low-fluence irradiation with new infrared device: a report of 25 patients. *Dermatol.Surg.* 32, 601-610.

Sadick, N. S., (2006). Update on Non-Ablative Ligth Therapy for Rejuvenation: A Review. *Lasers in Surgery and Medicine* 32, 120-128.

Sadick, N. S., (2007). Combination radiofrequency and light energies: electro-optical synergy technology in esthetic medicine. *America Society for Dermatologic Surgery* 31, 1211-1217.

Sadick, N. S., Alexiades-Armenakas, M., Bitter, P., Hruza, G., Mulholland, S., (2006). Enhanced Full-Face Skin Rejuvenation Using Synchronous Intense Pulsed Optical and Conducted Bipolar Radiofrequency Energy (ELOS): Introducing Selective Radiophotothermolysis. *Journal of Drugs in Dermatology* 4, 181-186.

Shindo, Y., Witt, E., Han, D., Epstein, W., Packer, L., (1994). Enzymic and non-enzymic antioxidants in epidermis and dermis of human skin. *J.Invest Dermatol.* 102, 122-124.

Smalls, L. K., Randall, W. R., Visscher, M. O., (2006). Effect of dermal thickness, tissue composition, and body site on skin biomechanical properties. *Skin Res.Technol.* 12, 43-49.

Snoeckx, L. H. E. H., Cornelussen, R. N., van Nieuwenhoven, F. A., Reneman, S., an der Vusse, G. J., (2007). Heat shock proteins and cardiovascular pathophysiology. *Physiological Reviews* 81, 1461-1497.

Souil, E., Capon, A., Mordon, S., Dinh-Xuan, A. T., Polla, B. S., Bachelet, M., (2001). Treatment with 815-nm diode laser induces long-lasting expression of 72-kDa heat shock protein in normal rat skin. *Br.J.Dermatol.* 144, 260-266.

Stadelmann, W. K., Digenis, A. G., Tobin, G. R., (2006). Physiology and Healing Dynamics of Chronic Cutaneous Wounds. *The American Journal of Surgery* 176, 26S-38S.

Stureson, C., Andersson-Engels, S., (1995). A mathematical model for predicting the temperature distribution in laser-induced hyperthermia. Experimental evaluation and applications. *Phys.Med.Biol.* 40, 2037-2052.

Swelstad, M. R., Gutowski, K. A., (2006). Facial Rejuvenation. *Clinical Obstetrics and Gynecology* 49, 353-366.

Tandara, A. A., Kloeters, O., Kim, I., Mogford, J. E., Mustoe, T. A., (2007). Age effect of HSP70: Decreased resistance to ischemic and oxidative stress in HDF. *Journal of Surgical Research* 132, 32-39.

Tasab, M., Batten, M. R., Bulleid, N. J., (2000). Hsp47: a molecular chaperone that interacts with and stabilizes correctly-folded procollagen. *EMBO J.* 19, 2204-2211.

Tasab, M., Jenkinson, L., Bulleid, N. J., (2002). Sequence-specific recognition of collagen triple helices by the collagen-specific molecular chaperone HSP47. *J.Biol.Chem.* 277, 35007-35012.

Troy, T. L., Thennadil, S. N., (2001). Optical properties of human skin in the near infrared wavelength range of 1000 to 2200 nm. *J.Biomed.Opt.* 6, 167-176.

Tuchin, V. V., Yaroslavsky, A. N., Jacques, S. L., Popp, J., (2010). Biophotonics for dermatology: science & applications. *J.Biophotonics.* 3, 9-10.

Tzaphlidou, M., (2007). The role of collagen and elastin in aged skin: an image processing approach. *Micron* 35, 173-177.

Vaalamo, M., Leivo, T., Saarialho-Kere, U., (2006). Differential Expression of Tissue Inhibitors of Metallproteinases (TIMP-1, -2, -3, and -4) in Normal and Aberrant Wound Healing. *Human Pathology* 30, 795-802.

van Gemert, M. J., Jacques, S. L., Sterenborg, H. J., Star, W. M., (1989). Skin optics. *IEEE Trans.Biomed.Eng* 36, 1146-1154.

Vandesompele, J., De, P. K., Pattyn, F., Poppe, B., Van, R. N., De, P. A., Speleman, F., (2002). Accurate normalization of real-time quantitative RT-PCR data by geometric averaging of multiple internal control genes. *Genome Biol.* 3, 1-11.

Verbeke, P., Clark, B. F. C., Rattan, S. I. S., (2007). Reduced levels of oxidized and glycoxidized proteins in human fibroblasts exposed to repeated mild heat shock during serial passaging in vitro. *Free Radical Biology & Medicine* 31, 1593-1602.

Verrico, A. K., Haylett, A. K., Moore, J. V., (2001). In vivo expression of the collagen-related heat shock protein HSP47, following hyperthermia or photodynamic therapy. *Lasers Med.Sci.* 16, 192-198.

Verrico, A. K., Moore, J. V., (1997). Expression of the collagen-related heat shock protein HSP47 in fibroblasts treated with hyperthermia or photodynamic therapy. *Br.J.Cancer* 76, 719-724.

Watanabe, S., (2008). Basics of laser application to dermatology. *Arch.Dermatol.Res.* 300 Suppl 1, S21-S30.

Weiss, R. A., McDaniel, D. H., Geronemus, R. G., (2006). Review of Nonablative Photorejuvenation: Reversal of the Aging effects of the Sun and Environmental Damage Using Laser and Light Sources. *Seminars in Cutaneous Medicine and Surgery* 22, 93-106.

Welch, A. J., Gardner, C. M., (1997). Monte Carlo model for determination of the role of heat generation in laser-irradiated tissue. *J.Biomech.Eng* 119, 489-495.

Welch, A. J., Motamedi, M., Rastegar, S., LeCarpentier, G. L., Jansen, D., (1991). Laser thermal ablation. *Photochem.Photobiol.* 53, 815-823.

Welch, A. J., Pearce, J. A., Diller, K. R., Yoon, G., Cheong, W. F., (1989a). Heat generation in laser irradiated tissue. *J.Biomech.Eng* 111, 62-68.

Welch, A. J., Torres, J. H., Cheong, W. F., (1989b). Laser physics and laser-tissue interaction. *Tex.Heart Inst.J.* 16, 141-149.

Welch, A. J., van Gemert, M. J., (1995). *Optical-Response Of Laser-Irradiated Tissue.* Kluwer Academic Publishers.

West, M. D., (2007). The cellular and molecular biology of skin aging. *Archives of Dermatology* 130, 87-95.

White, W. M., Makin, I. R. S., Barthe, P. G., Slayton, M. H., Gliklich, R. E., (2007). Selective creation of thermal injury zones in the superficial musculoaponeurotic system using intense ultrasound therapy - A new target for noninvasive facial rejuvenation. *Archives of Facial Plastic Surgery* 9, 22-29.

Wilhelm, K. P., Cua, A. B., Maibach, H. I., (2007). Skin aging. *Archives of Dermatology* 27, 1806-1809.

Yaar, M., Eller, M. S., Gilchrist, B. A., (2007). Fifty years of skin aging. *Journal of Investigative Dermatology* 7, 51-58.

Zeller, T., Wild, P., Szymczak, S., Rotival, M., Schillert, A., Castagne, R., Maouche, S., Germain, M., Lackner, K., Rossmann, H., Eleftheriadis, M., Sinning, C. R., Schnabel, R. B., Lubos, E., Mennerich, D., Rust, W., Perret, C., Proust, C., Nicaud, V., Loscalzo, J., Hubner, N., Tregouet, D., Munzel, T., Ziegler, A., Tiret, L., Blankenberg, S., Cambien, F., (2010). Genetics and beyond--the transcriptome of human monocytes and disease susceptibility. *PLoS.One.* 5, e10693.

Samenvatting

Het effect van warmtepulsen op huidverjonging

De vorming van rimpels is één van de aspecten van het verouderen van huid die voort komt uit een gedegeneerde dermis. Het verouderde netwerk van eiwitten, de spiersamentrekkingen en de zwaartekracht resulteren in het rimpelen van de huid. Momenteel gaan de ontwikkelingen voor huidverjonging in de cosmetische industrie erg snel. Slechts enkele technieken zijn toepasbaar voor het verjongen van de dermis. Één van de meest veelbelovende technieken is het gebruik van niet-ablatieve lasers. Deze techniek is klinisch getest en wordt veelal gebruikt om de huid te verjongen. Echter, de achterliggende fysiologie zal nog moeten worden bevestigd.

Het is verondersteld dat de warmte die gegenereerd wordt door een laser een warmteshock veroorzaakt waar fibroblasten op reageren. Deze warmteshock brengt een cascade aan reacties teweeg, onder andere de productie van 'heat shock proteïnen', die de collageensynthese zouden stimuleren. Naast het thermische effect heeft de laser ook een fotochemisch effect. Het huidige proefschrift richt zich op het effect van de thermische puls op de collageenproductie van de dermale fibroblasten in kweek en in *ex-vivo* huid.

Een model is ontwikkeld dat de interactie van fotonen met huid en de veroorzaakte temperatuursontwikkeling berekent. Dit model werd gecombineerd met een transportmodel om de verdeling van de temperatuursverhoging in de huid te beschrijven. Vervolgens werd het model gebruikt om de optimale laserparameters, voor het beschrijven van de warmte verdeling als gevolg van een laser in de huid, te bepalen als functie van tijd en plaats.

Om het effect te onderzoeken van warmteshocks op menselijke huid, werd het aanvankelijke onderzoek uitgevoerd op celkweken. De dermale fibroblasten werden in kweek gebracht en blootgesteld aan temperaturen van 45°C en 60°C en met een pulsduur van 2 seconden. De resultaten van deze studie toonden aan dat deze temperaturen collageentype I synthese stimuleerden. Daarna werd er een studie uitgevoerd met dezelfde temperaturen, 45°C en 60°C. Echter een variatie in pulsduur: 2, 4, 8, 10 en 16 seconden, werd toegepast. Geconcludeerd kan worden uit deze studie dat 8 tot 10 seconden bij 45°C de optimale duur van de blootstellingstijd is waarbij de collageentype I synthese het hoogst is.

Om te kijken of fibroblasten in de huid hetzelfde reageren als in kweek, werd een *ex-vivo* huidstudie gedaan. Humane huidstukjes werden ondergedompeld in verwarmde PBS van 45°C en 60°C. De 45°C warmteshock leidde niet tot schade, echter de 60°C warmteshock lijkt vroege schade rond de cellen in de huid aan te tonen. Verder is aangetoond dat procollagentype I evenals type III geupreguleerd was door zowel de 45°C als de 60°C warmteshocks.

Om grip te krijgen wat laseropwarming voor invloed heeft op de huid, werd een pilot gedaan waarbij huidstukjes werden opgewarmd met behulp van een laser. De resultaten van dit onderzoek toonden aan dat de 45°C lasershock de huidstukjes niet beschadigde. De 60°C warmteshock, daarentegen, leek de aanwezigheid van hsp27 rond de cellen aan te tonen wat een aanwijzing is van vroege schade. De resultaten van de genexpressie lieten zien dat de 45°C warmteshocks leidden tot een verhoogde expressie van procollagentype I.

Samenvattend, hebben we in dit proefschrift aangetoond dat een temperatuur van 45°C zowel op fibroblasten als in huid *ex-vivo* een upregulatie van collageentype I teweegbrengt. Voorts toonden de celstudies de relevantie aan van de combinatie van tijd en temperatuur; een optimale duur van de blootstellingstijd van 8 tot 10 seconden bij 45°C resulteerde in de hoogste hoeveelheid collageentype I. Ook werd de schadelijke aard van een 60°C warmteshock aangetoond. Het aantonen dat de collageensynthese door de 45°C hitteschok kan worden verbeterd, is een volgende stap naar een beter begrip van de fysiologische processen die tot huidverjonging leiden.

Dankwoord

Het voltooien van een promotie onderzoek is vergelijkbaar met kampioen worden. Het vereist optimisme, veel inzet, hard werken, gedrevenheid en ook vertrouwen. Vertrouwen in jezelf, maar ook in anderen, want hoewel promoveren een solistische aangelegenheid lijkt, niets is minder waar. Daarom wil ik middels dit dankwoord de gelegenheid aangrijpen om een aantal mensen te bedanken voor hun steun, zowel van wetenschappelijke als persoonlijke aard.

Graag wil ik iedereen bedanken die direct of indirect een bijdrage heeft geleverd aan de totstandkoming van dit proefschrift. Een aantal mensen wil ik specifiek bedanken. Allereerst Frank en Paco bedankt voor het mogelijk maken van mijn project binnen deze bijzondere constructie tussen Philips en TU/e. Door de samenwerking heb ik kunnen profiteren van de faciliteiten alsmede de kennis van beide zijdes. Cees, bedankt voor het vertrouwen en je positieve relativerende kijk op zaken. Tom, bedankt voor je nuchtere en fysieke kijk op het onderzoek, het heeft me veel geholpen. Moniek, ontzettend bedankt voor je onuitputtelijke optimisme en gedrevenheid. Jouw input is vele malen erg nuttig gebleken. Ook Kang Yuen, Sarrita en Marina, bedankt voor het zorgvuldig uitvoeren van talrijke analyses. Ook de studenten Steven, Ying, Aaron en Claudia en verscheidene projectgroepjes wil ik bedanken voor hun inzet en bijdrage. Zij hebben wat van mij geleerd, maar bovenal heb ik ook zeker wat van hun geleerd. Debbie, Roel en Marion, het was bijzonder prettig dat er ook andere mensen met *ex-vivo* huid bezig waren, zodat we de lugubere verhalen konden delen.

Door het samenwerkingsverband tussen Philips en TU/e heb ik heel veel fijne collega's gehad. Ik zou mijn kamergenootjes bij Philips alsook op de TU/e specifiek willen bedanken voor hun gezelschap. Alberto, "good luck with your thesis, I'm sure you'll get there!" en Callina en Sipke, als was het niet lang, het was altijd reuze gezellig en bovenal leerzaam. Ook Robbert, Lenieke, Marieke en Linda wil ik zeker niet vergeten te bedanken voor hun motiverende woorden en overheerlijke hamburgerlunches! Danook Jeroen, Rudi, Marc en Yavat wat hebben we toch gelachen over de meest uiteenlopende zaken. Heerlijk even het verstand op nul en discussieren over helemaal niks. Natuurlijk ook mijn koffiemaatjes Robbert, Peter, Marc en Bas. Wat hebben we menig ochtend slaperig uit onze ogen zitten kijken, maar ook jullie relativerende woorden waren een welkome ontspanning.

Ik wil het personeel van de afdelingen plastische chirurgie en de operatiekamers in het Catharina Ziekenhuis in Eindhoven bedanken voor alle emmertjes met huid. In het bijzonder de plastisch chirurgen Van Rappard en Hoogbergen die deze samenwerking mogelijk hebben gemaakt alsook Marjolein (en je directe collega's) en de OK-receptie.

Lieve dames van Nayade, wat was het toch heerlijk om zo lang bij jullie te kunnen blijven. We hebben samen heel wat meegemaakt. Het was heerlijk om “stoom” af te kunnen blazen tijdens een training of een wedstrijd. Nu ik klaar ben is het voor mij helaas tijd om naar de Classic dames te gaan, maar ik hoop jullie daar te zijner tijd toch ook weer te zien. Bedankt voor al die jaren van gezelligheid en sportiviteit!

Johanneke en Rudi, Elise en Gertjan, Niels en Mirelle, Lydia en Arjan, Anne en Peter, Daan en Karlijn, Dennis en Ilse, Joost en Anouk, Bjorn en Sabine, Rob en Lindsay bedankt voor jullie interesse, medeleven en luisterende oren en natuurlijk voor de gezelligheid tijdens uitjes, etentjes en BBQs.

Lieve papa en mama, jullie wil ik in het bijzonder bedanken voor alle steun en het onvoorwaardelijke vertrouwen dat jullie altijd in me hebben gehad. Jullie hebben mij gevormd tot wie ik nu ben en daarvoor ben ik jullie eeuwig dankbaar. Chris, Ine, Roel, Willemijn, Wim, Liesbeth, Hennie en Harry, bedankt voor jullie steun.

Lieve Henk, mijn laatst dankwoorden zijn voor jou. Jouw onvoorwaardelijke steun, liefde, geduld en vertrouwen hebben mij de kracht gegeven door te gaan. Het valt niet in woorden uit te drukken wat dat betekent voor mij, maar zonder jou zou ik nooit zo ver gekomen zijn. Ik kijk uit naar de vele mooie avonturen die wij samen zullen gaan beleven!

Susanne, juli 2010

Curriculum Vitae

Susanne Dams werd op 24 april 1979 geboren te Nuenen. In 1999 behaalde zij haar VWO diploma aan Scholengemeenschap Augustinianum in Eindhoven. Aansluitend studeerde zij Biomedische Technologie aan de Technische Universiteit Eindhoven. Als onderdeel van deze studie heeft zijn stage gelopen aan de University of California San Diego (De Verenigde Staten). Hier onderzocht zij de invloed van mechanische rek op de contractie van hartspiercellen. Haar afstudeerwerk in de vakgroep cardiovasculaire biomechanica richtte zich op het bepalen en modelleren van de viscoelastische eigenschappen van de thrombus van abdominaal aneurysma in de aorta. In 2006 startte zij met haar promotieonderzoek bij Philips Research Eindhoven in de groep Care & Health Applications. Zij deed haar onderzoek in samenwerking met de Technische Universiteit Eindhoven in de vakgroep Soft Tissue Biomechanics & Engineering, resulterend in dit proefschrift.

List of Publications

S.D. Dams, Y. Luan, A.M. Nuijs, C.W.J. Oomens, F.P.T. Baaijens. *Modeling and simulation of heat distribution in human skin caused by laser irradiation*. J. of Biomech. **(submitted)**

S.D. Dams, M.de Liefde-van Beest, A.M. Nuijs, C.W.J. Oomens, F.P.T. Baaijens. *Pulsed heat shocks enhance procollagen type I and procollagen type III expression in human dermal fibroblasts*. Skin Res. and Techn., 16(3): 354-364, 2010.

S.D. Dams, M.de Liefde-van Beest, A.M. Nuijs, C.W.J. Oomens, F.P.T. Baaijens. *Influence of pulse duration of heat shocks on collagen type I expression in human dermal fibroblasts*. **(submitted)**

S.D. Dams, M. de Liefde-van Beest, A.M. Nuijs, C.W.J.Oomens, F.P.T.Baaijens. *Heat shocks enhance procollagen type I and III expression in fibroblasts in ex vivo human skin*. Skin Res. Tech. **(submitted)**

The work described in this thesis has been carried out at the Philips Research Laboratories Eindhoven as part of the Philips Research programme.